T.C.
MANİSA CELAL BAYAR UNIVERSITY
GRADUATE SCHOOL OF NATURAL and APPLIED SCIENCE
INSTITUTE

DOCTOR of PHILOSOPY THESIS
CHEMISTRY DEPARTMENT
PHYSICAL CHEMISTRY DISCIPLINE

PROVIDING CONDUCTIVE PROPERTIES TO POLYOLEFINS; EXAMINING THEIR THERMAL AND MECHANICAL PROPERTIES

Ayşe Nur ÖZKAN

Supervisor
Prof. Dr. Kamil ŞİRİN

MANİSA–2024

Ayşe Nur ÖZKAN	**PROVIDING CONDUCTIVE PROPERTIES TO POLYOLEFINS; EXAMINING THEIR THERMAL AND MECHANICAL PROPERTIES**	**2024**

APPROVEL OF THE THESIS

The thesis entitled "Providing Conductive Properties to Polyolefins; Examining Their Thermal and Mechanical Properties", prepared by Ayşe Nur Özkan, was successfully defended as a doctoral thesis at the Department of Chemistry of the Institute of Sciences of Manisa Celal Bayar University on 03/05/2024 and was approved unanimously.

Supervisor	**Prof. Dr. Kamil ŞİRİN** Manisa Celal Bayar University
Examining Committee Member (Head of the Examining Committee)	**Prof. Dr. Yüksel ABALI** Manisa Celal Bayar University
Examining Committee Member	**Prof. Dr. Uğur AVCIBAŞI** Manisa Celal Bayar University
Examining Committee Member	**Assoc. Prof. Dr. Fatih DOĞAN** Çanakkale Onsekiz Mart University
Examining Committee Member	**Assoc. Prof. Dr. Yeliz YILDIRIM** Ege University

TAAHHÜTNAME

Bu tezin Manisa Celal Bayar Üniversitesi, Fen Bilimleri Enstitüsü, Kimya Ana Bilim Dalında akademik ve etik kurallara uygun olarak yazıldığını ve kullanılan tüm literatür bilgilerinin referans gösterilerek tezde yer aldığını, tamamen kendi çalışmam olduğunu, her alıntıya kaynak gösterdiğimi, tezin yazımında akademik ve etik kurallara aykırı herhangi bir yapay zeka ve program kullanmadığımı beyan ederim.

Bu doktora tezi, Yükseköğretim Kurulu Başkanlığının 09.03.2022 tarih, 19579 sayılı ve Lisansüstü Eğitim /Tez Yazım Dili konulu yazısına istinaden; 19.10.2022 tarih ve 24 sayılı Manisa Celal Bayar Üniversitesi Fen Bilimleri Enstitüsü Yönetim Kurulu Kararına göre: MCBÜ Lisansüstü Eğitim Öğretim Yönetmeliği'nin 9. maddesinin 10. fıkrası "Yabancı dilde öğretim yapılmayan programlarda (Türk Dili ve Edebiyatı Anabilim Dalı hariç) öğrencinin, danışmanın, enstitü anabilim/anasanat dalı kurulunun önerisi ve enstitü yönetim kurulunun onayı ile yüksek lisans tezi YÖK tarafından kabul edilmiş olan yabancı dillerde de yazılabilir." hükmü uyarınca İngilizce olarak hazırlanmıştır.

COMMITMENT

I hereby declare that; this thesis was written in Manisa Celal Bayar University, Graduate School of Natural and Applied Science Institute, Department of Chemistry, in accordance with the academic and ethical rules, and all the literature information used is included in the thesis by reference. It is entirely my own work. I declare that I did not use any artificial intelligence or programs that violate ethical rules.

Ayşe Nur ÖZKAN

CONTENTS

LIST of ABBREVIATIONS

HDPE	High Density Polyethylene
LDPE	Low Density Polyethylene
PANI	Polyaniline
PP	Polypropylene
PPY	Polypyrrole
PTH	Polythiophene
PMMA	Poly(methyl methacrylate)
SBR	Styrene butadiene rubber
PET	Polyethylene terephalate
NMP	N-Methyl-2-pyrrolidinone
DBSA	Dodecylbenzenesulfonic acid
MWCNT	Multi-walled carbonnanotube
PAA	Poly(acrylic acid)
PSS	Polystyrene sulphonic acid
FTIR	Fourier Transform Infrared Spectroscopy
XRD	X-Ray Diffraction
TGA	Termogravimetric Analyzer
DMA	Dynamic Mechanical Analyzer
SEM	Scanning Electron Microscope
DSC	Differential Scanning Calorimetry
ESD	Electrostatic Charge Dissipation
EMSE	Electromagnetic Shielding Efficiency

LIST of FIGURES

Page

LIST of TABLES

Page

ACKNOWLEDGEMENT

I would like to express my sincere gratitude to my valuable supervisor, Prof. Dr. Kamil ŞİRİN, who guided and encouraged me with his knowledge and experience at every stage of my thesis work. His continuous efforts throughout my career will always be appreciated.

I would like to thank Assoc. Prof. Fatih DOĞAN for ESD analyses and guidance about conductive polymers.

Some of analyses in this dissertation were carried out at the Manisa Celal Bayar University Applied Science and Research Center (ASRC). I would like to thank the ASRC management and team for their support.

I would like to express my appreciation to my husband, Eray ÖZKAN, who constantly supported and encouraged me during this study; and to my daughters, Neva and Sena, who understood that I could not spare much time for them during this dissertation. I also would like to thank my parents for their endless support.

Finally, I would like to thank the Manisa Celal Bayar University Scientific Research Project Coordination Unit for their financial support (Project Number 2020-116).

Ayşe Nur ÖZKAN
Manisa, 2024

ABSTRACT

PhD Dissertation

Manisa Celal Bayar University
Graduate School of Natural and Applied Science Institute
Department of Chemistry

Supervisor: Prof. Dr. Kamil ŞİRİN

Blends of high density polyethylene (HDPE) and low density polyethylene (LDPE) and conductive polyaniline (PANI) were prepared in order to impart antistatic properties to polyethylene, which is one of the most important materials widely used today. For the preparation of the blends, first of all, polyaniline was synthesized by oxidative polymerization method using ammonium peroxydisulfate and 1M HCl at 0°C. The obtained green powdered PANI was characterized by techniques such as FTIR (Fourier Transform Infrared Spectroscopy), XRD (X-Ray Diffraction) and thermal analysis.

Polyaniline added LDPE and HDPE blends were prepared by solution blending method. LDPE was dissolved in toluene in a magnetic stirrer at 80°C, and polyaniline was dissolved in NMP in an ultrasonic bath. PANI/LDPE blends were obtained by adding different ratios of polyaniline to LDPE solution. The interaction between PANI and LDPE was then characterized by FTIR, DSC (Differential Scanning Calorimetry), TGA (Thermogravimetric Analyzer), DMA (Dynamic Mechanical Analyzer), SEM (Scanning Electron Microscopy) and XRD techniques. The conductivities of PANI/LDPE blends were determined to be in the range of 10^{-6}- 10^{-9} S.cm^{-1}. When the antistatic decay times were examined, it was seen that all blends could provide ESD protection at 3 kV corona voltage. In addition, it was observed that LDPE blend, doped with 3 wt% polyaniline could also provide ESD (Electrostatic Charge Dissipation) protection at -3 kV and 6 kV corona voltages.

HDPE was dissolved in p-xylene in a magnetic stirrer at 100°C, and polyaniline was dissolved in NMP in an ultrasonic bath. PANI/HDPE blends were obtained by adding different ratios of polyaniline to the HDPE solution. The interaction between PANI and HDPE was then characterized by FTIR, DSC, TGA, DMA, SEM and XRD techniques. The conductivities of PANI/HDPE blends were determined to be in the range of 10^{-7}- 10^{-10} S.cm^{-1}. When the the antistatic decay times are examined, it was seen that all blends could provide ESD protection at 3 kV corona voltage.

Keywords: Polyolefins, Conductive Polymers, Polyanilin, Antistatic Applications

2024, 101 pages

ÖZET

Doktora Tezi

Ayşe Nur ÖZKAN

Manisa Celal Bayar Üniversitesi
Fen Bilimleri Enstitüsü
Kimya Bölümü

Danışman: Prof. Dr. Kamil ŞİRİN

Günümüzde yaygın olarak kullanılan en önemli malzemelerden polietilene antistatik özellik kazandırılması amacıyla, yüksek yoğunluklu polietilen (YYPE) ve alçak yoğunluklu polietilen (AYPE) ile iletken polianilin (PANI) harmanları hazırlandı. Harmanların hazırlanması için öncelikle 0 ºC'de amonyum peroksidisulfat ve 1M HCl kullanılarak oksidatif polimerizasyon yöntemi ile polianilin sentezlendi. Yeşil renkli toz halindeki polianilin FTIR, XRD ve termal analiz gibi tekniklerle karakterize edildi.

Polianilin katkılı AYPE ve YYPE karışımları çözelti ortamında harmanlama yöntemiyle hazırlandı. AYPE toluen içinde 80ºC'de ısıtıcılı manyetik karıştırıcıda, polianilin ise ultrasonic banyoda NMP içinde çözündü. Farklı oranlardaki (kütlece % 0.5, 1 ve 3) polianilinin AYPE çözeltisine eklenmesiyle PANI/AYPE harmanları elde edildi. PANI ve AYPE arasındaki etkileşim daha sonra FTIR, DSC, TGA, DMA, SEM ve XRD teknikleri ile karakterize edildi. PANI/AYPE harmanlarının iletkenlikleri 10^{-6}- 10^{-9} S.cm^{-1} aralığında olduğu belirlendi. Statik yük dağılımının süreleri incelendiğinde tüm harmanların 3 kV korona geriliminde ESD koruması sağlayabildiği görüldü. Bunun yanısıra kütlece %3 oranında polianilin ile katkılandırılmış olan AYPE blendinin -3 kV ve 6 kV korona gerilimlerinde de ESD koruması sağlayabildiği görüldü.

YYPE, p-xylene içinde 100ºC'de ısıtlıcılı manyetik karıştırıcıda, polianilin ise ultrasonic banyoda NMP içinde çözündü. Farklı oranlardaki polianilinin, YYPE çözeltisine eklenmesiyle PANI/YYPE harmanları elde edildi. PANI ve YYPE arasındaki etkileşim daha sonra FTIR, DSC, TGA, DMA, SEM ve XRD teknikleri ile karakterize edildi. PANI/YYPE harmanlarının iletkenlikleri 10^{-7}- 10^{-10} S.cm^{-1} aralığında olduğu belirlendi. Statik yük dağılımının süreleri incelendiğinde tüm harmanların 3 kV korona geriliminde ESD koruması sağlayabildiği görüldü.

Anahtar Kelimeler: Poliolefinler, İletken Polimerler, Polianilin, Antistatik Uygulamalar

2024, 101 Sayfa

GENİŞ ÖZET

Polimerler günlük yaşamımızda yaygın olarak kullanılan malzemelerdir. Giysilerden ev eşyalarına, ambalajlardan plastik bazlı birçok malzemeye kadar geniş bir kullanım alanına sahiptir. Düşük yoğunluklarından dolayı nispeten hafif, işlenebilir, esnek ve ayrıca ucuz olmalarından dolayı kullanımları giderek artmıştır.

Son yıllarda polimerlerin kullanım alanlarının artması, polimer bilimi ve teknolojisindeki çalışmaları hızlandırmış ve bilim insanları yeni polimerlerin sentezlenmesi ve mevcut polimerlerin özelliklerinin iyileştirilmesi üzerine çalışmalar yapmaktadır. Polimerler, iletkenlik değerleri 10^{-7} ile 10^{-14} S/cm arasında olan elektriksel olarak yalıtkan malzemeler olarak biliniyordu. 1977'de MacDiarmid ve Heeger'in poliasetileni indirgeme ve oksidasyon reaksiyonları yoluyla yalıtkan bir durumdan iletken bir duruma dönüştürmüşlerdir. İletken poliasetilenin icadından sonra birçok farklı iletken polimer geliştirilmiştir.

İletken polimerler arasında polianilin, monomerinin ucuz olması, sentezlenmesinin kolay olması, stabilitesi ve katkılama nedeniyle yüksek iletkenliği nedeniyle birçok uygulama için tercih edilen bir malzemedir. Polianilin, güneş pilleri, şarj edilebilir piller, sensörler ve kapasitörler, elektromanyetik radyasyon kalkanı, gaz ayırma membranları, elektrokromik cihazlar ve antistatik kaplamalar gibi çok çeşitli yeni nesil teknolojilerde kullanılmaktadır. Özellikle bilgisayar iç parçaları, veri depolama aygıtları ve çip taşıyıcıları gibi elektronik endüstrisinde iletken polimerlerin antistatik özellikleri oldukça önemli bir konudur.

Günlük hayatımızda birçok malzeme üzerinde elektrostatik birikim nedeniyle kıvılcım, yangın ve patlamalar meydana gelebilmektedir. Bu istenmeyen sonuçlar, cihazların arızalanmasının yanı sıra, insanların yaralanmasına ve hatta ölümüne neden olabilir. Ayrıca statik elektrik toz birikmesine neden olur ve bu da malzemelerin çekiciliğini azaltır. Bu sorunun önemi anlaşılmış ve sorunun çözümüne yönelik çalışmalara hız verilmiştir. Günümüzde antistatik ajanlar alanında iletken polimerler, karbon nanotüp, karbon siyahı, grafit, metaller ve metal oksitler gibi birçok malzeme geniş çapta araştırılmaktadır.

Bu çalışmanın amacı yüksek yoğunluklu polietilene ve alçak yoğunluklu polietilene iletken özellik kazandırmak ve elde edilen blendlerin elektrostatik yük dağıtma performansını araştırmaktır. İlk olarak polianilin, anilinin kimyasal oksidasyonu ile asidik ortamda sentezlendi. Polianilin oluşumunu doğrulamak için XRD (X-Işını Kırınımı), FTIR (Fourier Dönüşümlü Kızılötesi Spektrometre), DSC (Diferansiyel Taramalı Kalorimetre) ve TGA (Termogravimetrik Analiz) analizleri yapıldı. FTIR spektrumu incelendiğinde 1468 cm^{-1} ve 1566 cm^{-1}'de benzoid ve kinoid halka titreşimlerine ait pikler net bir şekilde görülmektedir. Bu da polianilinin indirgenmiş (benzenoid) ve oksitlenmiş (kinoid) emeraldin formunun elde edildiğini göstermektedir. TGA analizi tipik üç basamaklı bir bozunma davranışı gösterdi. Birinci bozunma su çıkışını, ikinci bozunma polianilinin deprotonasyonunu ve son ağırlık kaybı polianilin zincirinin kırılmasını temsil etmektedir. DSC analiz sonucuna göre 254,6°C'de camsı geçiş sıcaklığı bulunmuştur. Polianilinin iletkenlik ölçümü dört nokta prob tekniği ile ölçüldü ve $4,5x10^{-6}$ S/cm olarak bulundu.

Çalışmanın ikinci bölümünde çözelti harmanlama yöntemine göre düşük yoğunluklu polietilen (AYPE) /polianilin (PANI) blendleri hazırlandı. AYPE toluen içinde 80^{o}C'de ısıtıcılı manyetik karıştırıcıda, polianilin ise ultrasonic banyoda NMP içinde çözündü. Farklı oranlardaki (kütlece % 0,5, 1 ve 3) polianilinin AYPE çözeltisine eklenmesiyle PANI/AYPE blendleri elde edildi. PANI ve AYPE arasındaki etkileşim FTIR, DSC, TGA, DMA (Dinamik Mekanik Analiz), SEM (Taramalı Elektron Mikroskobu) ve XRD teknikleri ile karakterize edildi.

Polimer blendleri, kimyasal olarak bağlanmak yerine fiziksel olarak birleştirilen iki veya daha fazla polimerden yapılan karışımlardır. Polimerleri harmanlamanın amacı, tek tek bileşenlerin fiziksel özelliklerinden daha iyi özelliklere sahip yeni malzemeler elde etmektir. Kızılötesi spektroskopisinde, her iki malzemenin de spesifik piklerinin olduğu görüldü ve bu malzemelerin fiziksel olarak karıştığının kanıtıdır.

Blendlerin TGA analizi, iki basamaklı bozunma davranışı gösterdi. Birincisi çözgenin buharlaşmasından, ikincisi ise AYPE'nin bozunmasından kaynaklanmaktadır. Katkı maddelerinden genel beklenti, konakçı polimerin termal özelliklerini değiştirmeden karışımlar elde etmektir. Saf AYPE ve $LP_{0.5}$, LP_1 ve LP_3 blendlerinin en yüksek bozunma hızına karşılık gelen sıcaklık değerlerinin 478°C civarında olduğu görüldü. Bu, termal dayanıklılığında herhangi bir değişiklik olmadığını göstermiştir.

PANI ve AYPE karışmaz olduğundan, polianilin miktarının AYPE'nin erime sıcaklığı üzerinde önemli bir etkisi olmadığı görülmektedir. PANI'nin AYPE matrisine eklenmesi, erime sıcaklığında yaklaşık 1°C'lik bir düşüşle sonuçlandı. Bununla birlikte, blendlerdeki PANI miktarı arttıkça AYPE kristallik derecesi önemli ölçüde azalmıştır. Polianilin amorf olduğundan, blendlerin amorf fazı genişleyecektir; bu, polianilin konsantrasyonu arttıkça blendlerdeki kristallilik yüzdesinin giderek azalacağı anlamına gelir. SEM görüntülerinden polianilin parçacıklarının bir tarafta toplanma eğiliminde olduğu da açıkça görülmektedir. Bu eğilim polianilin'in AYPE içinde iyice dağılmasını zorlaştırır. Bu topaklanma, kristallik yüzdesinin ve hatta mekanik özelliklerin azalmasının nedenidir. Gerilme-gerinim sonuçlarına göre mekanik özelliklerde azalma söz konusudur.

X-ışını kırınım desenleri incelendiğinde, AYPE'nin 2 Θ ° =21,27° (110) ve 2 Θ° =23,46° (200) değerindeki iki farklı kırınım pikinin literatürle uyumlu olduğu görülmektedir. Tüm AYPE/PANI blendlerinin de XRD kırınım açılarının 21° ve 23° civarında olduğu görülmüştür.

Blendlerin iletkenlik ölçümleri üç farklı sıcaklıkta yapıldı ve 10^{-9} ve 10^{-6} S/cm aralığında iletkenlik değerleri elde edilmiştir.

Elektrostatik yük birikmesi malzemelerde birçok soruna neden olmaktadır. Dolayısıyla elde edilen malzemelerin antistatik koruma sağlayıp sağlamadığını anlamak için ESD (Elektrostatik Deşarj) analizleri yapılmıştır. Analizlerde AYPE ve blendlerin yüzeyleri üzerinde biriktirilen statik yüklerin dağılım süreleri belirlenmiştir. Analizler oda sıcaklığında malzemeler üzerine uygulanan değişik pozitif (3, 6, 9 kV ve negatif (-3, -6, -9 kV) korona voltajlarında gerçekleştirilmiştir. AYPE ‘nin yüzeyinde biriktirilen statik yükün dağılım süresi (300 saniyeye kadar)

ölçülememiştir. $LP_{0.5}$ ve LP_1 blendleri -3kV, 3kV, 6kV korona gerilimlerinde, LP_3 blendi ise 3 kV korona geriliminde oldukça iyi 1/e ve %10'luk kesme zamanı değerleri göstererek ESD koruması sağladığı söylenebilir.

Çalışmanın son bölümünde çözelti harmanlama yöntemine göre yüksek yoğunluklu polietilen/polianilin blendleri hazırlandı. YYPE P-xylen içinde 100°C'de ısıtıcılı manyetik karıştırıcıda, polianilin ise ultrasonik banyoda NMP içinde çözündü. Farklı oranlardaki (kütlece % 0,5, 1 ve 3) polianilinin YYPE çözeltisine eklenmesiyle PANI/YYPE blendleri elde edildi. PANI ve YYPE arasındaki etkileşim daha sonra FTIR, DSC, TGA, DMA, SEM ve XRD teknikleri ile karakterize edilmiştir.

PANI ve YYPE arasındaki etkileşimi anlamak için analizlere FTIR spektroskopisi ile başlandı. Kızılötesi spektruma göre her iki malzemenin kendisine ait pik noktaları görülmüştür ve bu da bu malzemelerin fiziksel olarak karıştığının kanıtıdır.

TG/DTG analizlerine göre blendler iki basamaklı bozunma sergilemişlerdir. Birinci basamaktaki bozunmalar çözücünün buharlaşmasından kaynaklanmakta olup ikinci bozunmalar ise polimer zincirinin bozunmasını göstermektedir. DTG analizine göre maksimum bozunma hızına karşılık gelen sıcaklıkta yaklaşık 1°C'lik bir artış vardır. YYPE blendlerinin termal dayanıklılığında yaklaşık 1°C'lik bir artış olduğu söylenebilir.

DSC analiz sonuçlarına göre, YYPE matrisine PANI ilavesinin erime sıcaklığında yaklaşık 1°C'lik bir düşüşle sonuçlandığını gösterdi. Bununla birlikte, karışımlardaki PANI miktarı arttıkça YYPE kristallik derecesi önemli ölçüde azaldığı görülmüştür. Polianilinin amorf yapısından dolayı, blendlerin amorf fazı genişleyecektir; bu, polianilin konsantrasyonu arttıkça blendlerdeki kristallik yüzdesinin giderek azalacağı anlamına gelmektedir.

X-ışını kırınım desenleri incelendiğinde, YYPE'nin $2\Theta^\circ = 21{,}18^\circ$ (110) ve $2\Theta^\circ = 23{,}55^\circ$ (200) değerindeki iki farklı kırınım pikinin literatürle uyumlu olduğu görülmektedir. Tüm YYPE/PANI blendlerinin de XRD kırınım açılarının 21° ve 23° civarında olduğu görülmüştür.

YYPE'deki moleküler zincirleri doğrusaldır ve daha yakın dizilirler, bu da güçlü moleküller arası kuvvetlere ve daha kristalin bir yapıya neden olur. Polianilin yapısından dolayı topaklanma eğilimindedir. Bu nedenle polianilin parçacıklarının toplanması, YYPE matrisinde uygun bir dolgu maddesi dağılımının oluşturulmasını zorlaştırır. Bu nedenle blendlerin mekanik özellikleri azalmıştır.

Karışımların iletkenlik ölçümleri üç farklı sıcaklıkta yapıldı. Sıcaklık arttıkça karışımların iletkenliği de arttı. ESD malzemesi olarak kullanılabilecek yeterli iletkenlik değerleri olan 10^{-7} ile 10^{-10} S/cm arasında iletkenlik değerleri elde edilmiştir.

Antistatik uygulamalar için ESD analizleri yapıldı. Karışımın yüzeyine oda sıcaklığında çeşitli pozitif (3, 6 ve 9 kV) ve negatif (-3, -6 ve -9 kV) korona voltajları uygulandı. Karışımların yüzeyindeki statik yük oluşumunun dağılma süresi belirlendi. 3kV korona gerilimindeki tüm PANI/YYPE blendlerinin 1/e süresi ve %10 kesme süresi kriterlerine göre ESD malzemesi olarak kullanılabileceği görülmüştür.

Yukarıda belirtilen bilgiler ışığında AYPE/PANI ve YYPE/PANI blendleri elektrik ve elektronik uygulamalar başta olmak üzere antistatik malzeme olarak pek çok kullanım alanı bulması beklenmektedir.

1. INTRODUCTION

Polymers are materials that are widely used in our daily life. It has a wide range of uses such as clothes, household items, packaging and many plastic-based materials. Polymers have a wide range of applications due to their molecular structure. They are relatively light, workable and flexible because of their low density. In addition, their use has increased gradually due to its cheapness. While polyethylene (PE) ranks first in plastic production and consumption in the world with 32%, polypropylene (PP) ranks second with 20%, poly(vinyl chloride) (PVC) ranks second with 17% (Sogancioglu et al., 2017).

In recent years, the increase in the usage areas of polymers has accelerated the studies in polymer science and technology, and scientists have started to work on synthesizing new polymers and improving their properties. Polymers were known as electrically insulating materials with conductivity values between 10^{-7} and 10^{-14} S cm^{-1}. It begins in 1977 after MacDiarmid and Heeger's conversion of polyacetylene from an insulating state to a conducting state by reduction and oxidation reactions (Hideki Shirakawa et al., 1977). Following the invention of electrically conductive polyacetylene, many different conductive polymers have been developed.

Among the conductive polymers, polyaniline is a preferred material for many applications because of its monomer being inexpensive, easy to synthesize, stability and high conductivity due to doping (Abraham et al., 1996). Polyaniline is used in a wide variety of next generation technologies such as solar cells, rechargeable batteries, sensors and capacitors, electromagnetic radiation shielding, gas separation membranes, electrochromic devices and antistatic coatings (Ivanov et al., 2003). Especially antistatic properties of conductive polymers is a very important issue in electronic industry such as computer internal parts, data storage devices and chip carriers.

The most important problem of electronic industry is electrostatic discharge. In our daily life, sparks, fires and explosions can occur due to electrostatic accumulation on many materials. These undesirable consequences can cause injury to

people and even death, as well as malfunction of devices. Also static electricity cause accumulation of dust which decreases the attractiveness of materials (Zhao et al., 2019). Importance of this problem understood and to solve problem the efforts has been accelerated. Nowadays, several materials such as conductive polymers, carbon nanotube, carbon black, graphite, metals and metal oxides have been widely researched in the field of antistatic agents. The conductivity value of the material to be used as antistatic agent should between 10^{-6} and 10^{-11} $S.cm^{-1}$ (Joelma et al., 2007).

The aim of this study is to provide conductive properties to polyolefins and to investigate the electrostatic charge dissipative performance of the polyolefin/polyaniline blends. Firstly, polyaniline was synthesized according to the chemical oxidation of aniline. To confirm the formation of polyaniline XRD, FTIR, DSC and TGA analysis are performed. Blends were prepared by loading 0.5, 1.0 and 3.0 wt % of PANI into HDPE and LDPE matrix in solution medium. The mechanical, morphological and thermal properties of so-called binary blends was also examined. Conductivities of blends are measured at three different temperature. Finally, antistatic decay time of blends was performed at Corona voltages between -9 kV and +9 kV.

2. GENERAL BACKGRAOUND

2.1. Polyolefins

Polymers are often utilized materials for both industrial and residential applications because of their appealing mechanical and physical qualities, which include high strength, ease of processing, low density, chemical resistance (Sirin et al., 2022). Polyolefins are group of polymers produced from olefin monomers such as ethylene, propylene, butylene and isoprene; polyethylene, polypropylene, polybutylene, polyisoprene (Beşergil et al., 2008). Olefines are unsaturated chemical compounds with at least one carbon- carbon double bond in organic chemistry. Olefins' double bonds make them an intriguing synthesis candidate for chemical reactions. There have been several prior attempts to produce longer hydrocarbons containing C–C bonds, especially using the low-molecular representatives propen and ethen. This double bond's placement increases the molecule's reactivity and opens up a variety of uses for it. Roughly 63% of the polymers produced worldwide come from the polyolefins industry. Globally, approximately 76 million metric tons (MMT) of polyethylene and 56 MMT of polypropylene are produced annually (Posch, 2016).The most widely used polyolefins are the polyethylene (PE) and polypropylene (PP). Either a free radical method (LDPE) or coordination catalysis (HDPE, i-PP) is used to generate polyolefins (Sauter et al., 2017).

2.1.1. Polyethylene

Polyethylene in its simplest form has long backbone covalently linked carbon atoms and hydrogen atoms which are attached to carbon atoms and the chain ends with methyl groups. Number of ethylene monomers polymerized to form this chain with formula $C_{2n}H_{4n+2}$, n is the degree of polymerization. Polyethylenes with different chain lengths from 1.400 molecular weights to 3.500.000 are available. Also, variations can be seen from branches change from alkyl groups to acid ester functionalities and from defects of vinyl groups. Chains with few defects have higher degree of crystallinity. The higher the concentration of the branches, the lower the density of the polymer. The density of polyethylene increase as the degree of crystallinity rises (Andrew Peacock, 2000). High density polyethylene (HDPE) and the low-density polyethylene

(LDPE) are the most commonly used polymers (Figure 2.1). The concentrations of monomer and polymer as well as the local reaction temperature determine the kind and degree of branching. Reactor shape and operation have a significant impact on the molecular weight distributions as well as the frequencies of long and short branches on polymer chains. Both crystalline and amorphous portions make up polyethylene. A higher degree of crystallinity can be achieved by more effectively packing molecules along linear polymer chains. Nevertheless, side-chain branching lessens the crystallinity (Şirin, 2008).

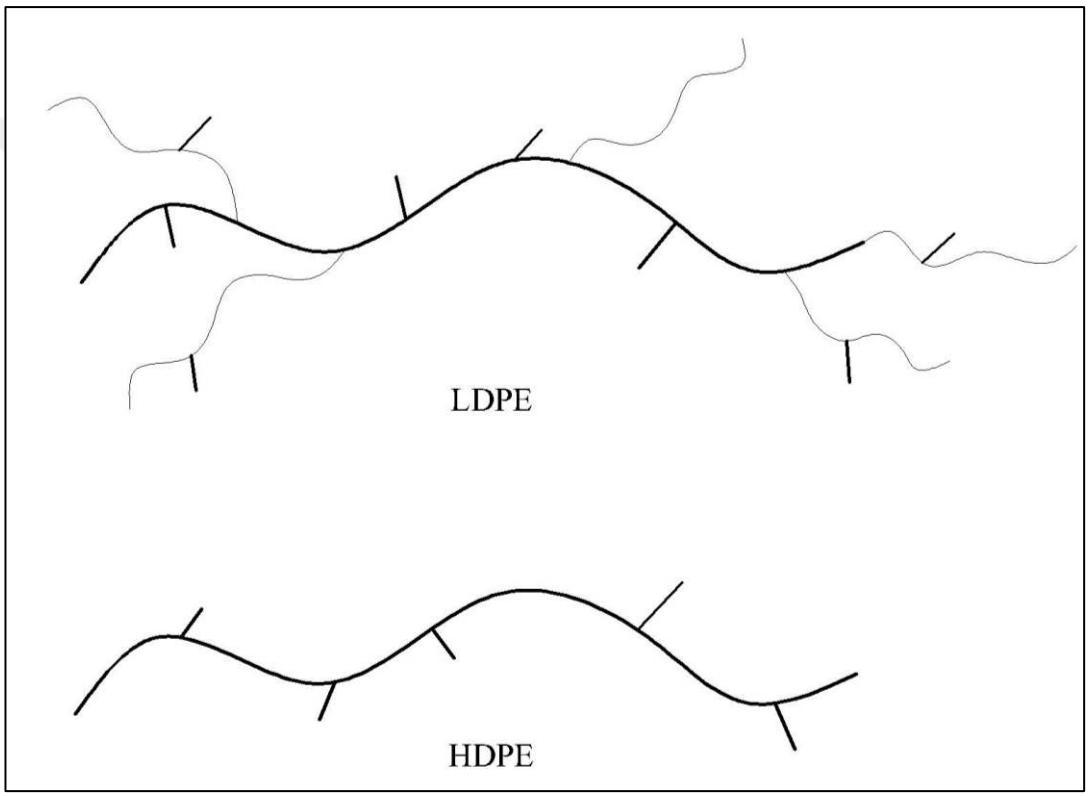

Figure 2.1. Linear Structure of LDPE and HDPE.

The density of LDPE varies between 0.91-0.93 g/cm^3. LDPE has a high degree of short and long side-chain branching. These branches reduce the tendency of the molecules to pack in hard, crystalline structure so lower density and crystallinity. LDPE is flexible and very resistant to breaking. It is used in the production of many plastic products, such as bottles, suitcases, frozen food packages, toys… LDPE is a partially crystalline thermoplastic as a result of free radical polymerization of ethylene under high pressure (Beşergil et al., 2008). In order to create LDPE, ethylene is

polymerized at high pressures (103–345 MPa) and high temperatures (200–350 ºC) with the addition of oxygen as a free-radical initiator.

Initiation: The free radicals are produced in this step by the decomposition of initiators. From various initiators most widely used are 2-2'-azo-bis-isobutyrylnitrile and benzoyl peroxide (Figure 2.2).

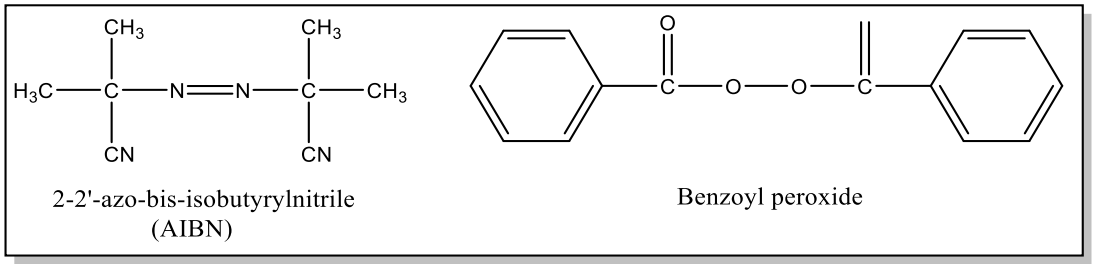

Figure 2.2. Initiators for polymerization of LDPE.

Propagation: The growth of the polyethylene chain occurs when the ethylene molecule is brought into close to the free radical by the force of the high pressure (Figure 2.3).

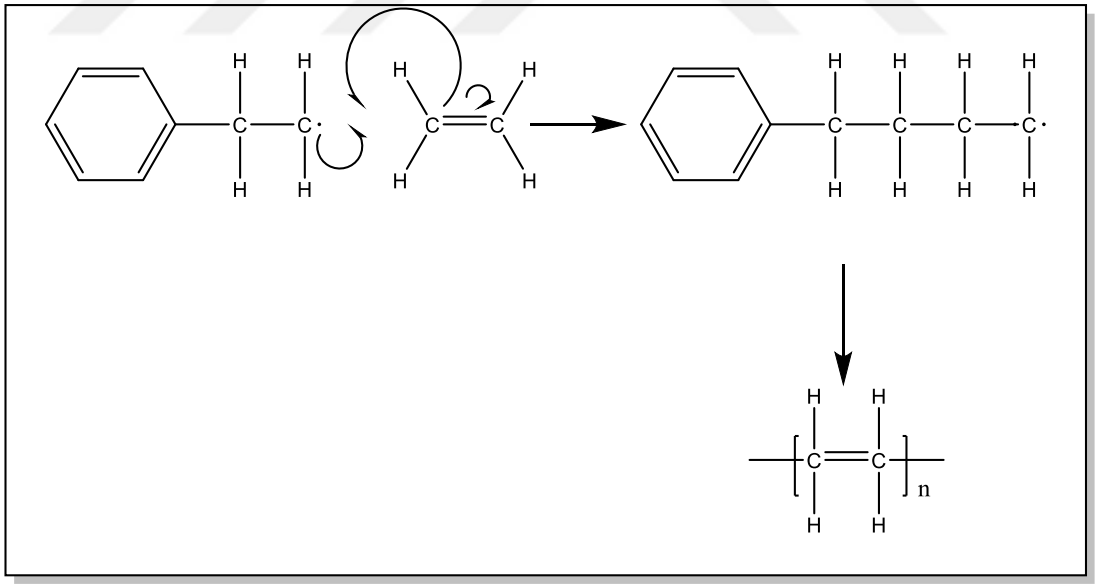

Figure 2.3. Propagation step of LDPE formation.

Termination: Termination can be three ways:

Coupling: When the two chains with radicals join, a single polymer molecule forms (Figure 2.4).

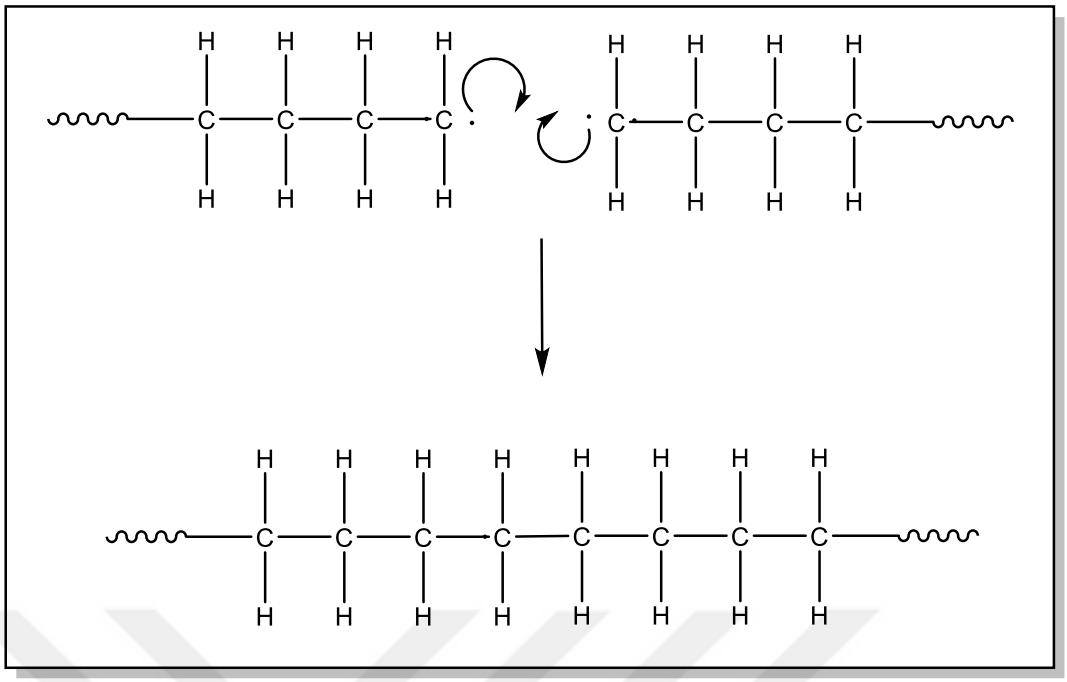

Figure 2.4. Termination step of LDPE by coupling way.

Disproportionation: When two chains with radicals meet, the result may be chain disproportionation (Figure 2.5).

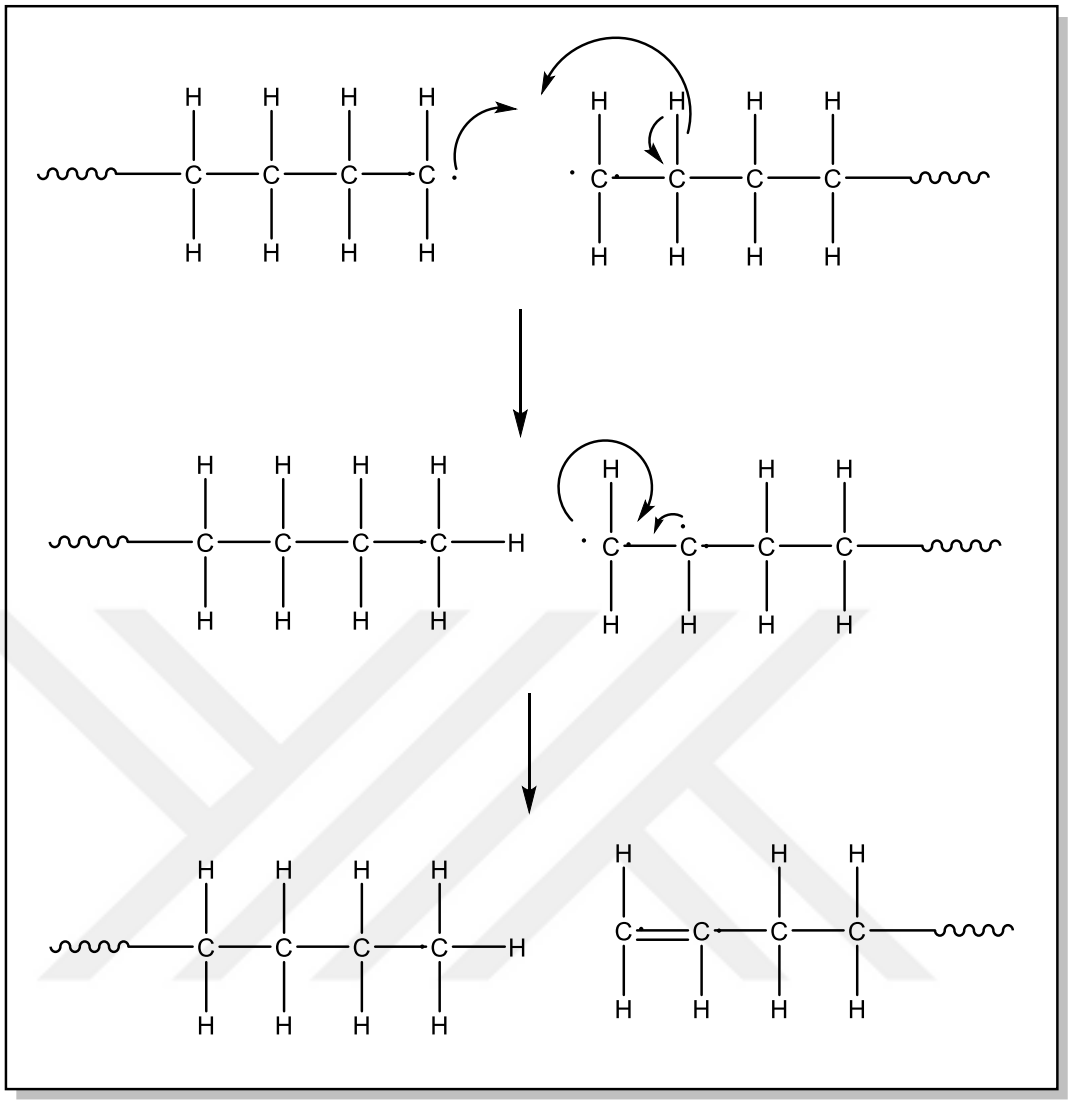

Figure 2.5. Termination step of LDPE by disproportionation.

Chain Transfer: Chain transfer is the process in which the free radical on a polyethylene chain is terminated by transferring to another molecule where further chain growth will occur (Figure 2.6).

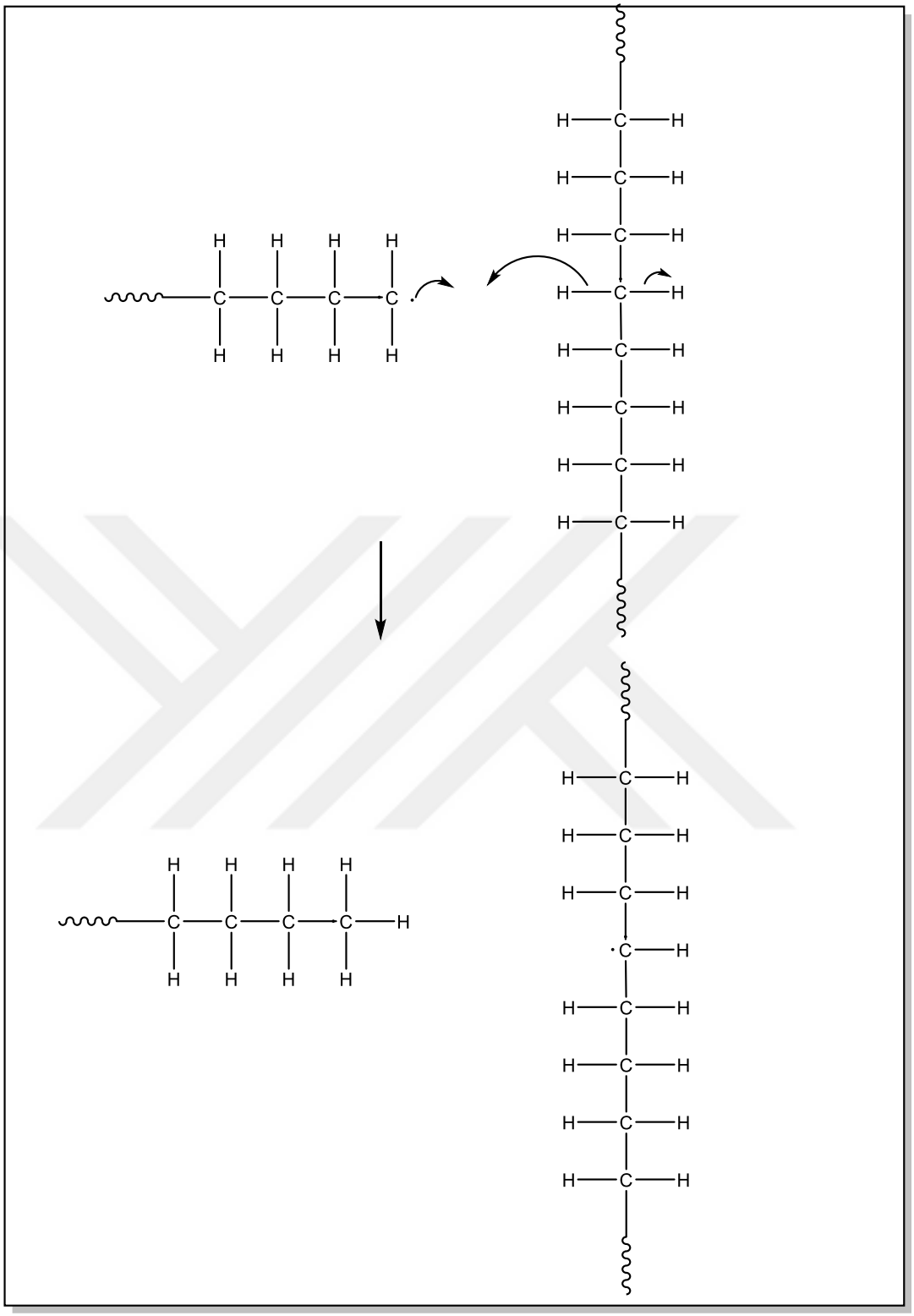

Figure 2.6. Termination step of LDPE by chain transfer (1).

When a new chain begins to form from the middle of the chain, a branched polyethylene occurs (Figure2.7).

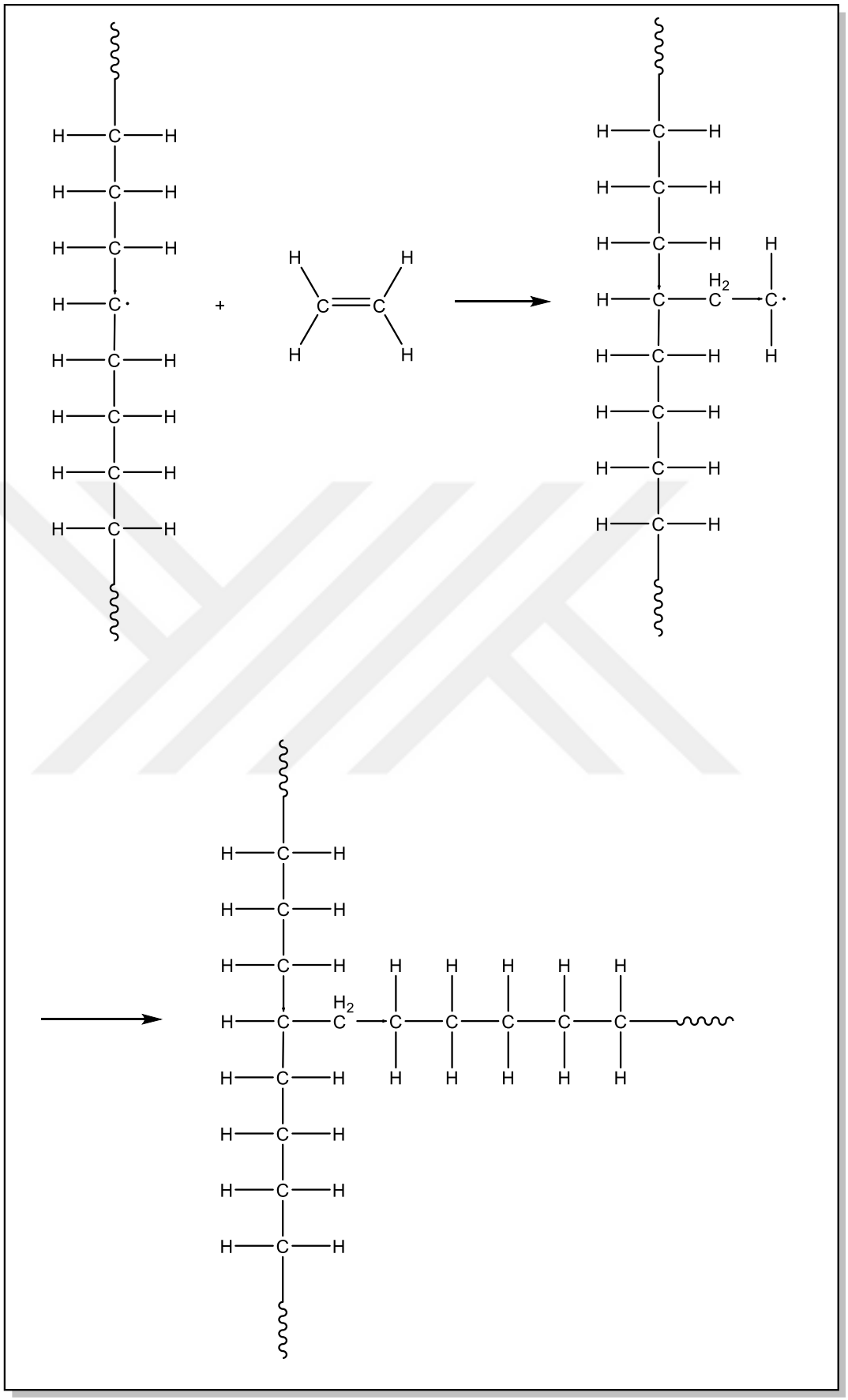

Figure 2.7. Termination step of LDPE by chain transfer (2).

The density of HDPE varies between 0.94-0.97 g/cm^3. With little branching HDPE has great crystalline region and therefore opaque and hard structure (Soganciogl u et al., 2017). Usage areas include shockproof tanks, packaging materials, pipes, etc. Keeping the branching under certain levels is achieved by special catalysts (eg Ziegler-Natta catalysts) and reaction conditions (Beşergil et al., 2008). HDPE was produced at lower pressures by using a Ziegler catalyst (Figure 2.8).

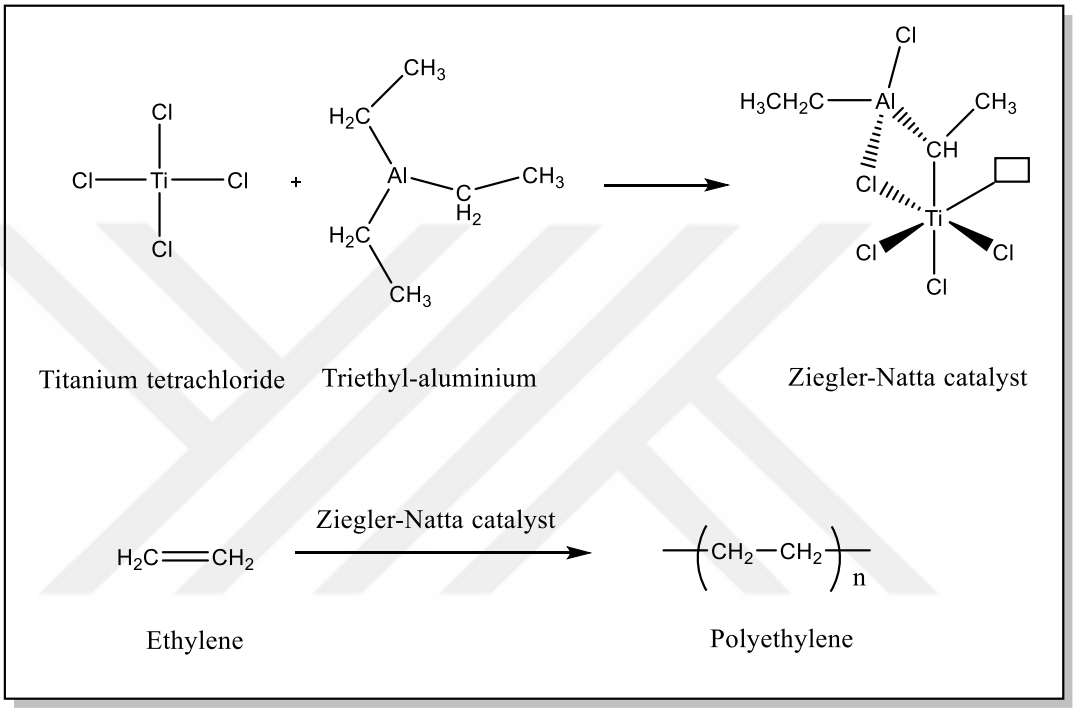

Figure 2.8. Production of HDPE.

2.2. Conductivity

Conductivity is the measure of electrical conduction and indicates the ability of the material to transport current. Materials can be classified as conductors, semiconductors and insulators. Conductors have over 10^2 S/cm conductivity values, semiconductors have between 10^2 S/cm and 10^{-8} S/cm conductivity values and insulators have less than 10^{-8} S/cm conductivity values (Sharaf, 2020). Metals are the most conductive materials and wood, ceramic and most of the polymers are the insulator materials (Figure 2.9).

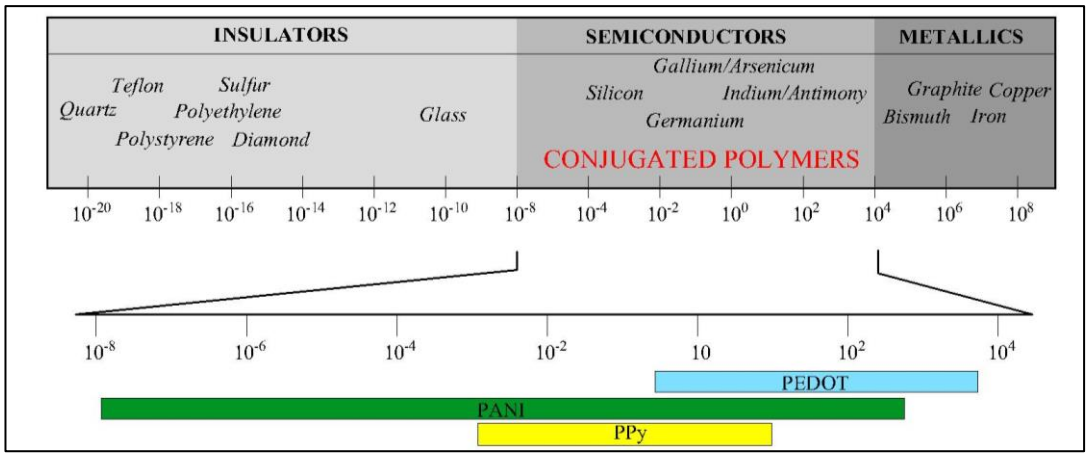

Figure 2.9. Scheme of electrical conductivity values of materials.

Electrical conduction occurs by the migration of ions or electrons. Migration of ions does not happen considerably in most covalent and ionic solids such as halides and oxides. In contrast, atoms tend to be fixed mainly in lattice locations and can only move through crystal defects. The ionic conductivity becomes significant at high temperatures, where the defective parts are very large, and the atoms have lots of thermal energy. For example, although pure NaCl is an insulator at room temperature, it has a conductivity value of ~ 10^{-3} S/cm at 800ºC. Ionic crystals, solid electrolytes, strong (liquid) electrolytes indicate ionic conduction. The conductivity of all materials except metals depends on temperature (A.R. West, 1987).

Electronic conductivity depends on the migration of electrons or their corresponding vacancies. Electronic structure of conductors and semiconductors can be explained by band theory.

2.2.1. Band Theory

The electrons of an atom are in the orbit of the atom. Each of the orbitals corresponds to its energy level. Electrons are in these energy levels (1s, 2s, 2p…). When two identical atoms are brought close to each other, their outer orbitals begin to overlap results in formation of two molecular orbitals. One of the molecular orbital is called ‘bonding’ with lower energy and the other one is called ‘antibonding’ with higher energy. For example, a metal composed of N atoms, each atom contributes

orbitals and the result is a band that contains N closely spaced energy levels (A.R. West, 1987).

The electrons in the valance band are responsible for electrical conductivity and chemical bonding. Bonding orbitals energy band is valance band and the antibonding orbitals of the energy band is conduction band as shown in Figure 2.10. Electrons in the valence band are excited by the applied energy and they are transferred to the conduction band. There is a gap (Eg) between valance band and conduction band. In insulators, the band gap between the valence band and the conduction band is larger than 3 eV so electrons cannot move from valance band to conduction band but in metals there is no band gap (Taherian, 2018).

Semiconductors have similiar structure at 0 K as insulators, but the band gap is much smaller in semiconductors. Electrons can excite from valance band to conduction band by reasonable thermal or optical energy. For example, at 300K a semiconductors electron (Eg=1eV) will excite to the conduction band, but an insulator with Eg = 10 eV will have almost no such excitations (Streetman et al., 2016).

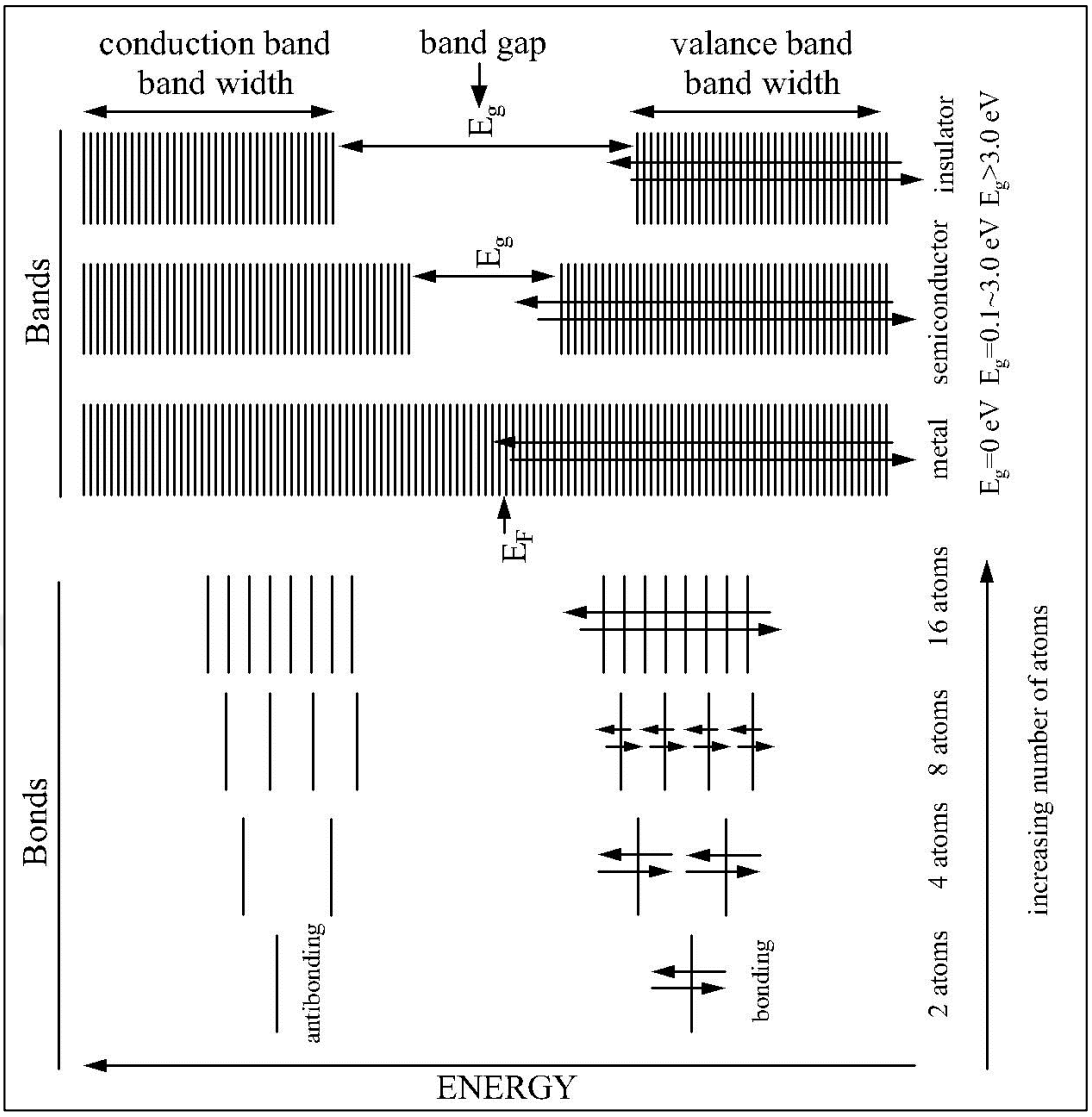

Figure 2.10. Schematic representation of bonds and bands.

2.3. Conductive Polymer

In the past, organic polymers are considered as excellent insulators which provide wide applications. The term conductive polymer emerged with the discovery of the conductivity of polyacetylene by Hediki Shirikawa, Alan Macdiarmid, and Allan Heeger in 1977 (Hideki Shirakawa et al., 1977). Following this invention, conductive polymers such as Polypyrrole, Polyaniline and Polythiophene took their place in the literature until the 1980s. Conductive polymers are classified in two different groups as extrinsic and intrinsic. Extrinsically conducting polymers are polymers that become conductive after the conductive agent (acetylene black, graphite, metal powders…) is added. Intrinsically conducting polymers have conjugated π-

electron systems to support electrical conduction without added conducting particles. Typical examples of ICPs are polyacetylene, polypyrrole, polyaniline, polythiophene. Electronic conductivity proceeds by transportation of electron from one polymer chain to another one in ICPs. Movement of electron between chains are called hopping (Kondratiev & Holze, 2021).

2.3.1. Doping

Conjugation alone is not sufficient for a polymer to be conductive. In 2000 Shirakawa, MacDiarmid and Heeger were rewarded by Nobel Prize that polyacetylene doped with bromine has a conductivity dramatically higher than pristine polyacetylene (Heeger, 2001). Doping is accomplished by reducing or oxidizing a polymer with conjugated π bonds with a suitable reagent to prepare conductive polymers (Kondratiev & Holze, 2021). Conjugated polymers have narrower band gaps and doping changes their band structure. Doping and undoping (de-doping) are reversible processes that chemical nature of the polymer do not change. Any conductivity value between the undoped and the doped form of the polymer can be obtained by controllably adjusting the doping level (Mishra, 2018).

The withdrawal of electrons from the structure (oxidation) is called p-doping, and the introduction of electrons from the outside into the chain structure (reduction) is called n-doping. In doping process, dopant ions are added which stabilize the charge on the polymer backbone by forming quasi-particles such as solitons, polarons and bipolarons (Kondawar & Patil, 2017).

Breakage of the double bond and formation of the positively charged radical on the polymer chain occurs by oxidation of a polymer with conjugated л bonds. These charge carriers on the polymer chain in conductive polymers are defined as polarons or radical cations. Then, after treatment with dopants again, it takes one more electron from the radical in the polaron to produce bipolarons. In linear conjugated polymers like Polyacetylene due the degeneracy of π electrons, charged ions, that are independent of one another, can move along the chain. The combination of separated charged ions are called a soliton. Depending on the dopant used, solitons can be negative or positive. New localized electronic states are formed in the middle of the

energy gap with soliton formation (Mishra, 2018). Thus, solitons, polarons and bipolarons that occur on the polymer chain settle into forbidden energy levels and give conductivity to the polymers as shown in Figure 2.11.

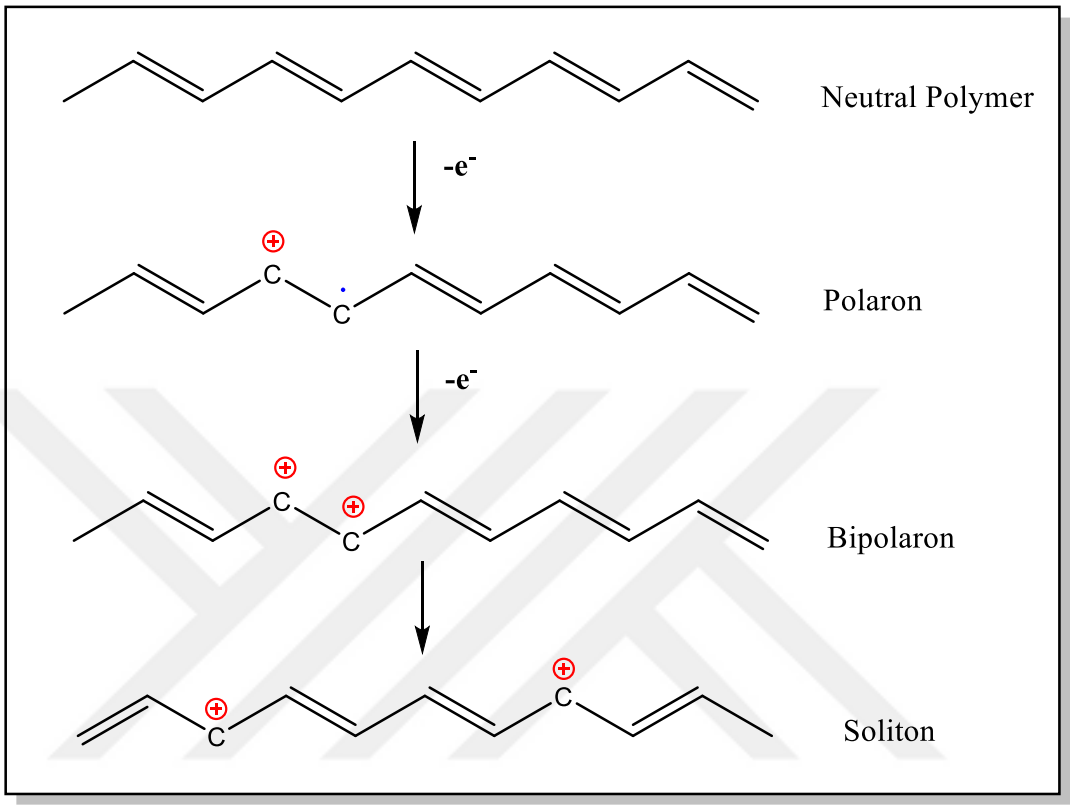

Figure 2.11. Schematic representation of polaron, bipolaron and soliton formation in polyacetylene.

Non-redox doping is the doping process without the addition and removal of electrons from the polymer backbone. For example, when emeraldine base form of polyaniline is treated with aqueous protonic acids the conductivity of the polymer increases nine to ten order magnitude (María et al., 2013).

2.3.2. Polyaniline

Although the emergence of intrinsically conducting polymers was with the discovery of polyacetylene in 1958, the history of polyaniline is even much older than polyacetylene. In 1862, Dr. Henry Letheby has reported synthesis of “a blue substance” which is obtained by electrolysis of aniline sulfate with reducing agent. It was called "aniline black" because of the dark color used in dyeing textile fabrics.

Polyaniline (PANI) has attracted the attention of researchers due to its cheapness of monomer and ease of synthesis (Bhandari, 2017).

2.3.2.1. Structure of Polyaniline

Although polyaniline is homopolymer, its molecular structure may contain benzenoid and quinonoid, or both in different proportions (Figure 2.12).

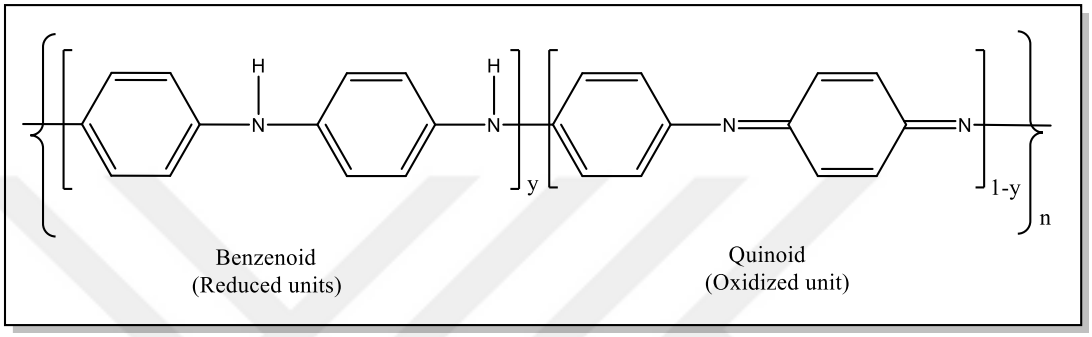

Figure 2.12. General Formula of PANI.

PANI can be found in three different redox states which are leucoemeraldine, emeraldine (salt/base) and pernigraniline as shown in Figure 2.13. Leucoemeraldine is composed of only benzenoid group which is fully reduced state. In this reduced unit H atoms are attached to the N atoms. Pernigraniline is composed of fully oxidized unit which is known as quinoid. Emeraldine consists of alternating reduced units (benzenoid) and oxidized units (quinoid) in equal amounts.

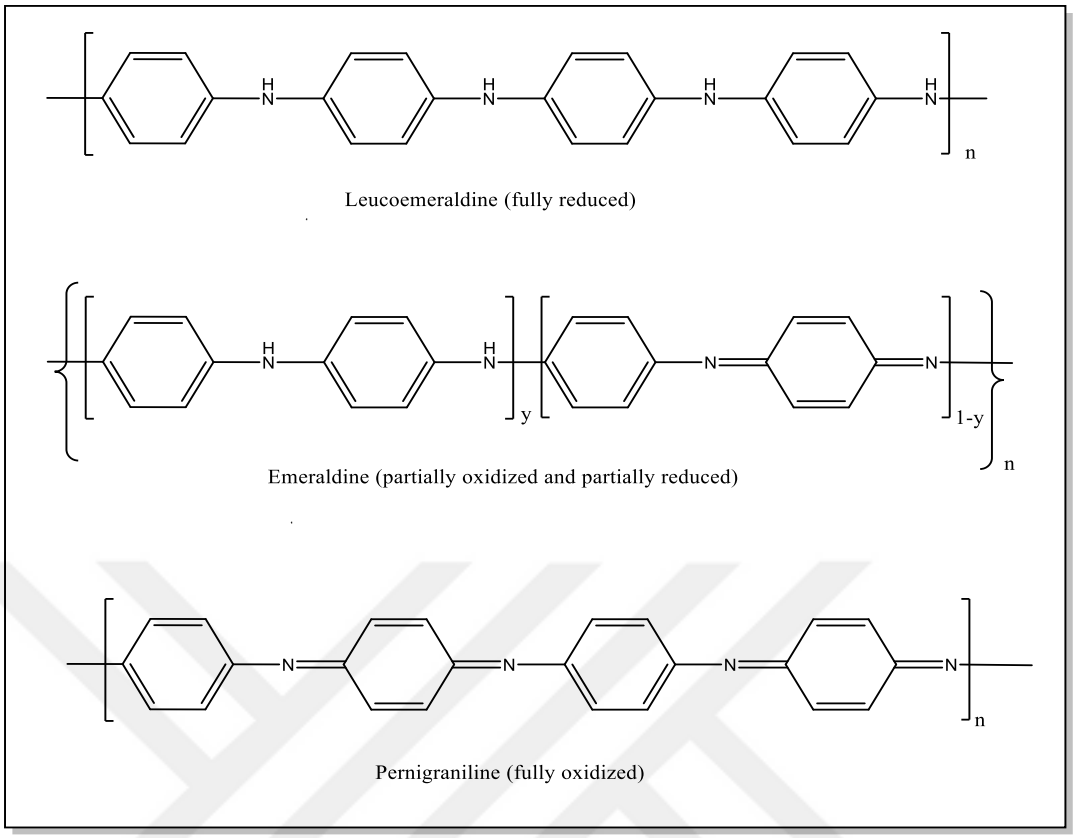

Figure 2.13. Chemical structure of polyaniline in different oxidation states.

Polyaniline has different colors in different oxidation states. Leucoemeraldine has light yellow color whereas pernigraniline is violet and both are nonconducting in nature (Bhandari, 2017). Emeraldine base (blue) is a semiconductor, becomes conducting emeraldine salt (green) after doping with protonic acids (Sanches et al., 2014). Emeraldine base and emeraldine salt forms of PANI can be modified by doping and de-doping with acid and base and the conductivity of PANI can be controlled from 10^{-11} to 10^{3} Scm^{-1} (Abd Razak et al., 2014) . While doping is a very important in PANI dopants do not chemically react with the polymer or form any chemical bonds and are located in the near vicinity of the polymer backbone (Bhandari, 2017).

2.3.2.2. Synthesis of Polyaniline

There are several methods to synthesis conductive polymers but two main methods stand out: Chemical and Electrochemical Methods. Polyaniline can be chemically synthesized by the oxidation of aniline with free radical initiators in the presence of aqueous acid. There are lots of oxidizing agents such as ammonium peroxydisulfate, ferric chloride, hydrogen peroxide, ceric nitrate and sulfate. Ammonium peroxydisulfate ($(NH_4)_2S_2O_8$) is more preferred because of its faster and easier solubility. The oxidation potential of the oxidants used to produce polyaniline should be greater than 0.7 V (Stejskal et al., 2015). Highest yield and conductivity of PANI is achieved with ammonium peroxydisulfate (E_0=1.94 V). Acidic pH conditions (pH<2.5) are required for chemical polymerization. Low acidic pH minimizes the formation of unwanted branched products (Bhandari, 2017). In synthesis of PANI, HCl and H_2SO_4 are used commonly as dopant.

By electrochemical polymerization, polyaniline can be obtained by three different techniques by applying a constant current (galvanostatic), a constant voltage (potentiostatic) and variable current and voltage (potentiodynamic) to an aqueous solution of aniline. To perform polymerisation bu using any of these techniques mentioned, three electrode (counter electrode, working electrode and reference electrode) is required. Polyaniline is produced on working electrode which can be indium tin oxide (ITO), platinumi glassy carbon (Molapo et al., 2012). The galvanostatic (constant current) method consists of a two-electrode assembly immersed in a monomer-containing electrolyte solution. A certain current is passed on the surface of a platinum foil electrode to form the PANI film. As a result of polymerization of aniline with potentiostatic method, powdered polymer which adheres weakly on the electrode is obtained. On the other hand, electrochemical oxidation of aniline can be performed with a continuous cycle between predetermined potentials. In this case, a polymeric film is produced that adheres tightly to the electrode surface. This thin film of polyaniline can then be reduced or oxidized for conductivity control. It is possible to produce a thicker free-standing, conductive films which can be peeled off from the electrode surface (S. Bhadra et al., 2009).

2.3.2.3. Polymerization Mechanism of Polyaniline

Whether polyaniline is synthesized chemically or electrochemically, the polymerization process proceeds with the formation of a radical cation.

First step is the oxidation of aniline to form a radical cation which has three resonant forms (Figure 2.14). The more reactive of these resonant forms is the one denoted by C because of substituent induction effect and its lack of steric hindrance.

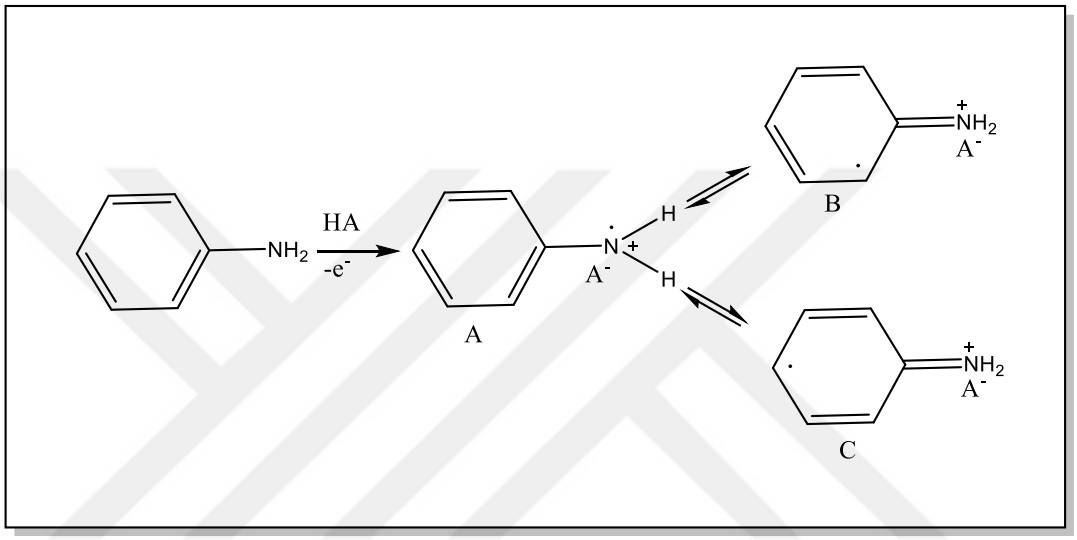

Figure 2.14. The oxidation of the aniline and its different resonant forms.

In the second step head to tail coupling reactions occur between radical cation and resonant form of it to yield dicationic dimer as shown in Figure 2.15. Finally in this step the dimer is oxidized to create cation-radical dimer.

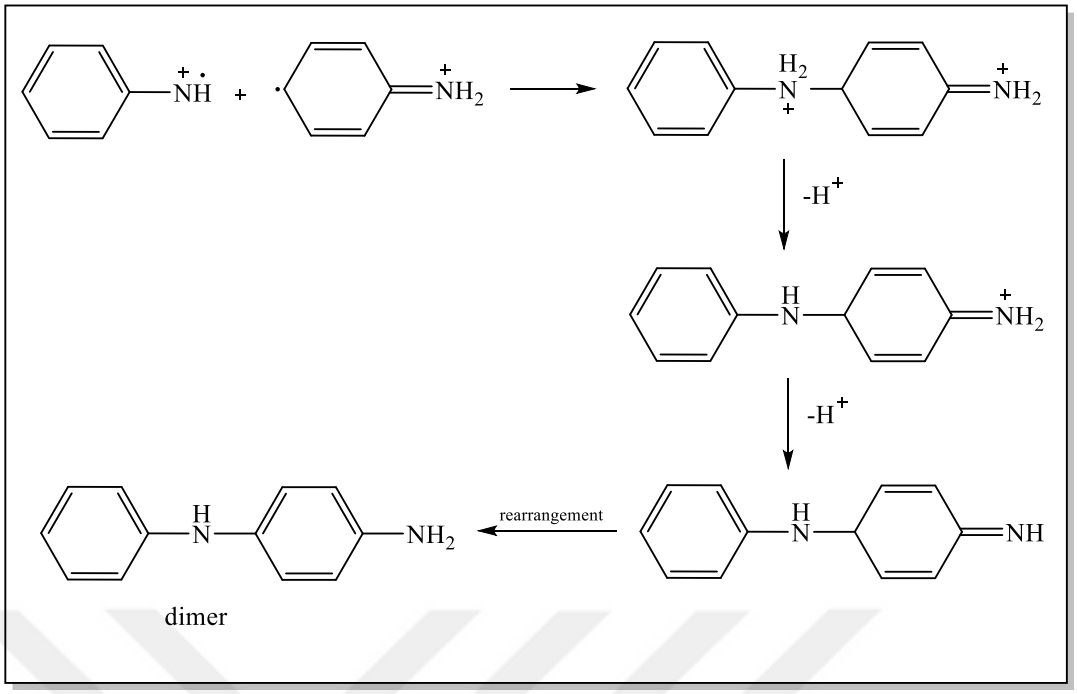

Figure 2.15. Formation of dimer.

In third step, If the formed radical prefers the radical cation monomer to react, a trimer is formed, and if the radical cation dimer is preferred, a tetramer is formed. With the continuation of these steps, the polymer is formed (Figure 2.16). Pernigraniline salt is formed as the initial product, but when all oxidants in the reaction are used up, emeraldine salt is formed (Molapo et al., 2012). Besides ideal polymerization, side reactions may occur and these are called chain defects.

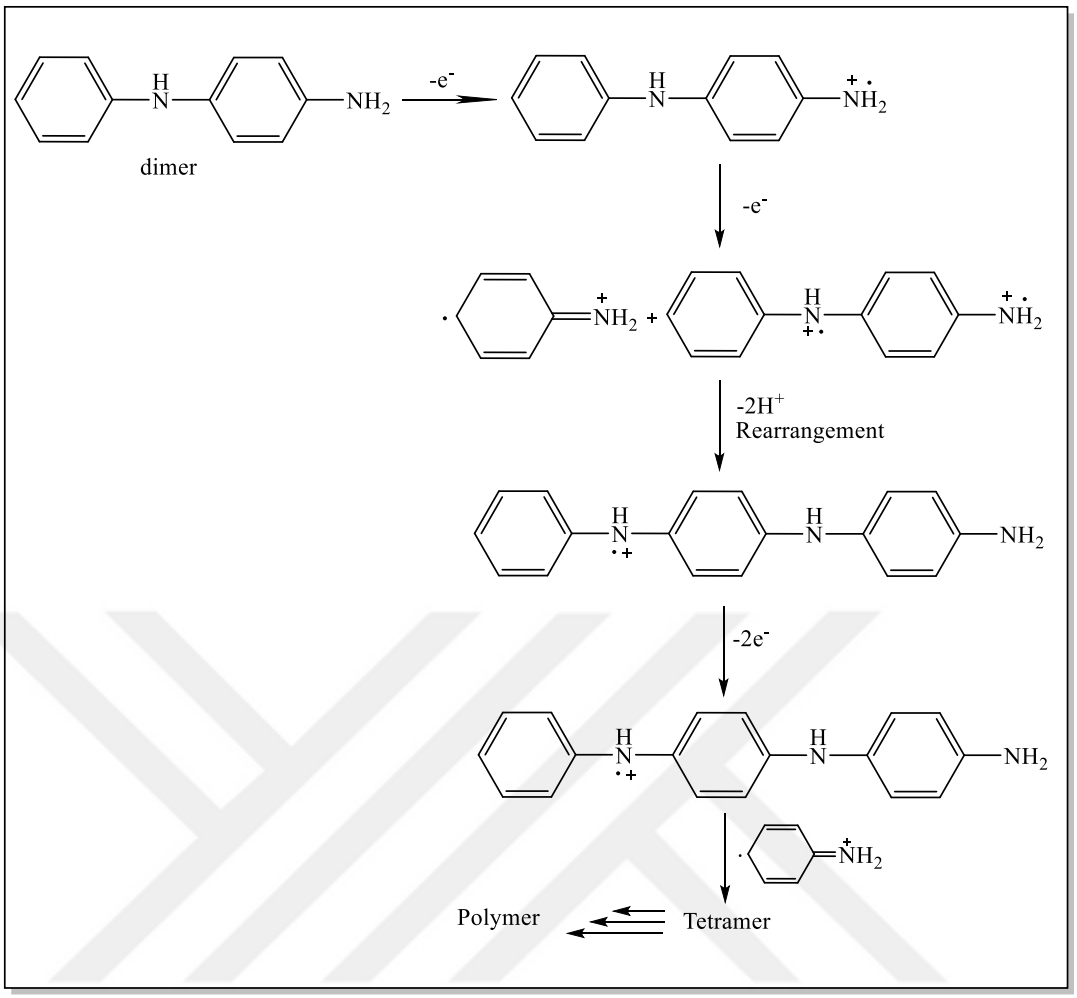

Figure 2.16. Formation of polymer.

2.3.2.4. Conductivity of Polyaniline

The electrical conductivity of PANI is one of the most important properties of interest. The conductivity of PANI ranges from 10^{-10} to 10^{2} S/cm, depending on the degree of oxidation or protonation, morphology, and synthesis methods. In the last parameter, especially the pH during synthesis and the type of counter-ions play an important role. Table 2.1. shows that the conductivity of polyaniline prepared using different acids varies considerably.

Table 2.1. Conductivity of Polyaniline Salts Produced by Oxidation of 0.2 M aniline with 0.25 M ammonium peroxydisulfate started at 20°C in the 1.2 M aqueous solutions of various acids.

Acid	**Conductivity** (S/cm)
Hydrochloric	11.9
Sulfuric	10.1
Methanesulfonic	9.7
Phosphoric	4.8
Hydrobromic	4.7
Camphorsulfonic	3.1
Picric	2.3
Citric	1.0
Succinic	0.28
Formic	0.21
Acetic	$4.2\ 10^{-2}$
No acid	4.4

Data are taken from ref (Stejskal et al., 2015)

Polyaniline generally exhibits semiconducting behavior, but in some cases its conductivity increases up to metallic conductivity. Transitions from semiconductor form to critical metallic conductivity can be achieved by doping. The formation of polaronic (cation radical) charge carriers due to doping in the polyaniline chain and its conjugated molecular structure enable effective charge transfer along the chain (Figure 2.17). As with the polyaniline base, the electronic structure of the undoped conjugated polymer is a large band gap insulator in a one-dimensional system. The conductivity is highly dependent on the degree of protonation and can range from 10^{-10} S/cm for the emeraldine base to 10 S/cm for the fully protonated emeraldine salt. The conductivity of PANI is increased up to 400 S cm^{-1} in the form of thin films from solution casting and protonation with camphorsulfonic acid (Stejskal et al., 2015).

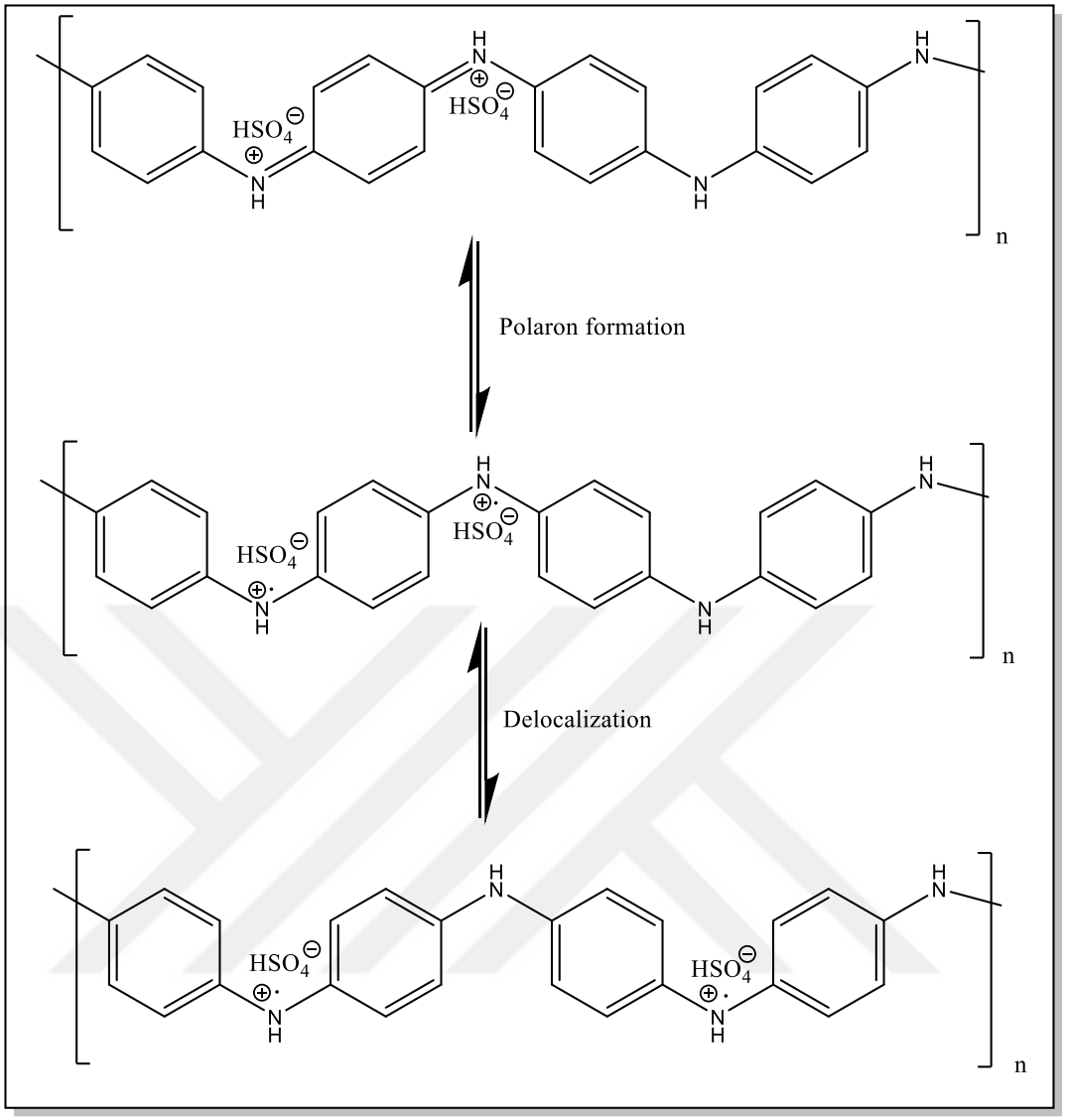

Figure 2.17. Polaron formation in PANI.

In addition to the electronic conductivity of the protonated emeraldine form, its ionic conductivity should also be considered. In this structure, there is one acid molecule per two aniline units. Acids interact with the imino group and provide a high level of conjugation. Interaction between the anion of the acid and polaron balances the positive charge. At the same time, the relatively free proton of the acid provides the proton conductivity to the material. The transportation of proton in a polymer takes place by hopping mechanism. Consequently, the emeraldine salt is a mixed conductor, and electrons and protons are simultaneously charge carriers. The conductivity of PANI is determined, as a rule, in the dry state. The increase in conductivity with increasing ambient humidity indicates that ionic conductivity may also have an important contribution. However, in many applications such as batteries,

biomedicine or corrosion protection, this polymer can also be used directly by immersion in an aqueous medium. Under these conditions, it has been suggested that the conductivity of PANI may be higher due to increased proton mobility in the aqueous medium and better contact between the metallic islands (Stejskal et al., 2015).

2.3.2.5. Superiority of PANI

PANI is a thermally stable, processable, and highly conductive polymer. Aniline monomer is cheaper than monomer of other conductive polymers. Besides the ease of synthesis of PANI, its electrical properties can be controlled reversibly by doping and protonation (S. Bhadra et al., 2009). In addition to its adjustable redox behavior, it has many applications such as gas sensors, electromagnetic shielding, supercapacitor and biosensor, owing to its wide conductivity range and nanostructured morphology (Bhandari, 2017).

2.4. Polymer Blends

Polymers have gained importance in many different industrial applications such as automotive, aircraft, packaging and electronics in recent years. Mechanical, thermal, morphological and rheological properties of polymers have been an important research area for many researchers. Methods such as adding fillers or blending are used to improve the mechanical properties of polymer materials or to obtain polymers with new properties (Kuleyin et al., 2022). Polymer blends are mixtures obtained by combining two or more polymers that are not chemically bonded to each other but brought together by physical methods. By blending the polymers, it is aimed to obtain new materials with superior qualities in addition to the physical properties of each component. Polymer blending is a technique that is easily applied without the need for complex chemical processes such as polymerization and provides the improvement of specific properties such as impact strength with low production costs (Utracki, 2002).

2.4.1. Miscibility of Polymer Blends

Polymer blends are divided into two groups as miscible (single phase) or immiscible (two or multi phases). Many of the polymer blends are immiscible. There are only few polymer blends based on miscible and partially miscible pairs. The thermal, mechanical, rheological, and other properties of blends strongly depend on miscibility (Barlow & Paul, 1981). In general, polymer blends can be fully miscible, partially miscible, or immiscible, depending on the ΔG_{mix} value. The free energy of mixing is defined by the following equation.

$$\Delta G_{mix} = \Delta H_{mix} - T.\Delta S_{mix} \quad \text{.....(2.1)}$$

ΔH in the equation represents the enthalpy change of the molten polymer mixture, ΔS represents the entropy change of the mixture at absolute temperature, and T is the absolute blend temperature (K). For miscibility, the free energy of mixing should be negative value. Due to the intertwined and complex nature of the polymer chain, the entropy change has a very small value and is often neglected. Therefore, miscibility of the polymers varies in proportion to the enthalpy change of the blend. If the enthalpy change of the mixture has positive values, the components that make up the blend act as two separate phases, forming the immiscible polymer blend. The enthalpy change is related to whether the mixture is exothermic or endothermic, and exothermic mixture indicates the miscibility of the polymers. Zero or negative enthalpy change can occur in the presence of strong hydrogen bonds, dipole, dipole and ionic interactions between the components (Şirin, 2008) (Thomas et al., 2013). The interactions between polymer pairs provide thermodynamic forces to polymers for miscibility. Single amorphous phase occurs in miscible blends which leads to single glass transition temperature (average glass transition temperature of blend components). In immiscible blends, a separate glass transition temperature appears for each blended polymer (Barlow & Paul, 1981).

Blends of immiscible polymers are frequently chosen over those of miscible polymers because they can incorporate some of the key attributes of each blend component. Optimal performance in immiscible blends is often achieved by reducing interfacial tension and enhancing adhesion between two phases. Immiscible blends can

be made more compatible by adding a functionalized polymer that can enhance particular interactions and chemical reactions in reactive systems, or by adding a third compatibilizing component (Akbari et al., 2007).

Multiphase systems occur when incompatible polymers are blended. Poor dispersion of the blends can lead to weak interface interactions between the components and the formation of unstable structures. In immiscible polymer blends, the compatibilization process is applied to establish interaction between the components and to provide adhesion at the interfaces. Compatabilizers reduce the interfacial tension and enable the blend morphology to reach a stable structure. Interfacial tension is a parameter revealed by the interactions between the components that make up the blend. The increase in interfacial tension causes the components to behave like two separate phases and to aggregate within themselves. In addition, the increase in interfacial tension results in decreased mechanical and thermal properties (Thomas et al., 2010).

2.4.2. Polymer Blend Processing

Generally, the blending methods are divided into two groups as solution blending method and melt belting method. In solution blending method, polymers dissolve in a certain or mixture of solvents and intensively stirred. The blend product is obtained after the evaporation of solvent. Solution blending is a method that is achieved quickly and without the need for huge energy consumption and has the potential to prevent unwanted chemical reactions. In melt blending method, the components are blended in molten state in extruders or batch mixers (Ezzati et al., 2017). Most widely used equipments are single-screw or twin-screw extruders for melt blending. Besides blending a pre-prepared polymer with a matrix polymer, chemical in situ polymerization method can also be used to prepare composites. In this method, a composite is formed by polymerizing the monomer on the host polymer (Pud et al., 2003).

2.5. Antistatic Behavior

Polymers such as polyolefins and polyesters are used in many fields such as textiles, packaging materials, automotive parts and electrical/electronic parts. These polymers are insulating materials however static charge can easily accumulate on such parts by contact or friction. This static charge may cause sparking and leading to damage in devices. A common approach in the electronics industry is to control the surface resistivity below 10^{10} Ω to avoid static charge accumulation. Antistatic agents are added to control the surface resistivity during the mixing process or applied to the surface of the polymers in a finishing process (Y. Li & Wang, 2012). Applying antistatic agents to the surface of the polymers are called external antistatics. External antistatics include surfactants and hydrophilic substances such as cationic, anionic, amphoteric, nonionic. Although surfactants or hydrophilic substances are inexpensive and easy to use, their antistatic effect is only achieved by adsorbed equilibrium moisture. This increases the ion mobility required for rapid discharge. Internal antistatics are added into the plastic material. They form conductive channels through the material allowing for surface-to-ground discharge or enrich at the surface to allow electron dissipation. By means electron hopping or tunnelling occur to disperse the accumulated surface charges. Internal antistatics include metal powder, metal oxide, carbon black, carbon nanotube, conductive fibers and intrinsically conductive polymers.

Antistatics have functional groups which may interact with polymers functional groups. Interaction reduces the static charge accumulation. Some functional groups are given in Table 2.2.

Table 2.2. Functional groups in antistatics.

Antistatic Type	Functional Groups
Amine group-containing antistatics	C=O, Cl^-, NH, S=O, SOH
Carbon and graphite fibers	OH, COOH
Carbon black	OH, COOH, SO_3, ONa
Carbon nanotubes	OH
Conductive Polymers	OH, NH, COOH, Cl, Br, SO_3Na
Esters	OH, ONa, S=O, C=O
Glycols	OH

Conductive coating is an effective method to prevent electrostatic charge or to rapidly disperse accumulated charges. In the preparation of coatings, adhesion of conductive or antistatic material to the surface is required. Metallic films, intrinsically conductive polymers, polyelectrolytes, surface active ionic antistatic agents can be used for coatings. The discharge mechanisms of coatings include ionic hopping and tunneling (Pötschke & Pionteck, 2016).

The general expectation from additives is that the use of small amount is effective. Basic properties of plastics such as strength, odor or color will not be affected. Additives should be non-toxic, economic, and environmentally friendly. Sometimes additives provide additional properties such as improved strength or flexibility and special optic effects. (Pionteck, 2016). In order to obtain good conductivity by using metal powder, it is necessary to use it at high concentration, which causes the system to become heavier. Intrinsically conductive polymers such as polypyrrole, polythiophene, polyaniline can contribute the matrix conducting property. Conductivity can be controlled by varying the concentration of additives (Y. Li & Wang, 2012).

2.6. Literature Review

Polymers are extensively utilized in numerous industries due to their exceptional chemical stability, affordability, ease of processing, and tolerance to high temperatures. Due to their outstanding qualities, PE and PP have been utilized as

blends in the production of materials for many years (Saltan et al., 2023). It is possible to give common polymers superior properties by preparing conductive polymer blends. Although conductive polymers have organic components like other organic insulator polymers, they are often not thermoformable. Conductive polymers have high electrical conductivity property but do not exhibit mechanical properties similar to other commercially available polymers. Conductive polymers are easy to process and disperse uniformly in organic solvents. When the conductive polymer and polyolefins are mixed, a new polymer present exceptional mechanical and processing properties with controlled conductivity level. Today, polymer materials have many application areas (Kumar et al., 2017). The use of conductive polymer blends are seen especially in batteries (Sivakkumar et al., 2009), optoelectronic devices (Dey & Kar, 2019), sensors and capacitors (Romero et al., 2020), electromagnetic radiation shielding (Moučka et al., 2011), antistatic coatings, electrochromic devices (Yildirim et al., 2008). In this study, we aimed to give polyethylene antistatic properties by doping it with a small amount of polyaniline. The studies carried out in recent years on obtaining new polymers by mixing commonly used polymers with conductive polymers are summarized here.

Omastova et al. investigated the influence of polypyrrole (PPy) amount in the PP/PPy, PE/PPy and PMMA/PPy composites on their conductivity. They prepared composites according to the chemical oxidative method. Depending on PPy content they obtained conductivitiy values from 10^{-11} to 1 S/cm. They also investigated the effect of processing on conductivity so they prepared PP/PPy blends with extruder at 170^{o}C. The conductivity value of mechanical mixing of PP/PPy was seven order lower than PP/PPy composites prepared by chemical oxidative method (Omastova et al., 1996).

Dey and Kumar prepared PMMA/PPy blends by chemical oxidative method using varying amounts of PMMA. Although PMMA is an insulator, all blends were in the semiconductor band due to the conductive nature of polypyrrole. Even though PPy has low photoluminescence emission efficiency, high PL intensity was achieved in PPy-PMMA blends. The PL emission intensity of the blends increases as an energy transfer took place from the donor PMMA to the acceptor PPy, which increased the emission intensity of PPy. Thus, it was stated that by adjusting the amount of PMMA

added to the PPy matrix, the PL intensity of the blend can be adjusted and the blend can be used as a promising material for optoelectronic devices (Dey & Kar, 2019).

To protect rubber againts oxidative aging, during the manufacturing process organic compounds were added to natural or synthetic rubber mixtures known as antioxidants. Abdelwahab et al were prepared polyfuran and polythiophene (Pth) blend by mechanical mixing to evaluate as antioxidants for styrene butadiene rubber (SBR) mixes. Polyfuran, polythiophene and their blends were incorporated in SBR mixes. Rheological and mechanical analysis were revealed that blends are efficient antioxidants for SBR mixes. Presence of heteroatoms with lone pair of electrons and conjugated system of these polymers make them good candidate for antioxidants (Abdelwahab et al., 2011).

Erdoğan et al prepared conductive Pth/polyethylene terephthalate (PET) composite fibers by in situ chemical polymerization method. Composite fibers with the lowest surface resistance of 80.0 kΩ at 5.7% PTh content were obtained. To examine the electromagnetic wave shielding properties of conductive composite fibers, the electromagnetic shielding efficiency (EMSE) of the composite in the radio and microwave frequency range were measured and they observed that the shielding efficiency decreased with the increase in frequency. They stated that PTh/PET composite fibers could not be used effectively as electromagnetic wave shielding but could be used as an electrostatic charge dissipation material (Erdoğan et al., 2012).

Zhang et al. prepared blends of conductive polymers by melt processing. The blends are composed of three components: Low-density polyethylene (LDPE), PANI doped with dodecylbenzenesulfonic acid (DBSA), and ethylene/vinyl acetate copolymer (EVA). For the PANI- DBSA/LDPE/EVA ternary blends with 2 and 20 weight percent PANI- DBSA, respectively, it was up to 10^{-9} and 10^{-5} S/cm (Zhang et al., 2004).

By melt blending in a torque rheometer, Oliveira et al. (Oliveira et al., 2016) prepared blends of; high-density polyethylene (HDPE), linear low-density polyethylene (LLDPE), and polyaniline (PANI) containing 5, 10, 15, 20, and 40

weight percent of polyaniline. The conductivity value increased to $3.7x10^{-6}$ S/cm by the addition of 40 weight percent of polyaniline.

Conductive polymers are very effective EMI shielding materials. Rashid et al. added PANI and NiFe nanoparticles to NBR rubber to obtain a material with highly flexible electromagnetic shielding properties. A shielding efficiency of 52 dB was achieved with a 0.5 mm thick composite film because of combined synergetic effect of PANI and NiFe nanoparticles. Maximum conductivity value of 167 S/cm was obtained from the 30% PANI loaded composite (Rashid et al., 2023).

In another study, flexible PET/Pani composite paper was prepared with bending durability and electromagnetic shielding performance was examined. In situ polymerization method is used to obtain PET/Pani composites. Maximum conductivity of 0,78 S/cm was obtained according to the reaction time. Electrical conductivity of composites were increased with polymerization time. They have achieved an effective shielding performance of up to 23.95 dB by coating PANI with a thickness of 0.29 mm on PET fibers. They stated that EMI Shielding remained at 99% even after the long-term cycle test of bending deformation. They also stated that this material can be used in advanced, smart and flexible electronic devices (Y. Zhang et al., 2020).

Novak et al have presented the electrophysical, mechanical and rheological properties of polyethylene compositions filled by polyaniline, multiwall carbon nanotubes and copper plate graphite. They stated that there is a decrease in specific electrical volume resistivity with an increase of the filler content up to 10 % vol. for compositions filled by CPG and 15 % vol. for compositions filled by MWCNT and PANI occurs at the percolation threshold. They noted that increasing the filler content by up to 30% by volume resulted in a decrease of tensile strength and relative elongation at the stretching for CPG and PANI filled PE compositions and a small increase in tensile strength for MWCNT. The melt flow index of PE/PANI and PE/MWCNT decreased but for PE/CPG increased (Novak et al., 2019).

In another study, blends of linear low-density polyethylene (LLDPE) and nanorod-polyaniline (NR-PANI) were prepared via extrusion. The content of

polyaniline in the blends was determined as 5, 10, 15 and 20 wt%. The conductivity of the blends increased with the addition of polyaniline. The highest conductivity value of 1.93 10^{-14} S cm^{-1} was obtained from a blend of 20wt% polyaniline. The blends were characterized with FTIR, XPS, ESR, XRD and DSC. The blends showed characteristic vibrational bands of both LLDPE and NR-PANI but they did not exhibit any chemical interaction. The crystallinity of LLDPE decreased as the amount of polyaniline in the blend was increased. The tensile strength and elongation at break of LLDPE decreased (due to a lack of interfacial adhesion between the NR-PANI and LLDPE) while the young's modulus increased with higher loading of polyaniline. The blends showed very good free radical scavenging capacity so they could be used as antioxidant packaging materials (Nand et al., 2012).

Zhu et al prepared the acrylic ester grafting epoxy(A-g-EP)/PANI composites containing 3%, 6% and 12% polyaniline by in situ polymerization method. To investigate the antistatic property of composites, they measure the surface resistivity. The surface resistivity of the composites of A-g-EP, PANI (3%)-A-g-EP, PANI (6%)-A-g-EP, and PANI (12%)-A-g-EP was 1.6×10^{11}, 1.2×10^{11}, 1.1×10^{7}, and 2.4×10^{5} Ω, respectively. For anti-electrostatic materials, coatings with a surface resistance less than 1.6×10^{9} Ω are considered. According to this information, they stated that composites containing 6% or more polyaniline will show antistatic properties. PANI-A-g-EP composites also exhibited anticorrosion property due to the electron transmission and passivation catalysis (Zhu et al., 2018).

Saini and Choudhary were investigated the electrostatic charge dissipation (ESD) and electromagnetic interference (EMI) shielding performance of the polyaniline based composites in the presence of poly(acrylic acid) (PAA) and polystyrene sulphonic acid (PSS). PSS and PAA are polymeric dopants and PANI was synthesized in the presence of these dopants by in situ polymerization method. The cotton fabrics were coated by immersion in PANI/PSS and PANI/PAA dispersions. In ESD analysis %10 cut-off decay time should be less than 2.0 s According to the ESD analysis composites showed rapid dissipation of static charges. In addition moderate EMI shielding performance was obtained with effectiveness value of -5,2 dB and -5,7 dB for PANI/PAA and PANI/PSS coated cotton fabrics, respectively (Saini & Choudhary, 2013).

Das et al prepared polyaniline- polystyrene- graphene oxide nanocomposites by the solution casting method. It is discovered that the composite (PANI-PS-GO) has an EMI SE of 40 dB. The results obtained suggest that the polymer nanocomposite system that has been proposed has great potential as an effective substitute for new EMI shielding materials in the X-band frequency region (Das et al., 2023).

Yu et al prepared a waterborne polyurethane/polyaniline composite and measured its resistance to corrosion. As evidenced by its capacity to resist immersion in 10% H2SO4 and 10% NaOH solution for 90 days without any paint flaking off, they claimed that this coating offers exceptional protection against acid and alkali resistance (Yu et al., 2024).

Polyaniline/graphene–coated polyamide6 nanofiber materials are produced through the electrospinning process by Tambakoozadeh et al. for electrochemical applications. When utilized as a separator in the cell, their specific capacitance was 423.28 F/g and their electrical conductivity was 1.02×10^{-4} S/cm. It is the conductivity value obtained when 0.5 M aniline in the polymerization process and 2 wt% graphene are added to nanofibers. As a result, the polyamide6 coated with a composite PANI/reduced graphene oxide may be suitable candidates for use in energy storage devices (Tambakoozadeh et al., 2019).

Jeevananda et al firsly utilizing xylene as the solvent, varying weight percentages of PANI functionalized c-MWNTs were combined with HDPE as the precursor master batch by the solution precipitation process. Then 20, 25 and 30 wt.% carbon black added to composite in melt mixer. According to the experimental findings, PTC intensity increased significantly and the hybrid nanocomposites with a little amount of PANI-MWNTs (0.50-0.75 wt%) had good conductivity (10 Ω) at ambient temperature (Jeevananda, 2018).

3. EXPERIMENTAL PART

3.1. Materials

3.1.1. Chemicals

Hydrochloric acid (HCl, 37%) was used as purchased from Aldrich Chemicals Co. The solution of an acid in a specific concentration was prepared using deionized water.

Ammonium peroxydisulfate (oxidant) [$(NH_4)_2S_2O_8$, 98%] was used as received from AFG Scientific.

N-methyl-2-pyrrolidinone (NMP, 99%,) toluene ($C_6H_5CH_3$, 99.5%, p-xylene (99%) from Aldrich Chemicals Co. were used as received.

Aniline monomer premium grade from Merck and low density polyethylene (LDPE) and high density polyethylene (HDPE) obtained from Petkim Petrochemical Company were used as received.

3.1.2. Instrumentation

3.1.2.1. Fourier Transform Infrared Spectroscopy (FTIR)

FTIR is a widely used technique that uses an infrared radiation beam to detect the functional groups in materials. Each bond in the molecule's absorption of IR radiation was evaluated using infrared spectroscopy, yielding a spectrum that is generally expressed as a percentage of transmittance vs wavenumber (cm^{-1}). It is necessary for a molecule to be IR active in order to identify its functional groups. A molecule having a dipole moment is said to be IR active. The covalent bond of a substance with an electric dipole absorbs energy from the IR radiation when it interacts with it, causing the bond to oscillate back and forth. As a result, IR radiations must be absorbed by the oscillation, which changes the net dipole moment of the molecule. It should be emphasized that since each bond in a molecule has a unique natural

vibrational frequency, different IR radiation (frequency) will be absorbed by different bonds in the molecule(Khan et al., 2018). For characterization of functional groups of molecules, Perkin Elmer-Spectrum BX FTIR spectrophotometer was used. FTIR spectra were recorded by preparing KBr pellets between 4000 and 400 cm^{-1}.

3.1.2.2. Thermogravimetric Analysis (TA) / Differential Thermal Analysis (DTA) System

Thermal analysis (TA) is the ability to evaluate a material's reaction to heating, cooling, or holding isothermal. TA involve measuring the physical properties of that sample as a function of temperature/time while applying a controlled temperature program to the sample. In addition to evaluating a material's actual physical properties, TA is used to estimate a material's lifetime in different conditions, characterize and design the methods employed in its fabrication, and provide light on its mechanical and thermal histories. The technique known as thermogravimetry (TG) or thermogravimetric analysis (TGA) measures a polymer's mass as a function of time or temperature while the sample is kept at a specific temperature program. The graph of the changing mass percentage depending on time or temperature is called a thermogram or thermal decomposition curve. Thermal analyzes can be performed in a single stable gas atmosphere or in atmospheres containing more than one gas (Prime et al., 2009). Hitachi TG/DTA 7300 is used for TG/DTG analysis (Figure 3.1). We used this TG/DTG to measure the highest rate of decomposition, and % weight losses of polyaniline powder and the blends of polyethylene/ polyaniline. Prior to starting the TG/DTG tests, the thermal analyzer system's mass and temperature calibration were performed. For mass calibration, certified etalon (20.05 mg) was utilized. The melting points of tin and indium supplied by Exstar were utilized to perform temperature calibration.

Figure 3.1. Hitachi 7300 TG/DTA Instrument.

3.1.2.3. Differential Scanning Calorimetry (DSC)

DSC is a technique where the difference in energy inputs into a substance and reference material is measured as a function of temperature under controlled temperature program. At a particular rate heating, cooling and isothermal conditions can be applied to the sample and reference. Applications of many materials from polymers to ceramics can be made with the DSC. Evaluation of glass transition, melting temperature, crystallization temperature, kinetic studies, specific heat measurements, curing studies, calculating degree of crystallinity are the examples of DSC applications. And also MDSC (Modulated Differential Scanning Calorimetry) technique can be used to differentiate the reversing and non-reversing heat flow. Conventional DSC measures total heat flow whereas MDSC separates the total heat flow signal into two parts: Reversing and Non-reversing heat flow (Buehler et al., 1998). Melting, heat capacity and glass transition are reversing heat flow but evaporation, crystallization, decomposition, cross-linking are non-reversing heat flow. Sometimes these transitions can overlap. To separate these transitions MDSC technique can be used. In this thesis to separate glass transition temperature of polyaniline MDSC was used but for PE/PANI blends conventional DSC was used. In

order to check the accuracy of instrument, the melting points of indium provided by TA, were used. DSC analyzes were performed in TA DSC 250 (Figure 3.2).

Figure 3.2. TA DSC 250 Instrument.

3.1.2.4. X-Ray Diffraction Analysis (XRD)

X-Ray Diffraction (XRD) methods are based on the crystals' ability to diffract X-rays in a characteristic way that allows the structure of crystal phases to be studied. The angle of diffraction of X-rays varies depending on the distance between the atomic layers that make up the crystal structure. The diffracted X-rays form the diffraction pattern of that sample. Bragg explained the X-ray diffraction theories by assuming the angular distribution of the scattered rays and their diffraction from the lattice planes (Figure 3.3).

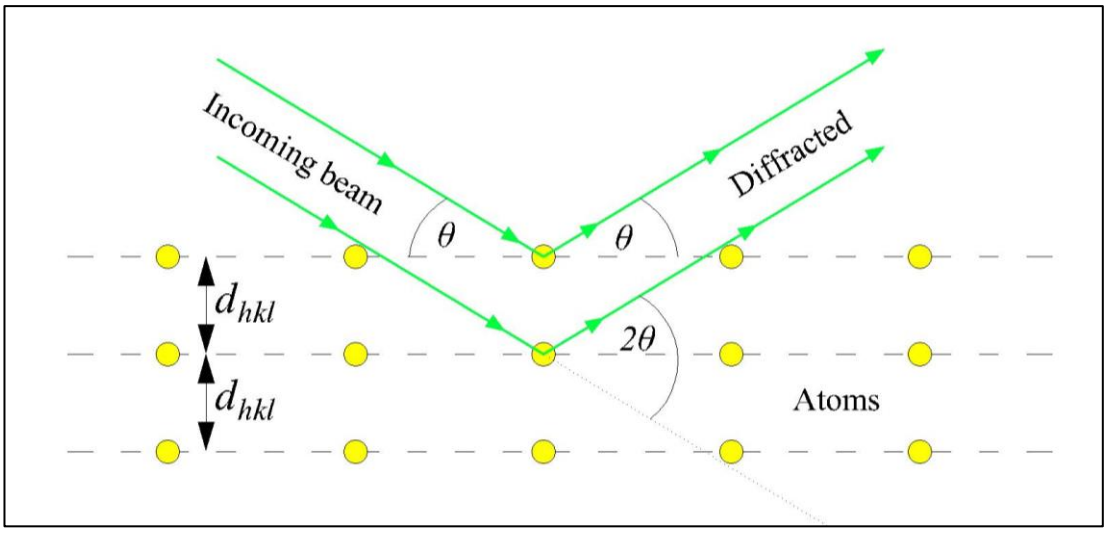

Figure 3.3. Bragg's diffraction.

$$2d \sin\theta = n\lambda \quad \text{.....(3.1)}$$

In this equation, d is the distance between the crystal planes, Θ is the angle of the incident and scattered beam, n is the degree of diffraction, and λ is the wavelength of the X-ray used (Epp, 2016). Two basic information is obtained from the X-ray diffraction pattern of any crystal: (1) diffraction angles; (2) diffraction intensities. X-ray diffraction patterns of the samples were taken by the PANalytical EMPYREAN XRD instrument (Figure 3.4). The instrument is suitable for the analysis of powder or bulk samples. For all samples the diffraction patterns were taken at a diffraction angle 2Θ from 5^{o} – 85^{o}.

Figure 3.4. PANalytical EMPYREAN XRD instrument.

3.1.2.5. Scanning Electron Microscope (SEM)

Scanning electron microscope (SEM) is used to investigate the morphology and microstructure of materials. SEM images are obtained by the interactions of electrons on the surface of the sample and the conversion of the electronic signals obtained as a result of these interactions into images. The primary electrons sent to the sample eject the electrons around the atoms on the surface and form secondary electrons. Another electron that emerges in the interaction of electrons with the surface is backscatter electrons. Backscattering electrons do not provide information about surface morphology like secondary electrons but provide information about surface composition. During the formation of secondary electrons, an electron from the higher orbit replaces the electron that is removed from the orbital. In the meantime, an X-ray

specific to that atom emerges. Element information can be obtained with this system called energy dispersive X-ray spectroscopy (EDX) (Michael Dunlap & J. E. Adaskaveg, 1997; Vernon-Parry, 2000). SEM images were taken at different magnifications to examine the morphological features of the samples used in the study. Images were obtained with the ZEISS GEMINI 500 SEM instrument (Figure 3.5).

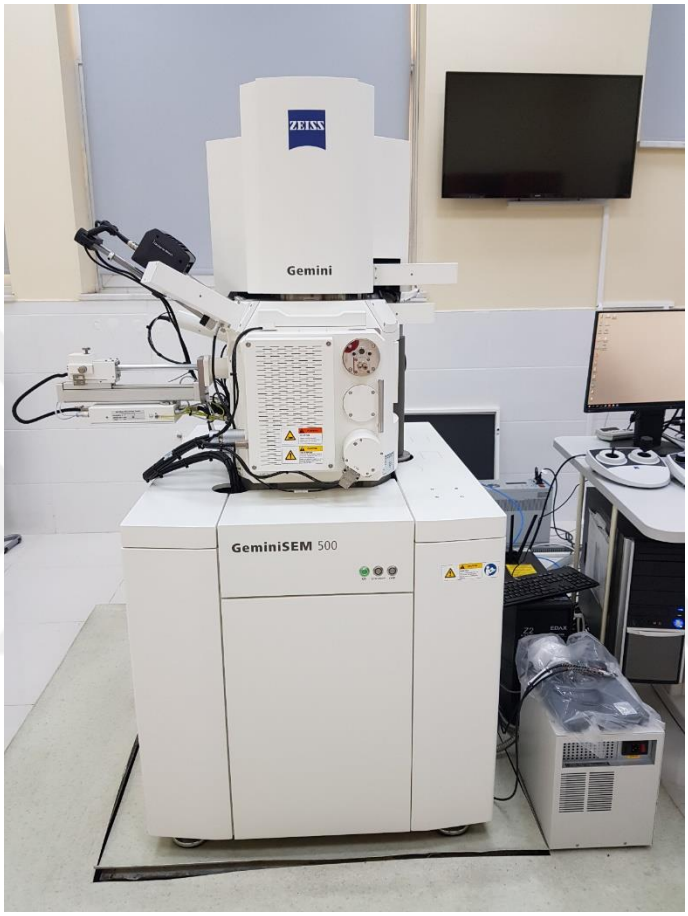

Figure 3.5. ZEISS GEMINI 500 SEM instrument.

3.1.2.6. Conductivity Measurements

Conductivity measurements are made by four-point probe technique. Four points touch the sample surface. These four points are arranged side by side with equal distance between them (Figure 3.6). Current is passed through the outermost probes 1 and 4. If the sample has resistance, there will be a voltage drop when current flows through the sample. The voltage variation is also measured via two internal probes (2 and 3) (Waremra & Betaubun, 2018). Conductivity (σ) is given by:

$$\sigma = (\frac{ln2}{\pi t})(\frac{I}{V})$$.....(3.2.)

Where conductivity (σ) in S/cm and applied current (I) is in mA, voltage in V andt is the thickness of pellet.

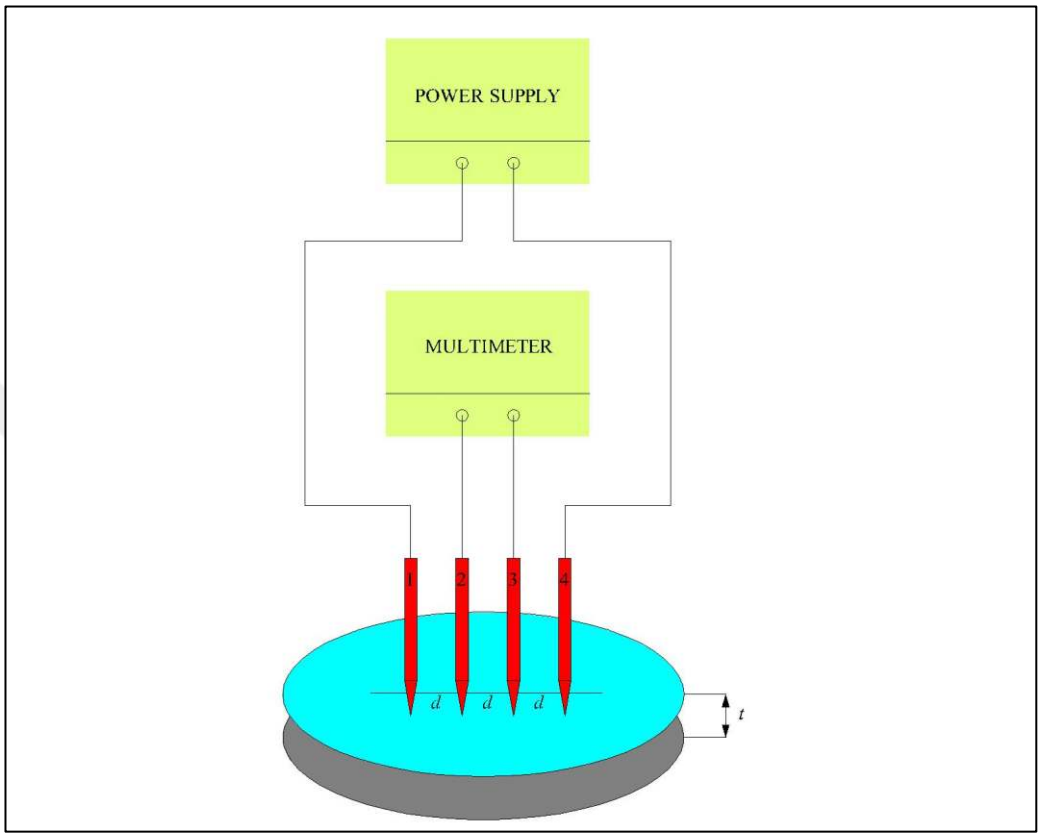

Figure 3.6. A schematic diagram of a four-point probe.

The conductivities of blends were measured with Keithley 2400 electrometer in pellet form under hydraulic pressure of 1600 kg/cm^2 (Figure 3.7).

Figure 3.7. Keithley 2400 Electrometer.

3.1.2.7. Electrostatic Charge Dissipation (ESD) Analysis

The term Electrostatic Charge Dissipation (ESD) refers to the transfer of charge between two objects at different electrical potentials, which can occur through direct contact or an induced electric field. It is a physical mechanism caused by charge imbalance. Friction between various materials is typically the cause of this imbalance of electrons on the material's surface. Recently, with the development of the electronics industry, some problems such as electrostatic charge dissipation (ESD) have emerged. Especially 60% of the damages seen in integrated circuits are caused by ESD (Hwang, 2004). In order to solve this problem, adding semiconductor materials into the materials commonly used in the industry is a good alternative to eliminate this problem. The semiconductor to be used as an additive agent should have

conductivity in the range of 10^{-6} to 10^{-11} S/cm. The simplest way to learn the materials ESD capability is to apply some charge on the material and see how quickly that charge disappears. ESD applications of blends were carried out by Static Decay Meter (model 406D), Electrotech Systems, USA) and Charge Decay Time Analyzer (JCI 155v6, John Chubb Instrument, UK) (Figure 3.8). At room temperature at different positive (3, 6 and 9 kV) and negative corona voltages (-3,-6 and -9 kV) applied to the blends surface. We determine the dissipation time of static charges accumulation on the surface of the blends.

Figure 3.8. Charge Decay Time Analyzer.

3.1.2.8. Dynamic Mechanical Analysis

Dynamic mechanical analysis (DMA) is a technique that measures the properties of materials that deform under stress. In the DMA experiment, an oscillating force is applied to a sample at a certain temperature and/or frequency and the response of the material to this force is measured. Stress is the applied force and strain is the deformation of the sample. In ideal elastic materials, when the load is removed, the material returns to its original state. Viscous behavior is the opposite of elastic behavior. Some materials like polymers show both viscous and elastic behavior called viscoelastic material (Deshmukh et al., 2020). We performed our analysis in TA Q800 DMA instrument with a ramp force rate of 1 N/min at 25^{o}C (Figure 3.9). The applied frequency was 1 Hz and tensile film clamp was used to obtain stress-strain curve.

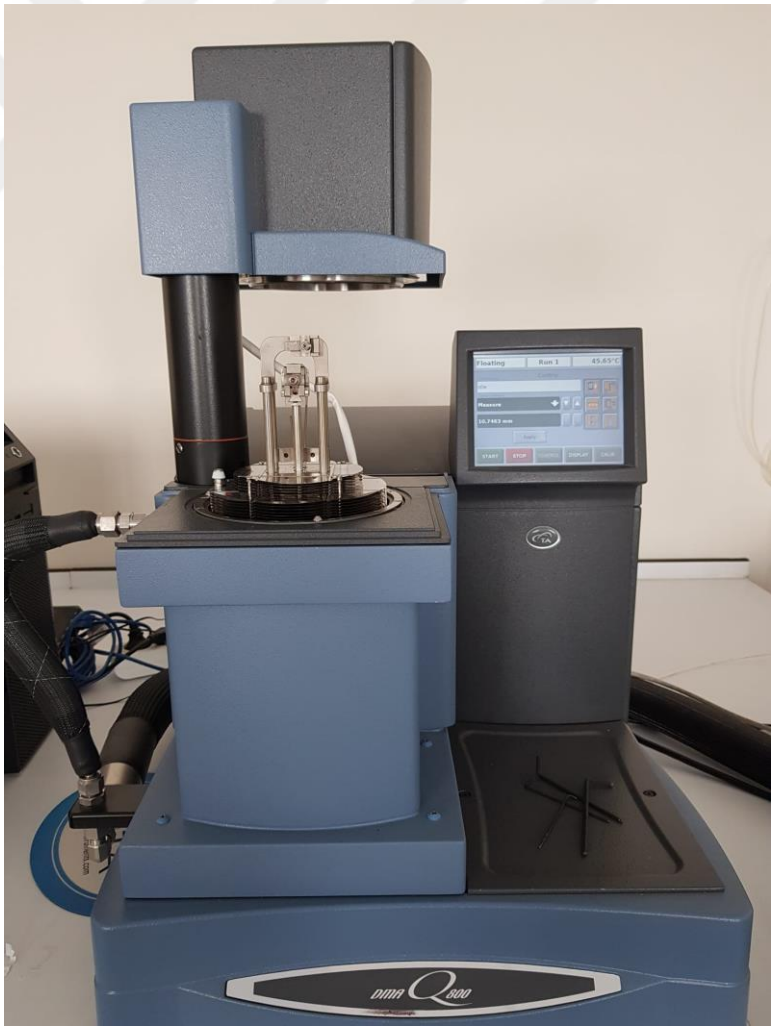

Figure 3.9. TA DMA Q800 Instrument.

3.2. Methods

3.2.1. Synthesis of Polyaniline

Polyaniline was synthesized in acidic medium by chemical oxidation of monomer. 6 ml aniline was dissolved in 200 ml (1 M) HCl in a 500 ml beaker which was kept in ice bath (0-5 °C). In a separate beaker 11,4 g ammonium peroxydisulphate was dissolved in 100 ml of deionized water. The ammonium peroxydisulphate solution was then added drop wise to the aniline solution under constant stirring (400 rpm) (Figure 3.10).

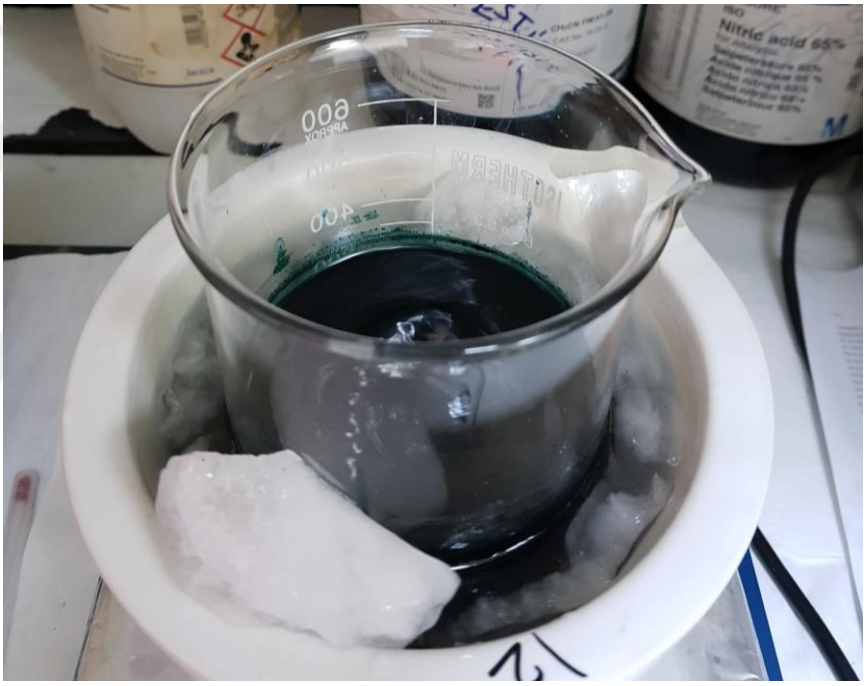

Figure 3.10. Polyaniline synthesis.

After the completion of addition, the mixture was kept overnight at refrigerator (4 °C). The greenish precipitate was centrifuged and washed multiple times with deionized water. To remove the water from powder form of PANI, the precipitate was kept in vacuum oven at 70 °C overnight (Choudhary et al., 2018). Greenish polyaniline can be seen in Figure 3.11. Polyaniline was characterized by FTIR, DSC, TGA, and XRD analysis. The results of these analysis are presented in Results and Discussion section.

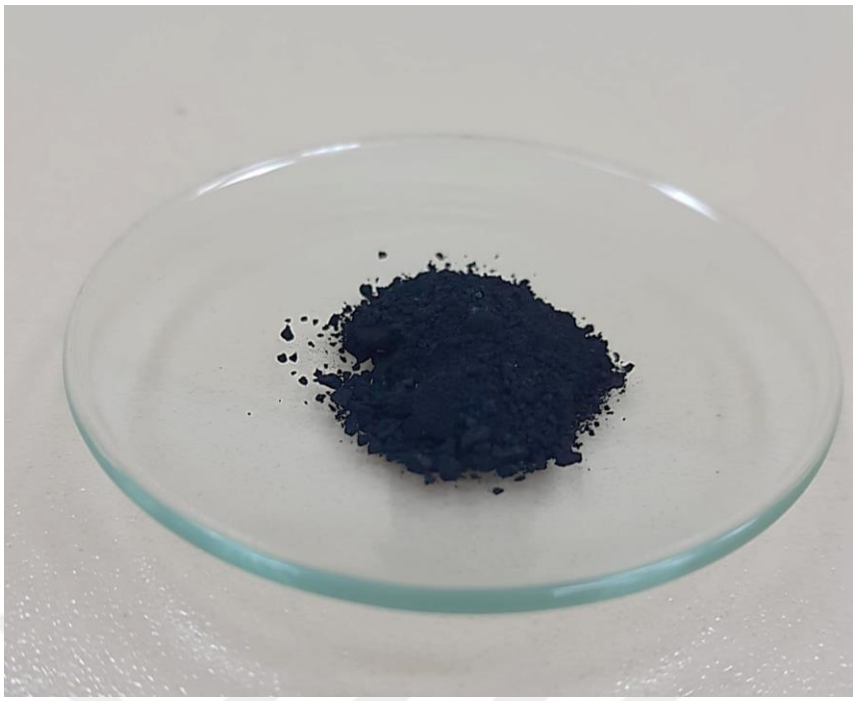

Figure 3.11. Synthesized powder polyaniline.

3.2.2. Preparation of Low-Density Polyethylene-Polyaniline Blends

The blends were prepared by solution blending method. In the process of obtaining polymer blends within this study, trial and error process was employed for selecting the solvent, determining the solvent quantity, and petri dish dimensions. Controlled experiments were conducted to identify the optimal choices. First of all, solvent selections were made in which polyaniline and LDPE can be dissolved. Polyaniline was tried to be dissolved in different solvents in ultrasonic bath. These solvents are; acetonitrile, dichloromethane, ethanol, cyclohexane, chloroform, dimethylformamide, tetrahaydrafuran, pyridine, n-hexane, n-methyl-2-pyrrolidone (NMP), and toluene. As a result of these experiments, it was observed that PANI dissolved most effectively in NMP. Experiments were conducted with varying volumes of NMP ranging from 5 to 10 ml to determine the optimal volume. It was observed that the most suitable volume was 8 ml. Toluene was employed in a magnetic stirrer at room temperature for the dissolution of LDPE. Subsequently, it was stirred in an ultrasonic bath at 50°C, yet dissolution did not occur. Later, dissolution of LDPE in toluene was achieved in a heated magnetic stirrer at 80°C. Experiments were conducted with varying volumes of toluene ranging from 50 to 150 ml to determine the optimal volume. It was observed that the most suitable volume was 100 ml. Finally,

the decision regarding the size of the petri dish for pouring the blends was made. Initially, the blend was poured into a glass petri dish with a diameter of 20 cm, but a uniform structure could not be obtained after the solvent evaporated. Subsequently, it was poured into a glass petri dish with a diameter of 10 cm, resulting in the desired uniform structure. The blends were prepared according to the obtained optimal selections as follows. 3g LDPE was dissolved in 100 ml of toluene by heating at 80°C on magnetic stirrer. 15 mg PANI was put into 8ml NMP and kept in an ultrasonic bath for 20 minutes and dissolved. Then PANI solution was added to the LDPE solution. After 15 minutes, the mixture was poured into a glass petri dish and kept for 1 hour at room temperature and then in a vacuum oven at 70°C overnight (Figure 3.12).

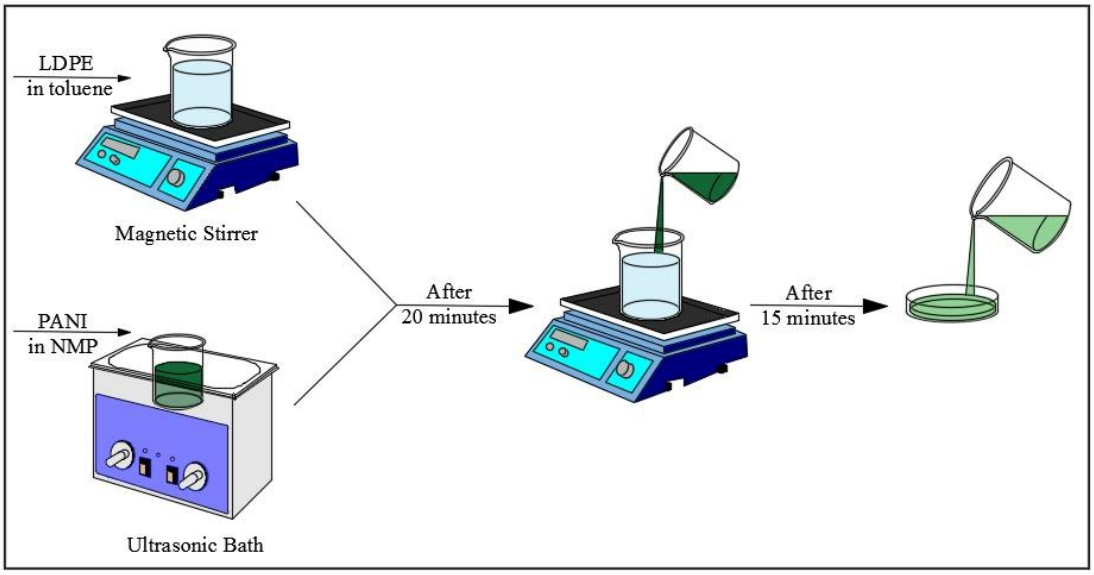

Figure 3.12. Schematic representation of the preparation of the LDPE/PANI blend.

Subsequently, the amount of polyaniline was increased to 30 mg and 90 mg, and PANI/LDPE mixtures were prepared in different proportions. Blends of low density polyethylene/ polyaniline (LDPE/PANI), containing 0,5- 1-3 wt % polyaniline have been obtained (Figure 3.13). The abbreviated nomenclature $LP_{0.5}$, LP_1 and LP_3 correspond to LDPE containing 0.5 wt%, 1 wt% and 3 wt% PANI for all blends with HDPE and PANI, respectively.

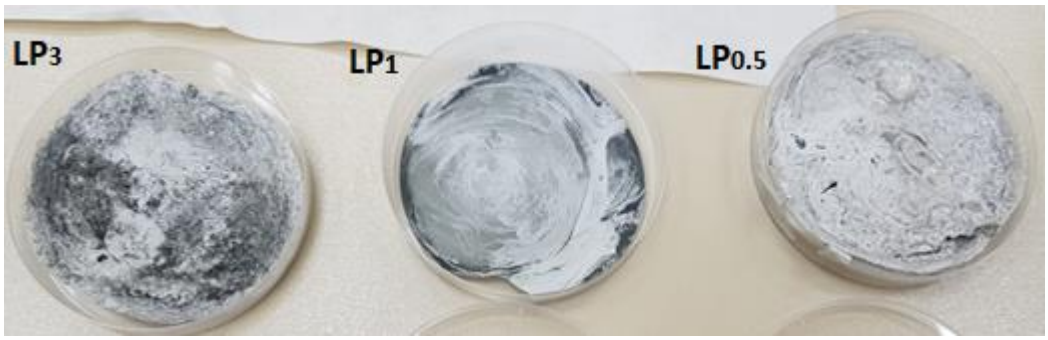

Figure 3.13. Images of LP_3, LP_1 and $LP_{0,5}$.

3.2.3. Preparation of High-Density Polyethylene-Polyaniline Blends

The blends were prepared by solution blending method. To dissolve HDPE p-xylene was chosen as solvent. 3 g HDPE was dissolved in 100 ml p-xylene by heating at 100°C on magnetic stirrer. 30 mg PANI was put into 8 ml NMP and kept in an ultrasonic bath for 20 minutes and dissolved. Then PANI solution was added to the HDPE solution. After 15 minutes, the mixture was poured into a glass petri dish and kept for 1 hour at room temperature and then in an vacuum oven at 70°C overnight. Blends of polyethylene/polyaniline (HDPE/PANI), containing 0,5- 1-3 wt% polyaniline have been obtained (Figure 3.14).

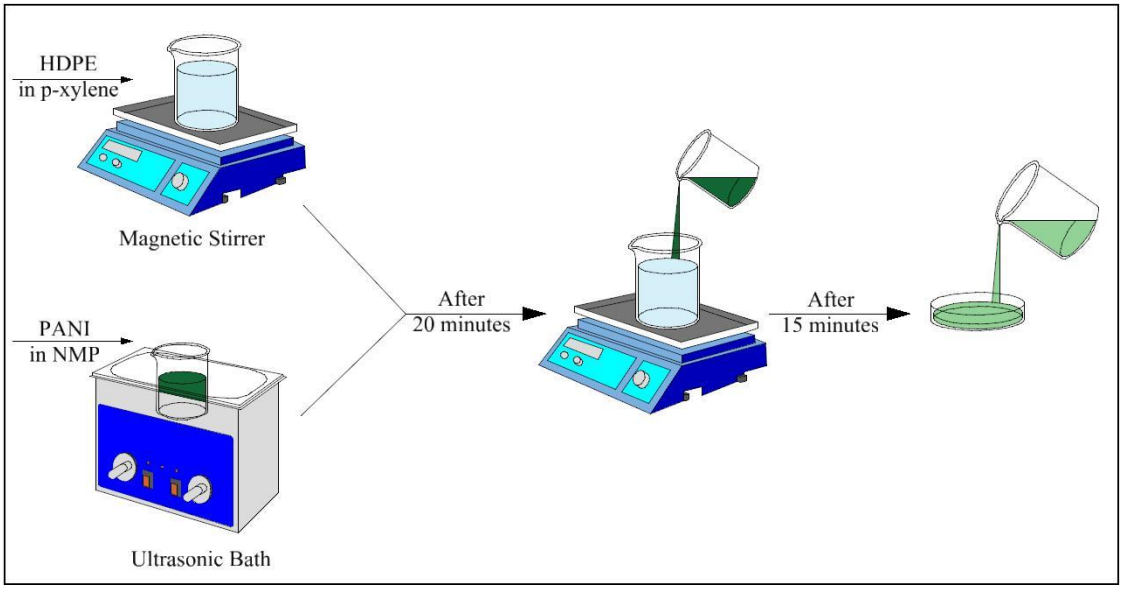

Figure 3.14. Schematic representation of the preparation of the HDPE/PANI blend.

Subsequently, the amount of polyaniline was increased to 30 mg and 90 mg, and PANI/HDPE mixtures were prepared in different proportions. Blends of high density polyethylene/ polyaniline (HDPE/PANI), containing 0,5- 1-3 wt % polyaniline have been obtained (Figure 3.15). The abbreviated nomenclature $HP_{0.5}$, HP_1 and HP_3 correspond to HDPE containing 0.5 wt%, 1 wt% and 3 wt% PANI for all blends with HDPE and PANI, respectively.

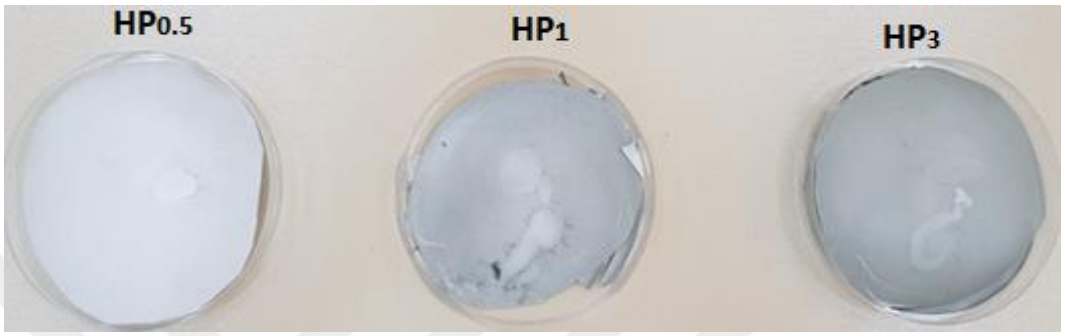

Figure 3.15. Images of $HP_{0.5}$, HP_1 and HP_3.

4. RESULTS and DISCUSSION

4.1. Characterization of Polyaniline

Polyaniline was synthesized by chemical oxidation method. Dark green color in a powder form indicates that polyaniline in salt form (conductive form) has been synthesized. Polyaniline was characterized by FTIR Analysis, Thermal Analysis (DSC and TGA), X-Ray Diffraction Analysis, Conductivity Measurement Analysis, Morphological Analysis (SEM). In this section, the results of the synthesized polymer are discussed in detail.

4.1.1. Fourier Transform Infrared Spectroscopy (FTIR) Analysis

FTIR spectra of polyaniline was recorded by preparing KBr pellets between 4000 and 400 cm^{-1}. Infrared spectra of polyaniline is presented in Figure 4.1. The characteristic bands at 3422 cm^{-1}, 2872 cm^{-1}, 1566 cm^{-1}, 1468 cm^{-1}, 1290 cm^{-1}, 1242 cm^{-1} and 790 cm^{-1} were attributed to N-H streching, C-H streching, C=C streching in a quinoid ring, C-C streching in a benzenoid ring, C-N streching, C-N bending and C-H (out of plane) vibrations, respectively. The prominent peak observed at 1114 cm^{-1} was regarded as an indicator of electron delocalization, making it a distinctive feature associated with the conductivity of PANI. (Zengin et al., 2002).

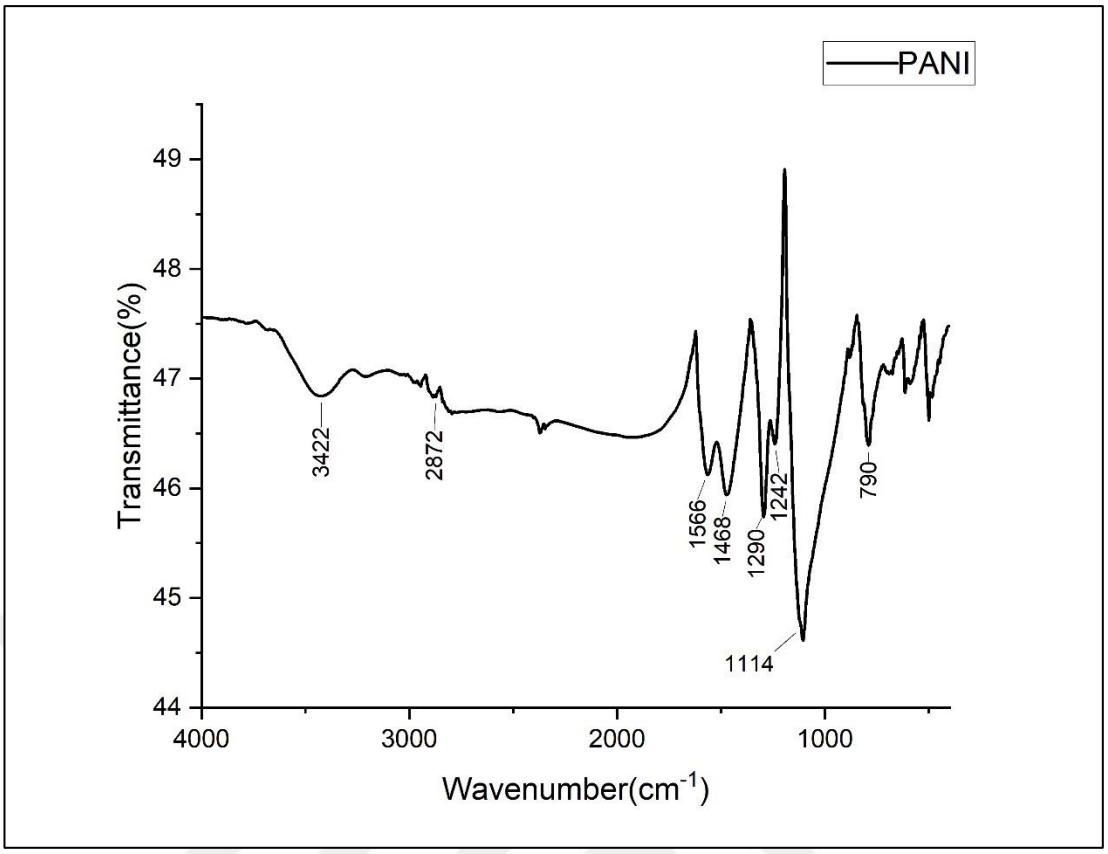

Figure 4.1. FTIR Spectrum of PANI.

4.1.2. Thermal Analysis of Polyaniline

Thermal analyzes of polyaniline were performed with TGA and DSC instruments.

4.1.2.1. Thermogravimetric Analysis (TGA)

TG/DTG curves which are shown in figure 4.2, were obtained for approximately 10 mg of sample weight by heating up to 750°C at a heating rate of 10°C/min under nitrogen gas. Polyaniline showed a typical three step decomposition behavior like previous studies (Kim et al., 2001; Joelma et al., 2007). In the first step at approximately 100 ºC, 8% weight loss is seen which attributed to loss of water. Second weight loss which is 18% in the temperature range of 136 - 360 ºC may attributed to deprotonation of PANI. Last weight loss which is 34% represents the chain break of the polyaniline as seen in Figure 4.2 in the temperature range of 360 - 700 ºC.

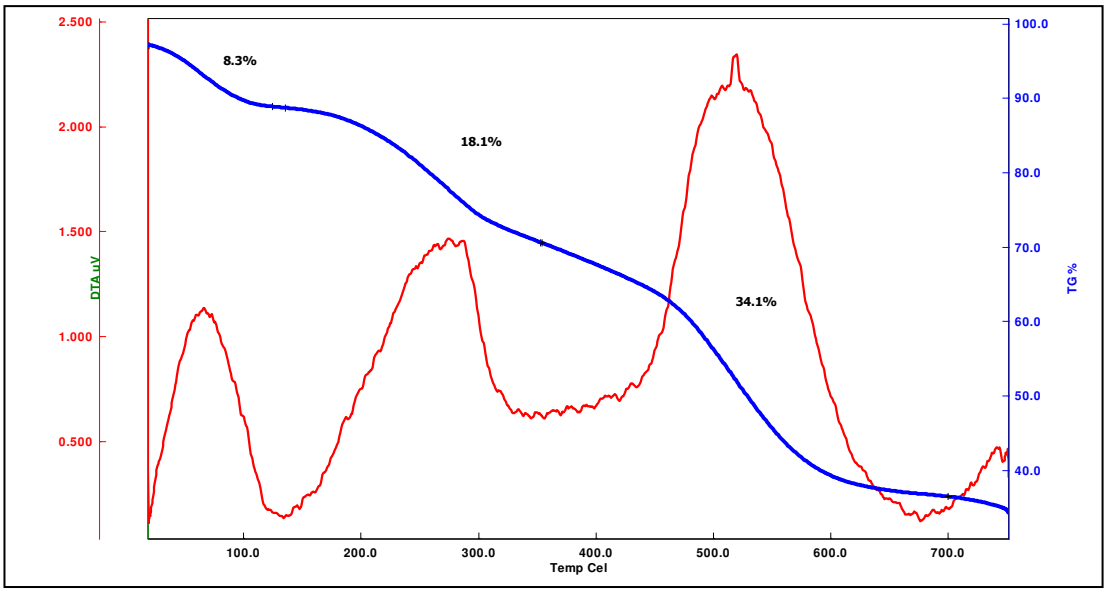

Figure 4.2. TG/DTG Thermogram of PANI.

4.1.2.2. Differential Scanning Calorimetry (DSC)

DSC analyzes of polyaniline were performed from 25°C to 300°C at a rate of 10°C min^{-1} under nitrogen gas and t-zero aluminum hermetic pan was preferred. Two endothermic peak were observed in Figure 4.3, first one can be due to the moisture loss and second one is for the loss of bound water which is consistent with the literature (S. Bhadra & Khastgir, 2009).

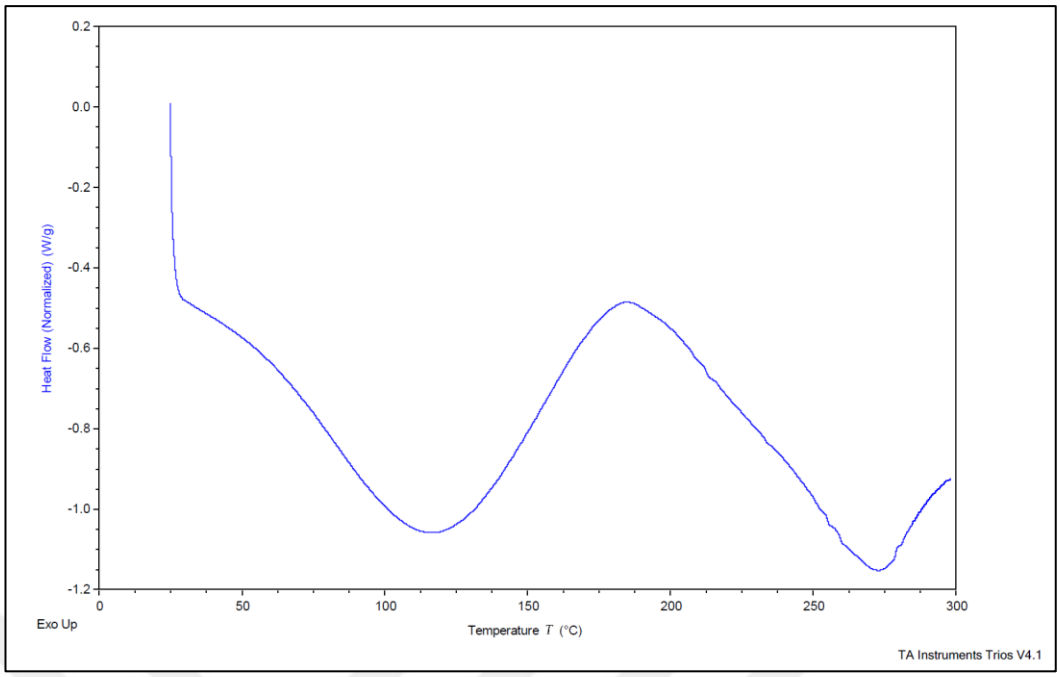

Figure 4.3. Conventional DSC Graph of PANI.

By plotting heat flow versus temperature and attributing a rapid discontinuity (slope shift) in the figures to the glass-rubber transition, the Tg of PANI can be found using DSC. The DSC plot also shows the occurrence of chemical changes, such as breakdown depending on temperature, and physical changes, such as loss of moisture and other constituents (S. Bhadra & Khastgir, 2009). It is either difficult to determine the glass transition temperature for PANI using conventional DSC due to potential overlap with other thermal transitions. Using MDSC, polyaniline was studied in order to gain a deeper understanding of any potential thermal transitions that might be concealed in the conventional DSC peaks. MDSC analyzes of polyaniline were performed from -50 °C to 400°C at a rate of 5°C min^{-1} under nitrogen gas and the period modulation was 60 s, temperature amplitude of modulation was 1°C. Reversing heat flow, non-reversing heat flow and total heat flow are shown in figure 4.4. According to the reversing heat flow there is an evident glass transition at 254.6°C which is consistent with the literature (Ding et al., 1999).

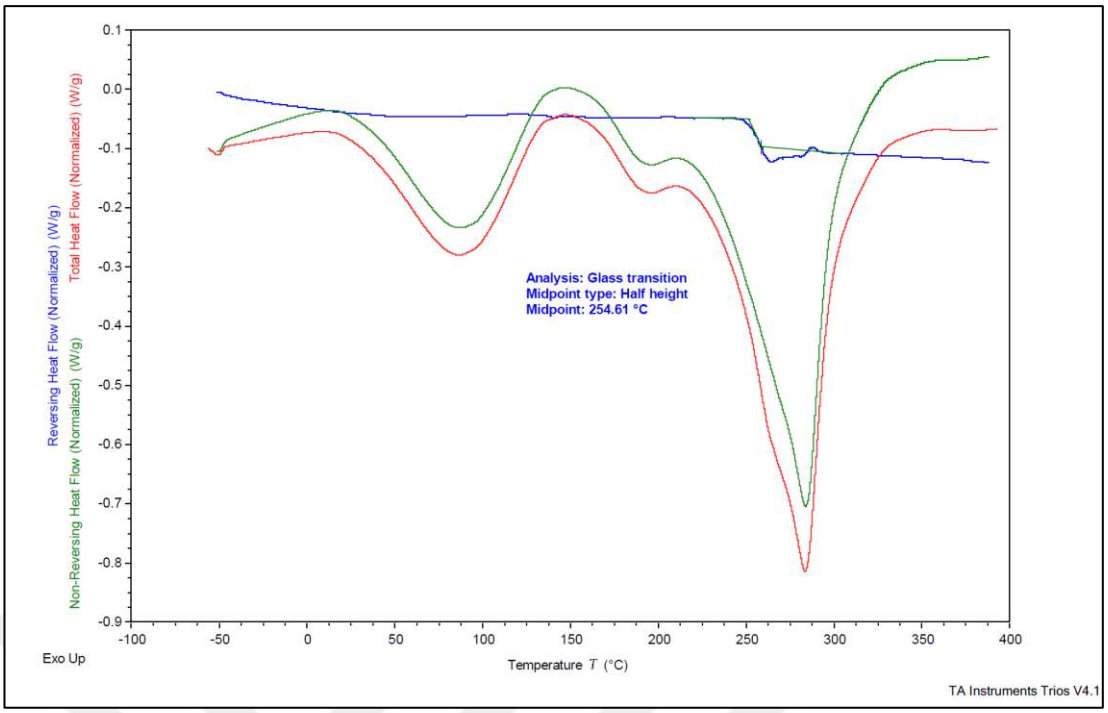

Figure 4.4. MDSC Graph of PANI.

4.1.3. X-Ray Diffraction Analysis

Diffraction patterns in the range of 10^{o} – 80^{o} 2Θ were taken for polyaniline (Figure 4.5). Powder samples were placed in the sample holder with the help of a stand and the analysis was done at room temperature. Polyaniline consists of a broad peak with two lower peaks. These two seperate peaks at 20.22˚ and 25.12˚ diffraction angles, which are attributed to the (020) and (200) Bragg Reflections of orthorhombic structure of polyaniline (Choudhary et al., 2018).

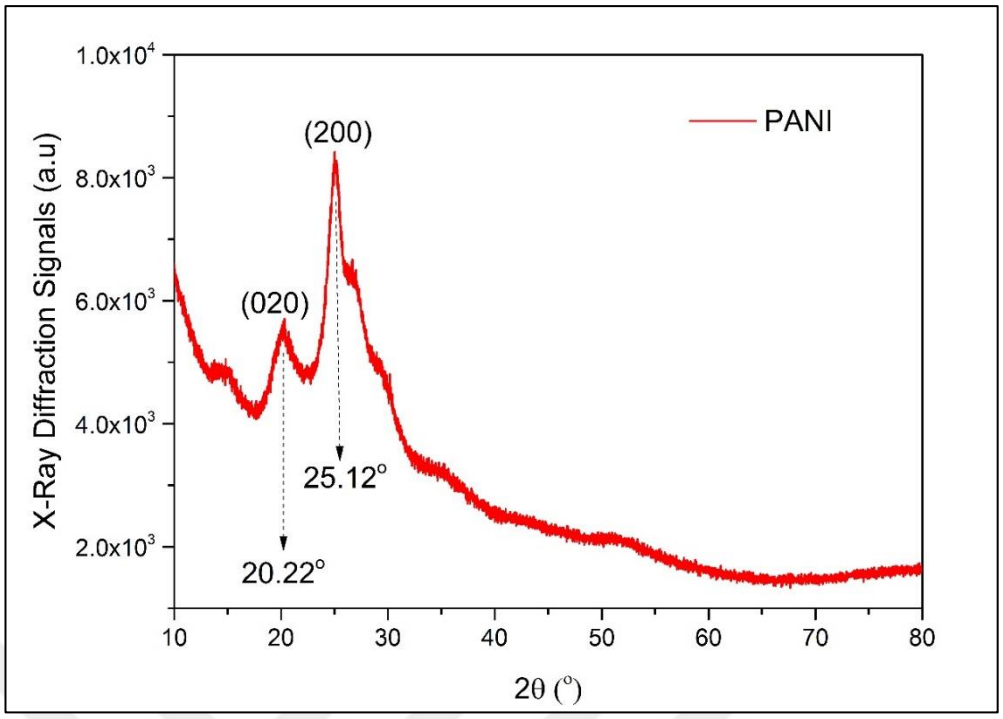

Figure 4.5. XRD Pattern of PANI.

4.1.4. Conductivity Measurements

The conductivity of the pure polyaniline is measured at three different temperatures. As seen in Table 4.1, the conductivity value increases as the temperature increases. In the literature, they attribute the increase in conductivity with the increase in temperature to the increase in the efficiency of charge transfer (Kulkarni & Viswanath, 2004). Additionally, the conductivity value of pure polyaniline was found to be compatible with the literature. (Udayaraj et al., 2023).

Table 4.1. Conductivity values of PANI at different temperatures.

	Conductivity (24^0C) (S/cm)	Conductivity (35^0C) (S/cm)	Conductivity (50^0C) (S/cm)
Pure PANI	$4.5\ 10^{-6}$	$6.6\ 10^{-6}$	$3.1\ 10^{-5}$

4.1.5. Morphological Analysis (SEM)

SEM images were taken at different magnifications to examine the morphological features of the polyaniline synthesized in the study. The SEM images display the polymer's usual characteristics. SEM image of polyaniline in Figure 4.6

shows a cottony coral like appearance. There are networks which can be the reason of charge transport and also the conductivity.

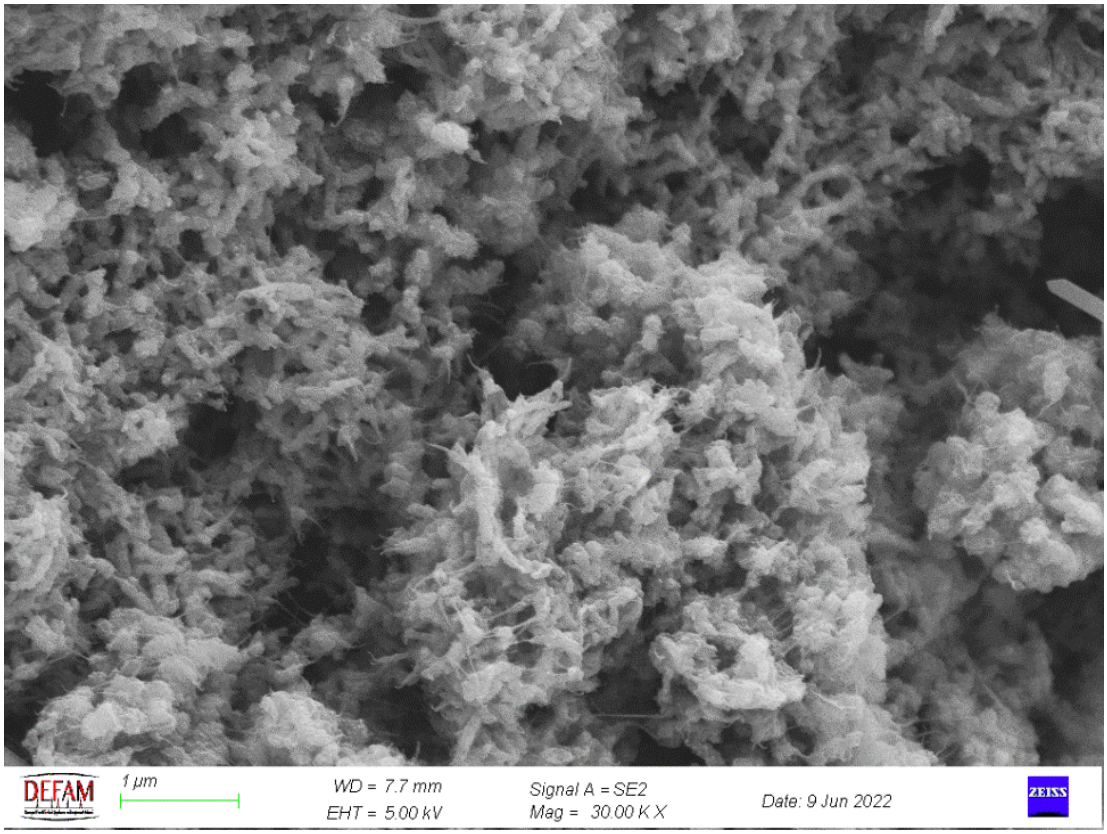

Figure 4.6. SEM Images of PANI.

4.2. Characterization of Low Density Polyethylene-Polyaniline Blends

Polyethylene (PE) has good processability, strong resistance to chemicals, and exceptional mechanical qualities. The emeraldine type polyaniline (PANI) was produced chemically through chemical oxidation of aniline at 0°C. As stated in Chapter 3 (Section 3.2.2), polyaniline and powdered low density polyethylene (LDPE) were mixed by the solution blending method. The abbreviated nomenclature $LP_{0.5}$, LP_1 and LP_3 correspond to LDPE containing 0.5 wt%, 1 wt% and 3 wt% PANI for all blends, respectively. FTIR analysis, TG/DTG analysis, DSC analysis, XRD analysis, SEM analysis, DMA analysis, Conductivity Measurements and ESD analysis were performed for characterization of blends.

4.2.1. FTIR Analysis

FTIR spectra of the blends were obtained by preparing KBr pellets between 4000 and 400 cm^{-1}. The FTIR spectra of LDPE blends prepared with various amounts of PANI are shown in Figure 4.7. The bands seen at 2913, 2846, 1466, 1369 and 715 cm^{-1} in the spectrum given were attributed to $-CH_2$ asymmetric vibration, $-CH_2$ symmetrical vibration, bending deformation vibration, $-CH_3$ symmetrical strain vibration and oscillating strain vibration of LDPE, respectively. The 3445 cm^{-1} broad N-H peak specific for polyaniline is also seen in the spectrum. As stated in the literature (Nand et al., 2012) the presence of specific peaks for both PANI and LDPE are proof that these materials are physically blended.

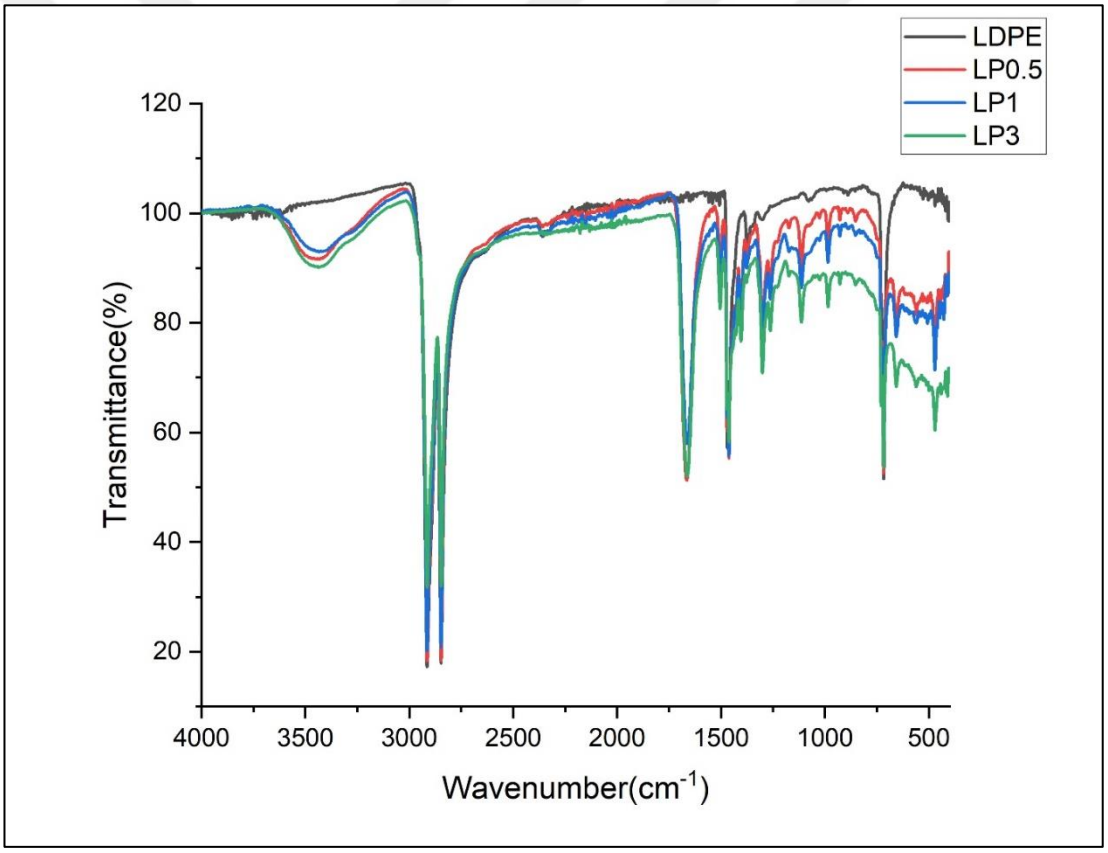

Figure 4.7. FTIR Spectra of LDPE, $LP_{0.5}$, LP_1 and LP_3.

4.2.2. TG/DTG Analysis

Thermogravimetric analyzes were carried out at a heating rate of 10°C/min, starting from room temperature up to 600°C. The temperature values corresponding to the highest decomposition rate of the blends, % mass losses were measured. Figure 4.8

shows the TG/DTG analysis of pure LDPE and its blends. Accordingly, it is seen that pure LDPE decomposes in one step, but blends decompose in two steps. The degradation curve of the blends seen in the first step is thought to be due to solvent evaporation. The second decomposition is caused by decomposition of LDPE. It was observed that the temperature values corresponding to the highest degradation rate of pure LDPE and $LP_{0.5}$, $LP_1$and LP_3 were around 478°C. There is not a clear change in the thermal stability of polyethylene. In other words, there is no difference in the temperature at which polyethylene chains begin to deteriorate. In addition, when mass losses were examined, it was observed that all of them decomposed.

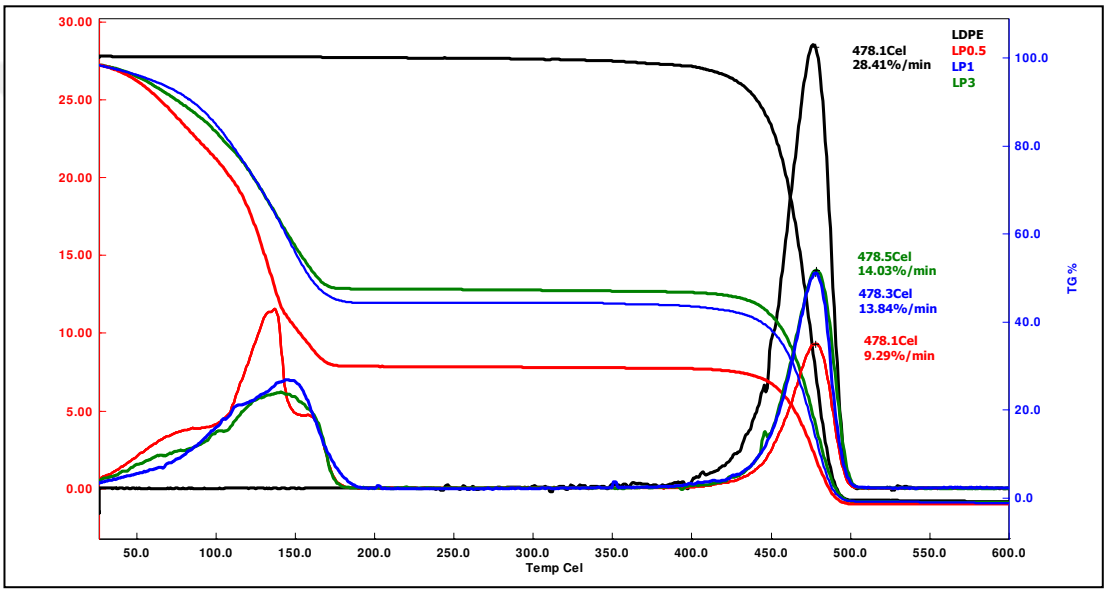

Figure 4.8. TG-DTG thermogram of LDPE, $LP_{0.5}$, LP_1 and LP_3.

4.2.3. DSC Analysis

DSC analyzes of LDPE and the blends were carried out starting from room temperature up to 250°C at a heating rate of 10°C/min with a three-step program (heating, cooling and second heating). A 50 mL/min flow rate of inert nitrogen gas was utilized, and an aluminum t-zero hermetic pan was chosen. Calibration of the DSC were carried out before starting the experiments. In order to conduct calibration, indium and sapphire supplied by TA, were used. Figure 4.9 shows the second heating of the DSC thermograms of LDPE blends doped with polyaniline.

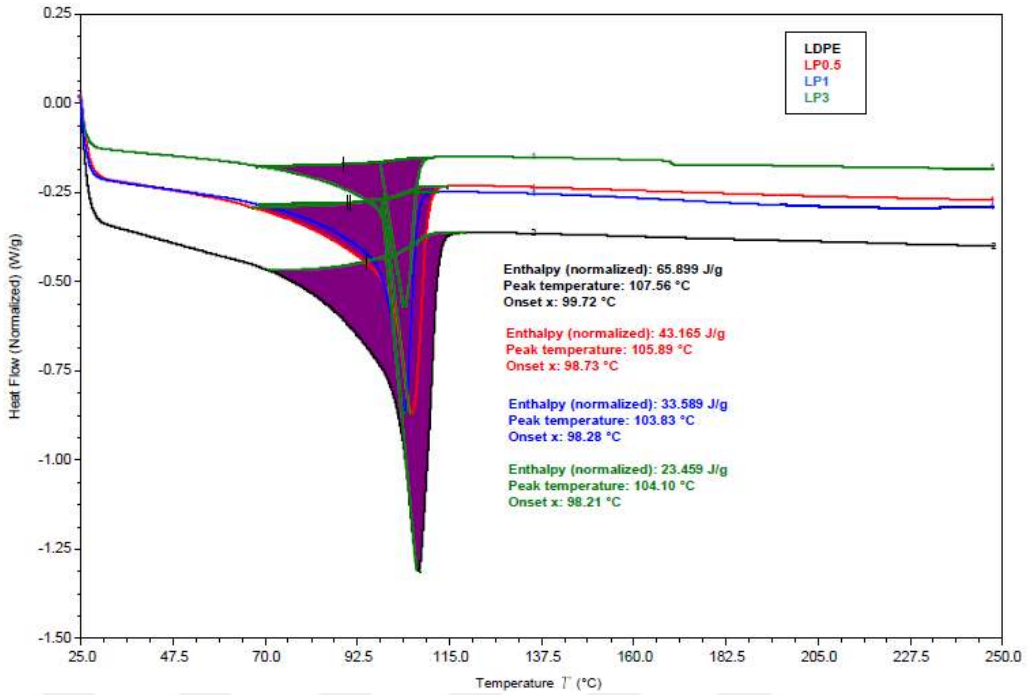

Figure 4.9. DSC thermogram of LDPE, $LP_{0.5}$, LP_1 and LP_3.

Melting temperature (Tm), heat of fusion (ΔH), and degree of crystallinity values (Xc) were found from this thermogram and are given in Table 4.2. The heat of fusion was used to assess the samples' degree of crystallinity, Xc. Equation 4.1 was used to calculate the crystallinity Xc (%) based on DSC data as follows:

$$Xc\ (\%) = \frac{\Delta H}{\Delta H^{\circ}}\ 100 \qquad \text{.....(4.1.)}$$

where ΔH° is the specific heat of melting of perfect crystal of LDPE and ΔH° = 293 J/g has been utilized in this study (D. Li et al., 2019). PANI and LDPE are immiscible, so melting temperature of LDPE does not appear to be significantly impacted by the amount of PANI (Passador et al., 2017). A decrease of approximately 1°C in melting temperature was observed while adding of PANI to the LDPE matrix. But, when the PANI amount in the blends increases, the degree of LDPE crystallinity significantly decreases. Because polyaniline is amorphous, the blends' amorphous phase will grow, which causes the percentage of crystallinity in the composites to gradually decrease as polyaniline concentration increases (Yilmaz, 2007).

Table 4.2. DSC data of LDPE and blends.

	T_m	ΔH, j/g	X_c (%)
LDPE	99.7	65.9	22.5
$LP_{0.5}$	98.7	43.2	14.7
LP_1	98.3	33.6	11.5
LP_3	98.2	23.5	8.0

4.2.4. XRD Analysis

X-ray diffraction patterns of the samples were taken with the PANalytical EMPYREAN XRD device. Diffraction patterns for all samples were taken from 10^o – 80^o at a diffraction angle of 2Θ. Figure 4.10 shows the X-ray diffraction pattern of LDPE blends doped with 3 wt% PANI-1 wt% PANI-0.5 wt% PANI. Ortho hexagonal, metastable monoclinic, and stable orthorhombic crystal forms make up commercial polyethylene. Two distinct diffraction peaks at 2 Θ =21.27° (110) and 2 Θ =23.46° (200) of LDPE are seen in pattern which are consistent with the literature (Depan et al., 2021). These peaks indicates that LDPE used in this study has orthorhombic structure.

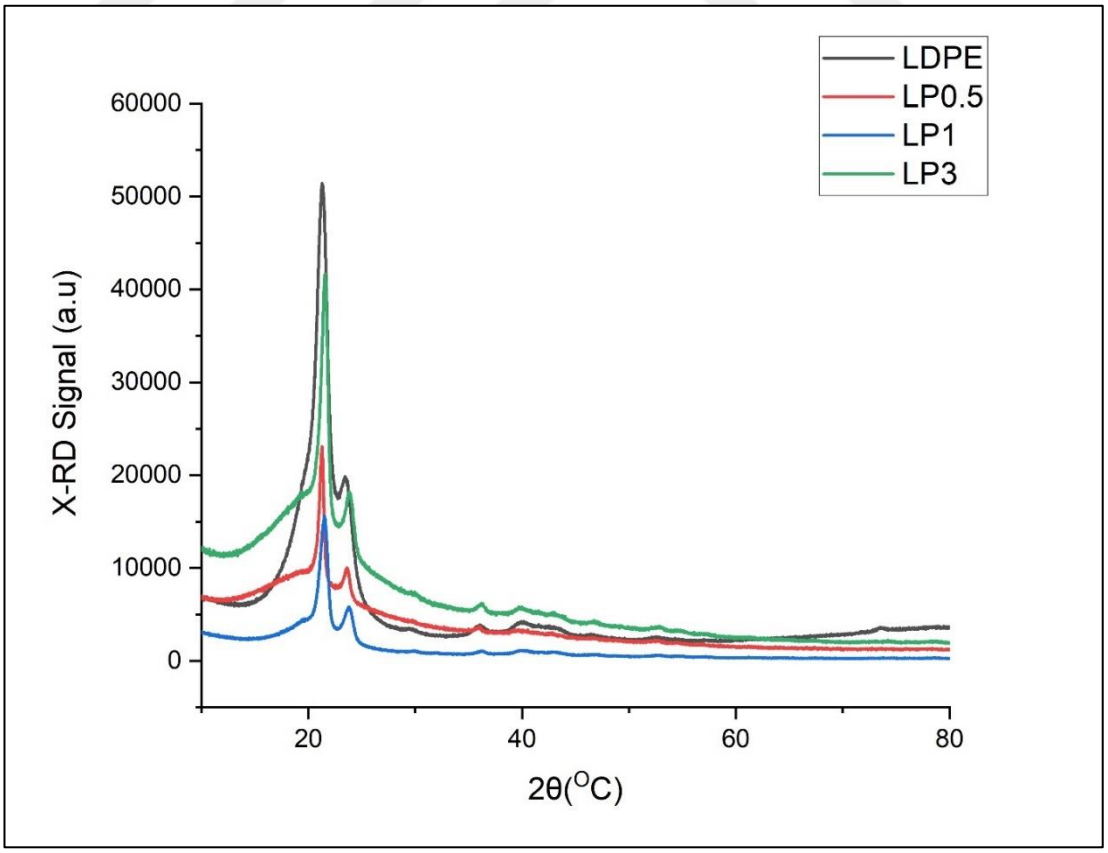

Figure 4.10. X-ray diffraction pattern of LDPE, $LP_{0.5}$, LP_1 and LP_3.

Table 4.3. XRD data of LDPE and blends.

Sample	$2\Theta_1$	$2\Theta_2$
LDPE	21.27	23.46
$LP_{0.5}$	21.28	23.61
LP_1	21.50	23.79
LP_3	21.55	23.85

The addition of the PANI to the LDPE showed that the X-ray diffraction peaks at 2 Θ did not change much, which are given in Table 4.3, but blends' peak intensities indicated a slight decrease. Decreases of peak intensities can be attributed to decreases of crystallinity (Bhadra et al., 2016).

4.2.5. Mechanical Properties

Mechanical analysis were performed in TA Q800 DMA instrument with a ramp force rate of 1 N/min at 25°C. The applied frequency was 1 Hz and tensile film clamp was used to obtain stress-strain curve. Stress-strain curves of LDPE and its blends with different PANI contents are given in Figure 4.11.

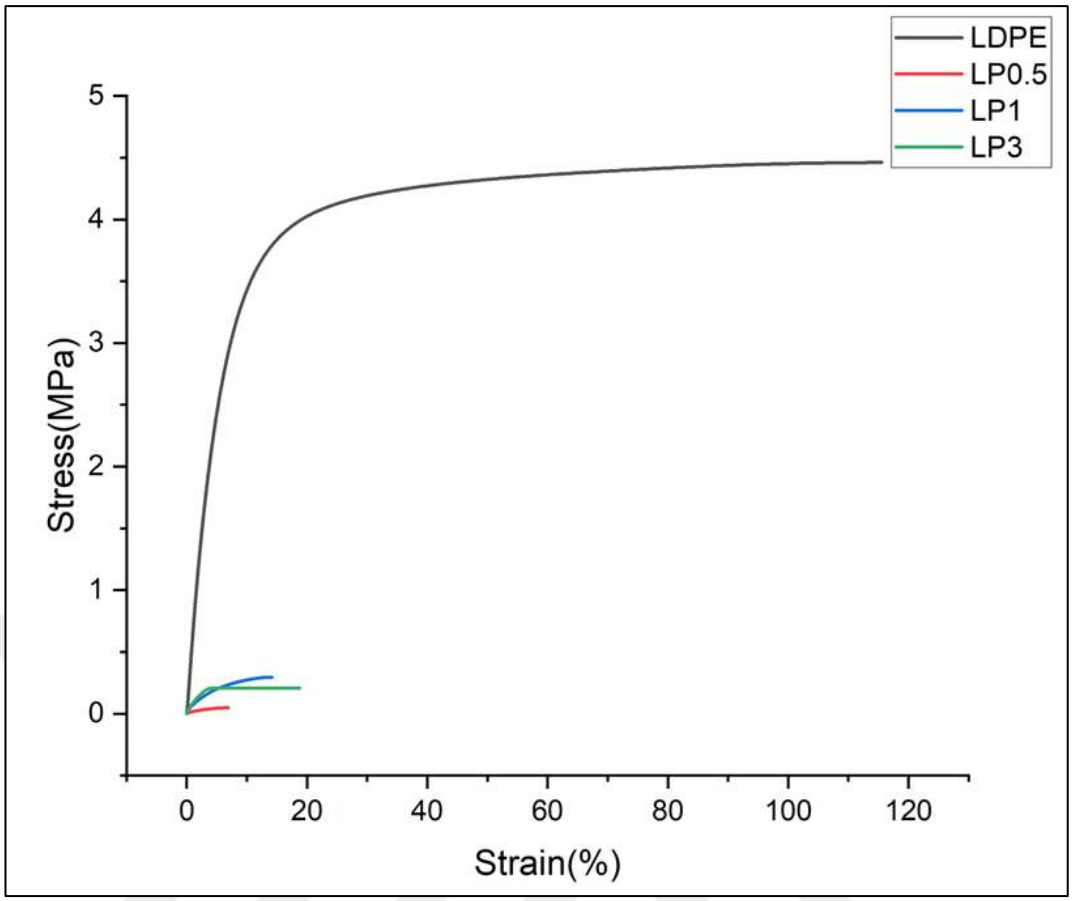

Figure 4.11. Stress-strain curves of LDPE, $LP_{0.5}$, LP_1 and LP_3.

The mechanical behavior of LDPE was significantly altered by the addition of PANI. Since the PANI is polar and the polyethylene is nonpolar, it may be inferred that there is no adhesion between the phases and that the addition of PANI has a detrimental effect on the mechanical characteristics of the polymer matrix. In conductive polymers, a conjugated carbon chain is made up of alternating single and double bonds (π bonds) which are strongly polarized, delocalized, and electron-dense (Namsheer & Rout, 2021). Due to the conjugated carbon chain of polyaniline, the aggregation of polyaniline particles make it difficult to establish a proper filler distribution in the PE matrix. Therefore, the mechanical properties of blends decrease. There is a decrease in mechanical strength of blends which were summarized in Table 4.4.

Table 4.4. Stress-Strain results of LDPE and its blends.

Sample	Stress (MPa)	Strain (%)
LDPE	4.46	115.57
$LP_{0.5}$	0.05	6.91
LP_1	0.29	14.24
LP_3	0.21	18.81

4.2.6. SEM Analysis

SEM images were taken at different magnifications to examine the morphological features of the samples used in the study. Images were obtained with the ZEISS GEMINI 500 SEM instrument. SEM image of pure LDPE in film form is given in Figure 4.12. According to the morphological images, the film surfaces of pure polyolefins are smooth.

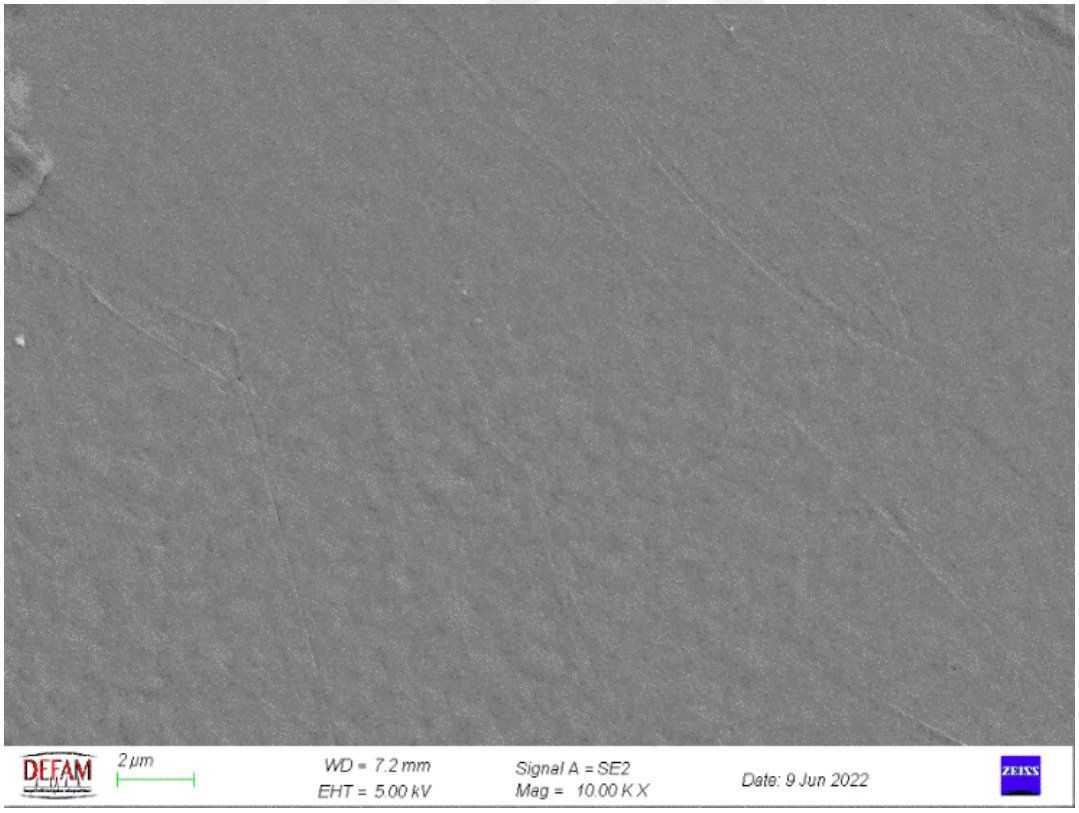

Figure 4.12. SEM Image of LDPE.

SEM images of the blends (Figure 4.13) were examined how much the morphology of the LDPE changed and whether polyaniline aggregated or not. It can

be seen that when 0.5 wt% PANI is added to completely smooth pure LDPE, solid particles begin to cluster. These images support the decrease in mechanical properties. When the amount of polyaniline is increased to 1%, these clusters increase even more and appear as nodules. But the LDPE blend, which is doped with 3 wt% polyaniline, shows regular structures and micro-channels resembling hexagons. This can lead to an increase in conductivity of the structure. Clusters are also seen in the SEM image of the LP_3 coded blend.

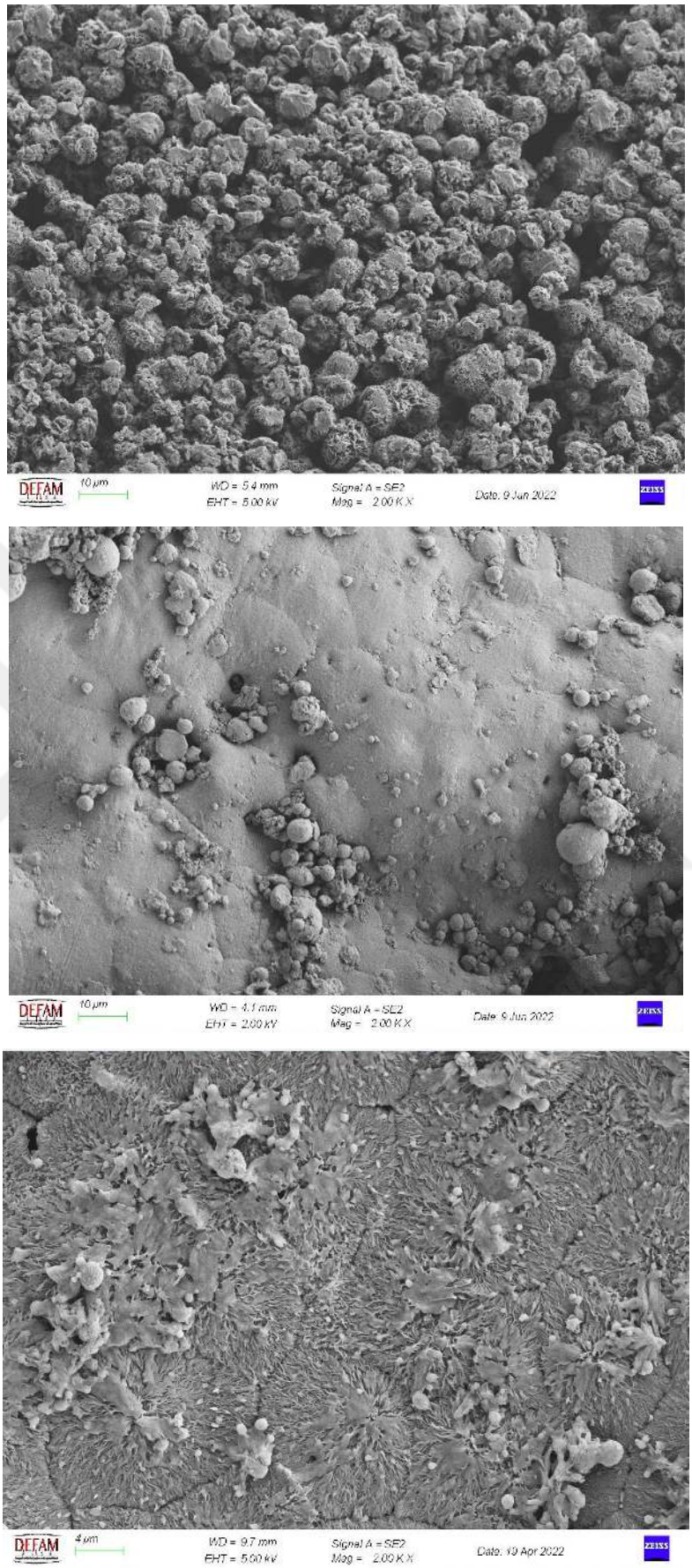

Figure 4.13. SEM Images of $LP_{0.5}$, LP_1 and LP_3 blends respectively.

4.2.7. Conductivity Measurements

The conductivities of the synthesized materials were measured in the film form with Keithley 2400 electrometer. The conductivies of blends and LDPE at three different temperatures are given in Table 4.5.

Table 4.5. Conductivity Measurements of Blends and Pure Materials.

	Conductivity(24^0C) ($x10^{-9}$S/cm)	Conductivity(35^0C) ($x10^{-9}$S/cm)	Conductivity(50^0C) ($x10^{-9}$S/cm)
Pure LDPE	0.036	0.043	0.044
$LP_{0.5}$	4.9	520	1300
LP_1	17	3700	2900
LP_3	28	8100	3300

According to the literature, it is seen that the conductivity value tends to increase as the conductive additive is added (Omastova,' et al., 1996). When the conductivity measurements are examined, it is seen that the conductivity value of LDPE, which is 3.6 10^{-11} S/cm, increases as polyaniline is added. It is seen in the literature that materials with a conductivity value of 10^{-6} -10^{-11} S/cm can be used as antistatic materials (Joelma et al., 2007). The conductivity value of the blends obtained varies between 10^{-6} and 10^{-9} S/cm. For this reason, all blends are candidates to be used as antistatic materials.

4.2.8. Electrostatic Charge Dissipation (ESD) Analysis

Electrostatic charge dissipation (ESD) is one of the challenges that have lately emerged with the rise of the electronics sector. Particularly, ESD is responsible for 60% of the damages to integrated circuits (Hwang, 2004). A viable solution to this issue is to incorporate semiconductor materials into the materials that are frequently utilized in the sector. The simplest technique to determine whether a material can retain a charge is to apply a charge to it and observe how quickly it dissipates. Corona charging offers a quick, dependable, non-contact method for controlling the magnitude and polarity of charge deposits on any surface (Saini & Choudhary, 2013). At room temperature various positive (3, 6 and 9 kV) and negative corona voltages (-3, -6 and

-9 kV) applied to the blends surface. The dissipation time of the static charges accumulated on the surfaces of LDPE and its blends depending on the change of corona voltage were determined.

Firstly, pure LDPE ESD analyses were carried out. The LDPE surface was seen to accept extremely high surface voltages in both high positive and negative polarities of charge decay time curves. As predicted, static charge dissipation time (up to 300 seconds) for aggregation on the surface of LDPE could not be measured. The results obtained from the measurements are summarized in Table 4.6.

Table 4.6. Polarity values of pure LDPE at various corona voltages.

Corona voltage*(V)*	Corona time *(s)*	Surface humidity*(%RH)*	Surface temperature(^0C)	Surface voltage*(V)*	1/e time *(s)*	%10 Cut-off time*(s)*	Surface charge*(nC)*	Capacitans
-9000	0.030	36.2	28.8	-2131.4	nr	nr	-57.3	11.56
-6000	0.030	34.7	29.8	-1252.0	nr	nr	-53.20	18.25
-3000	0.008	34.6	29.1	-425.8	nr	nr	-1.82	1.85
3000	0.008	33.6	28.2	-152.3	nr	nr	-2.034	5.703
6000	0.030	33	27.5	1731.4	nr	nr	-0.24	0.07
9000	0.030	32.9	27.2	1802.6	nr	nr	59.56	14.19

nr:not reached

The effectiveness of the ESD control material is determined by how long it takes for the static charge to dissipate. ESD performance can be calculated using either the charge decay time of 1/e, or 10% of the voltage value, or about 37% of the voltage value. Thus, a good ESD control material's surface static load needs to be less than 1 and 2 s in order to meet the requirements of 1/e and 10% cut time standards (Doğan et al., 2018). Taking into account the performance of different corona voltages of $LP_{0.5}$ blend as given in Table 4.7, the blend at -3kV, 3kV and 6kV Corona voltage, according to the 1/e criterion (1/e time: 0.134 s for −3 kV; 1/e time: 1.025 s for 3 kV, 1/e time: 1.022 s for 6 kV) could serve as antistatic material . Also, cut-off time of synthesized blend was about below 2 s (%10 cut-off time: 0.248 s for −3 kV; %10 cut-off time: 2.361 s for 3 kV, %10 cut-off time: 2.354 s for 6 kV). As a result at -3kV, 3kV and 6kV Corona voltage $LP_{0.5}$ blend could serve as antistatic material.

Table 4.7. ESD values of $LP_{0.5}$ blend at various corona voltages.

Corona voltage *(V)*	Corona time *(s)*	Surface humidity *(%RH)*	Surface temperature *(^0C)*	Surface voltage *(V)*	1/e time *(s)*	%10 Cut-off time *(s)*	Surface charge *(nC)*	Capacitans
-9000	0.030	36.8	28.2	-135.1	9.307	27.213	-1373.96	4363.90
-6000	0.030	36.2	29.8	-96.6	34.401	nr	-487.02	2164.41
-3000	0.030	33	29.8	-13.6	0.134	0.248	-37.80	1191.41
3000	0.020	32.2	22.4	-707.0	1.025	2.361	nr	nr
6000	0.020	32.4	22.7	-690.6	1.022	2.354	nr	nr
9000	0.030	36.1	26.2	127.9	12.934	nr	629.95	2116.63

nr:not reached

The results of various corona voltages of LP_1 blend as given in Table 4.8, the blend at 3kV corona voltage (1/e time: 1.025 s ; %10 cut-off time :2.361s) could serve as antistatic material according to the 1/e and %10 cut-off time criterion.

Table 4.8. ESD values of LP_1 blend at various corona voltages.

Corona voltage *(V)*	Corona time *(s)*	Surface humidity *(%RH)*	Surface temperature *(^0C)*	Surface voltage *(V)*	1/e time *(s)*	%10 Cut-off time *(s)*	Surface charge *(nC)*	Capacitans
-9000	0.030	35.8	28.5	-991.2	nr	nr	-706.56	306.09
-6000	0.030	35.2	29.8	-550.6	nr	nr	-260.46	203.11
-3000	0.029	32.7	30.4	-249.6	nr	nr	-31.75	54.63
3000	0.020	32.4	22.4	-700.8	1.025	2.361	nr	nr
6000	0.030	34.8	28.2	329.6	23.213	23.275	6.61	8.61
9000	0.030	36.6	26.5	1021.9	35.401	35.526	386.42	162.38

nr:not reached

Taking into account the performance of various corona voltages of LP_3 blend as given in Table 4.9, the blend at -3kV, 3kV and 6kV Corona voltage, according to the 1/e criterion (1/e time: 0.115 s for −3 kV; 1/e time: 1.022 s for 3 kV, 1/e time: 1.010 s for 6 kV) could serve as antistatic material. Also, cut-off time of so-called blend was about below 2 s (%10 cut-off time: 0.256 s for −3 kV; %10 cut-off time:

2.361 s for 3 kV, %10 cut-off time: 2.292 s for 6 kV). As a result at -3kV, 3kV and 6kV Corona voltage, LP_3 blend could be used as ESD material.

Table 4.9. ESD values of LP_3 blend at various corona voltages.

Corona voltage *(V)*	Corona time *(s)*	Surface humidity *(%RH)*	Surface temperature *(^0C)*	Surface voltage *(V)*	1/e time *(s)*	%10 Cut-off time *(s)*	Surface charge *(nC)*	Capacitans
-9000	0.030	36.8	28.2	-504.0	nr	nr	-293.18	249.77
-6000	0.030	36.0	29.8	-410.0	nr	nr	-100.99	105.77
-3000	0.030	33.1	29.8	-13.7	0.115	0.256	-33.97	1064.89
3000	0.020	32.5	22.7	-695.7	1.022	2.361	nr	nr
6000	0.020	32.4	22.7	-171.4	1.010	2.292	nr	nr
9000	0.030	36.7	26.2	454.5	nr	nr	152.65	144.24

nr:not reached

4.3. Characterization of High-Density Polyethylene-Polyaniline Blends

Elevated tensile strength, excellent resistance to chemicals, high resistance to impact, and low moisture absorption capacity are all characteristics of HDPE. The emeraldine type polyaniline (PANI) was produced chemically through oxidation at 0°C as stated in Chapter 3 (Section 3.2.1). Conductive polyaniline emeraldine form and powdered high density polyethylene (HDPE) were mixed by the solution blending method. The abbreviated nomenclature $HP_{0.5}$, HP_1 and HP_3 correspond to HDPE containing 0.5 wt%, 1 wt% and 3 wt% PANI for all blends respectively. FTIR Analysis, TG/DTG analysis, DSC analysis, XRD analysis, SEM analysis, DMA analysis, Conductivity Measurements and ESD analysis were performed for characterization of blends.

4.3.1. FTIR Analysis

The FTIR analysis of blends were performed by Perkin Elmer-Spectrum BX FTIR spectrophotometer between 400 to 4000 cm^{-1}. The FTIR spectra of HDPE blends prepared with various amounts of PANI are shown in Figure 4.14. It was determined that the bands observed at 2916 and 2848 cm^{-1} corresponded to $-CH_2$

symmetrical and asymmetric vibration, respectively. The frequencies seen at 1472 and 1462 cm^{-1} in the spectrum were attributed to bending deformation, and 1365 cm^{-1} was attributed to -CH_3 symmetrical deformation vibration. The frequencies observed at 730 and 719 cm^{-1} in the spectrum were attributed to deformation vibrations. One of the most crucial markers utilized to differentiate poly (olefin) was the symmetric deformation vibration peak of -CH_3 at 1365 cm^{-1}. This peak in the spectrum could be used to confirm that the polyolefin-based mixture is HDPE (Gulmine et al., 2002). The 3413 cm^{-1} broad N-H peak specific for polyaniline was also seen in the spectrum. As stated in the literature the presence of specific peaks in both materials and the absence of other new formation peaks are proof that these materials are physically blended (Nand et al., 2012).

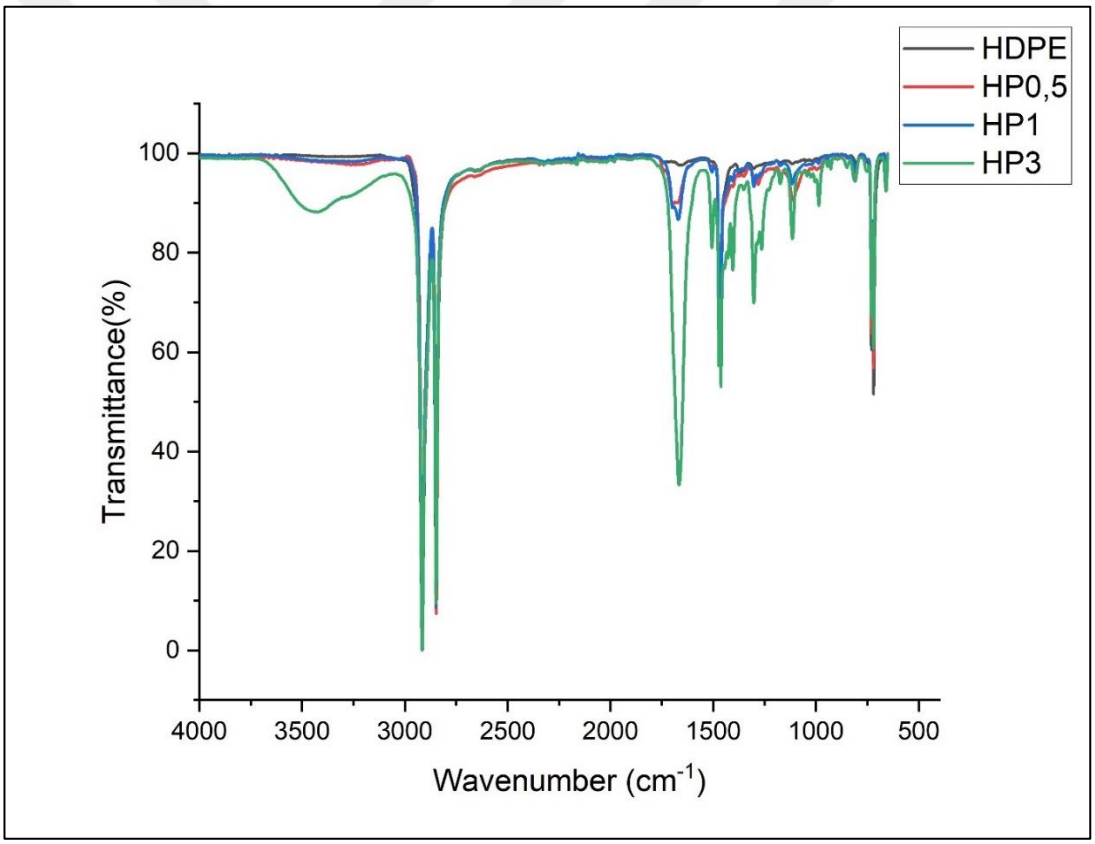

Figure 4.14. FTIR Spectra of HDPE, $HP_{0.5}$, HP_1 and HP_3.

4.3.2. TG/DTG Analysis

Thermogravimetric analyzes were performed starting at room temperature up to 600°C at a heating rate of 10°C/min. The temperature values that indicate the blends' maximum rate of degradation, % mass losses were examined. Figure 4.15 shows the

TG/DTG analysis of pure HDPE and its blends. The degradation curve of the blends seen in the first step is thought to be due to solvent evaporation. The second degradation was also caused by HDPE. Based on DTG analysis, the blends of HDPE, HP0.5, HP1, and HP3 have temperature values of 480.1°C, 481.9°C, 481.9°C, and 481.5 °C that corresponded to the maximum rate of decomposition, respectively. There is an increase of approximately 1°C in the thermal stability of HDPE with increasing polyaniline content. In other words, the degradation of HDPE will shift to higher temperatures. Additionally, when the mass losses were examined, it was observed that almost all of them decomposed.

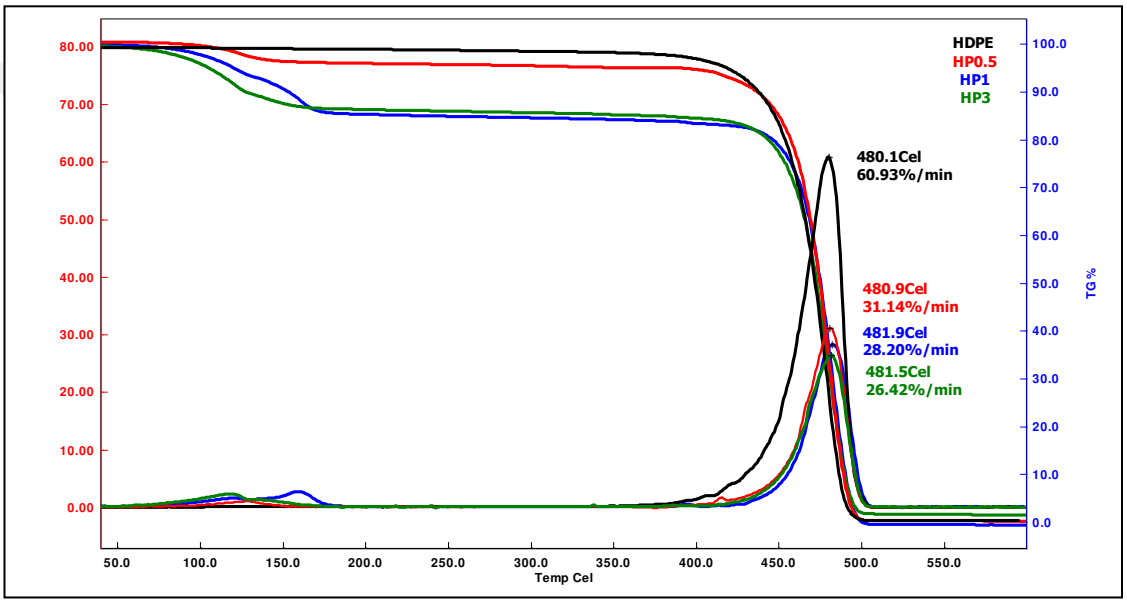

Figure 4.15. TG-DTG thermogram of HDPE, $HP_{0.5}$, HP_1 and HP_3.

4.3.3. DSC Analysis

DSC measurements were performed using TA DSC 250. Calibration of the DSC were carried out before starting the experiments. In order to conduct calibration, indium and sapphire supplied by TA, were used. The analyses were carried out starting at room temperature up to 250 °C at a rate of 10°C/min using a sequential three-stage program (heating–cooling–heating). A 50 mL/min flow rate of inert nitrogen gas was utilized, and an aluminum t-zero hermetic pan was chosen. Figure 4.16 shows the second heating of the DSC thermograms of HDPE and its blends doped with polyaniline.

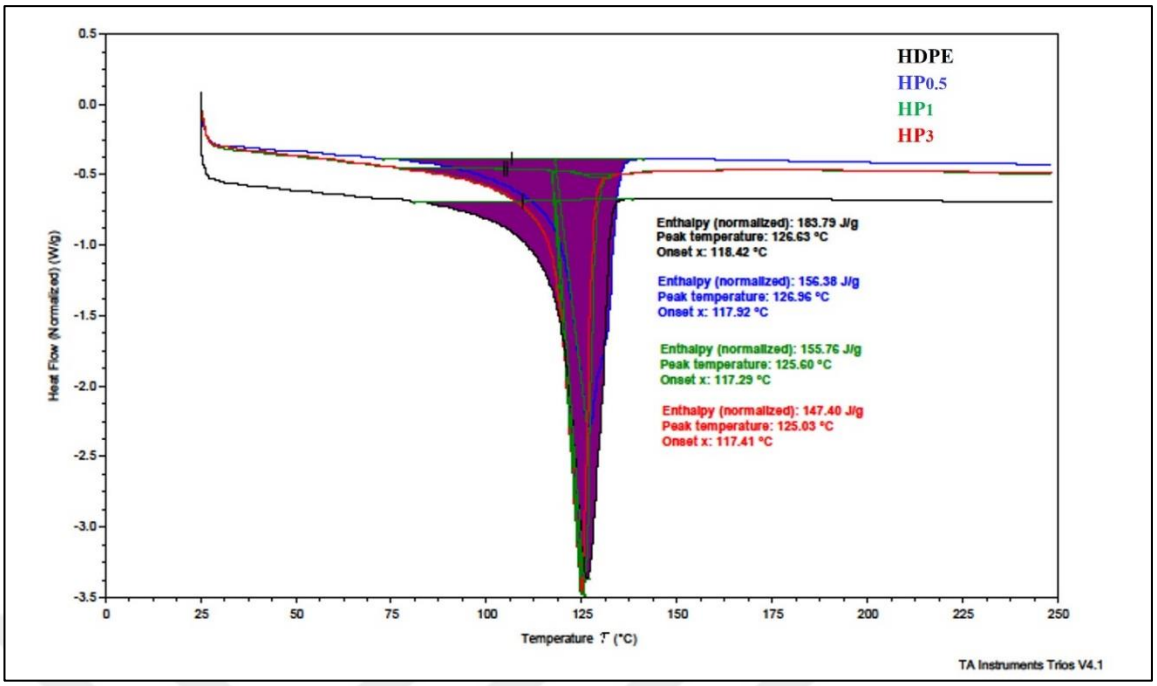

Figure 4.16. DSC thermogram of HDPE, $HP_{0.5}$, HP_1 and HP_3.

Melting temperature (T_m), ΔH, and degree of crystallinity values were found from this thermogram and are given in Table 4.10. The heat of fusion was used to assess the samples' degree of crystallinity, Xc. Equation 4.2 was used to calculate the crystallinity Xc (%) based on DSC data as follows:

$$X_c\,(\%) = \frac{\Delta H}{\Delta H^\circ}\,100 \qquad \text{(4.2.)}$$

where ΔH° is the specific heat of melting o perfect crystal of HDPE and ΔH° = 290 J/g has been utilized in this study (Yadegari et al., 2016). PANI and HDPE are immiscible, so melting temperature of HDPE does not appear to be significantly impacted by the amount of PANI (Passador et al., 2017). A decrease of approximately 1°C in melting temperature was observed while adding of PANI to the HDPE matrix. But, when the PANI amount in the blends increases, the degree of HDPE crystallinity decreases. Because polyaniline is amorphous, the blends' amorphous phase will grow, which causes the percentage of crystallinity in the composites to gradually decrease as polyaniline concentration increases.

Table 4.10. DSC data of HDPE and related blends.

Sample	T_m(°C/)	ΔH, j/g	X_c (%)
HDPE	118.4	183.8	63.4
$HP_{0.5}$	118.0	156.4	53.9
HP_1	117.3	155.7	53.7
HP_3	117.4	147.4	50.8

4.3.4. XRD Analysis

XRD patterns of the samples were obtained from the PANalytical EMPYREAN XRD device. Diffraction patterns for all samples were taken from 5° to 85° at a diffraction angle of 2θ. Figure 4.17 shows the X-ray diffraction pattern of HDPE, $HP_{0.5}$, HP_1 and HP_3. Ortho hexagonal, metastable monoclinic, and stable orthorhombic crystal forms make up commercial polyethylene. The flat zigzag chain conformation is present in orthorhombic and monoclinic phases. Two distinct diffraction peaks at 2θ =21.14° (110) and 2θ =23.28° (200) indicate that the HDPE used in this study has orthorhombic form (Benabid et al., 2019).

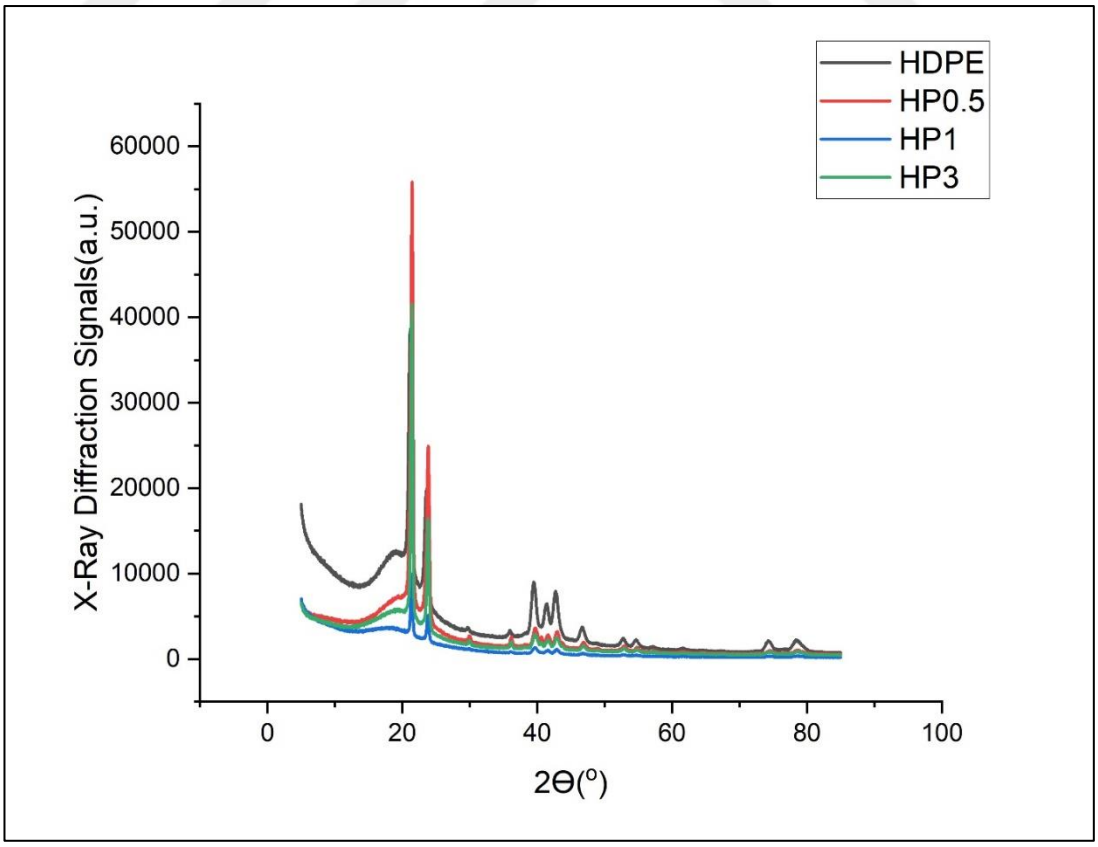

Figure 4.17. X-ray diffraction pattern of HDPE, $HP_{0.5}$, HP_1 and HP_3.

XRD patterns of all HDPE/PANI blends indicated the distinctive peaks of HDPE at approximately 21°, and 23° and other peaks. Significant X-ray diffraction peaks are given in Table 4.11.

Table 4.11. Diffraction angles of HDPE and related blends.

Sample	$2\theta_1$ *(°)*	$2\theta_2$ *(°)*
HDPE	21.18	23.55
$HP_{0.5}$	21.46	23.81
HP_1	21.44	23.80
HP_3	21.44	23.81

4.3.5. Mechanical Analysis

Analysis on a TA Q800 DMA instrument were performed with a ramp force rate of 1 N/min at 25ºC. The applied frequency was 1 Hz, and a tensile film clamp was used to obtain the stress-strain curve. DMA stress-strain curves of HDPE and its blends doped with 0.5 wt% PANI, 1 wt% PANI, and 3 wt% PANI are given in Figure 4.18.

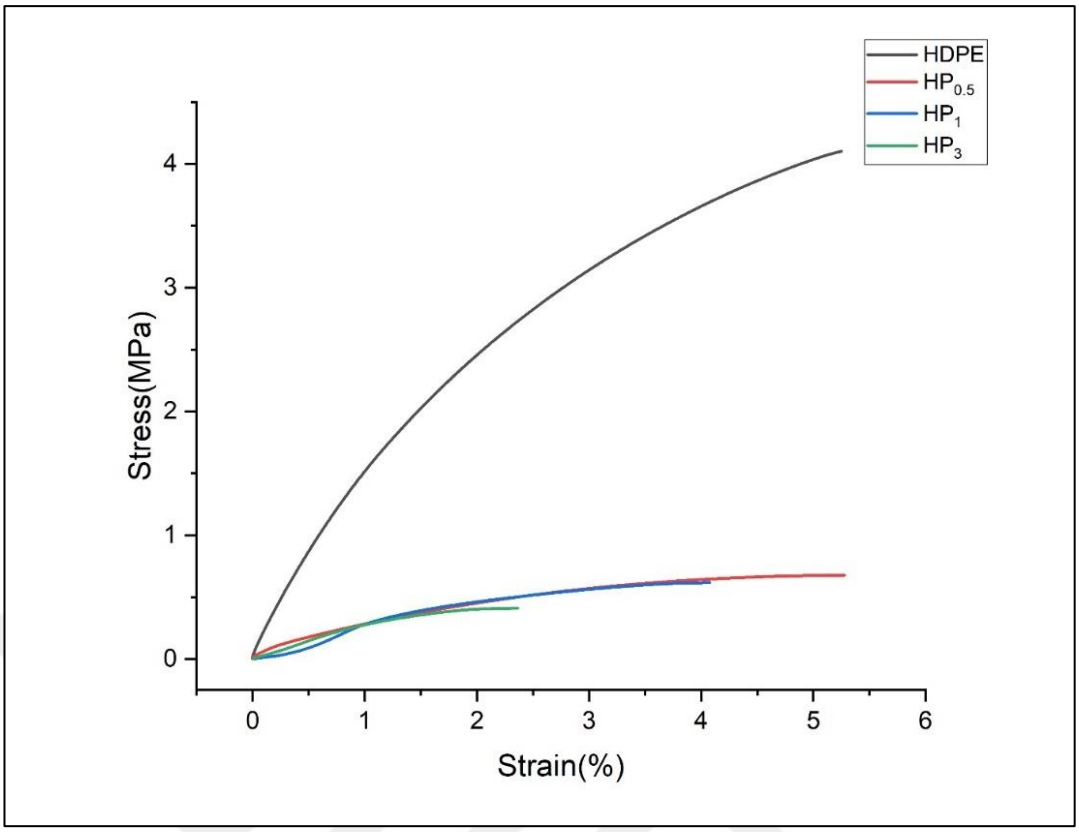

Figure 4.18. Stress-strain curves of HDPE, $HP_{0.5}$, HP_1 and HP_3.

Molecular chains in HDPE are linear, and they are packed closer, which results in strong intermolecular forces and a more crystalline structure (Elhrari, 2018). The mechanical behavior of HDPE was altered by the addition of PANI. Since the PANI is polar and the polyethylene is nonpolar, it may be inferred that there is no adhesion between the phases and that the addition of PANI has a detrimental effect on the mechanical characteristics of the polymer matrix. In conductive polymers, a conjugated carbon chain is made up of alternating single and double bonds (π bonds) which are strongly polarized, delocalized, and electron-dense (Namsheer & Rout, 2021). Due to the conjugated carbon chain of polyaniline, the aggregation of polyaniline particles makes it difficult to establish a proper filler distribution in the HDPE matrix. Therefore, the mechanical properties of blends decrease. Stress and strain values from the curves were summarized in Table 4.12.

Table 4.12. Stress-Strain results of HDPE and its blends.

Sample	Stress (*MPa*)	Strain (%)
Pure HDPE	4.10	5.25
$HP_{0.5}$	0.68	5.27
HP_1	0.62	4.08
HP_3	0.41	2.36

4.3.6. SEM Analysis

The SEM images were taken at different magnifications to examine the morphological features of the samples used in the study. Images were obtained with the ZEISS GEMINI 500 SEM instrument. SEM image of pure HDPE in film form is given in Figure 4.19, which exhibits a continuous homogeneous phase.

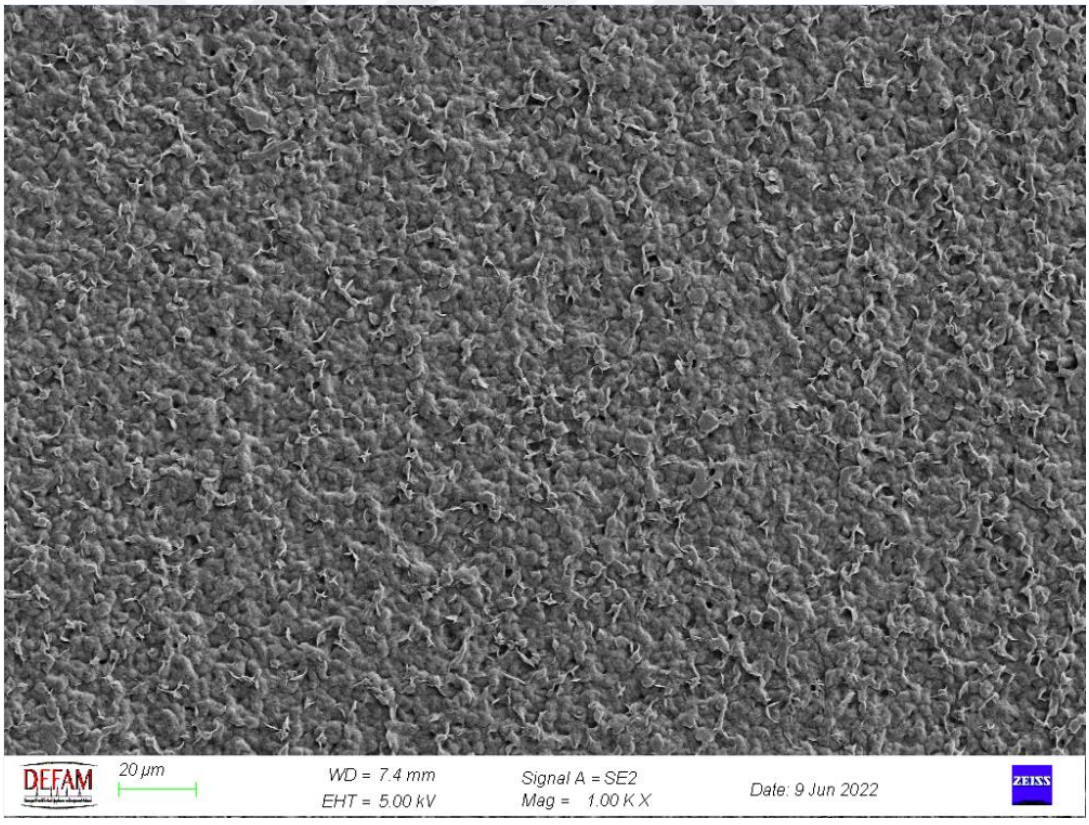

Figure 4.19. SEM Image of HDPE in film form.

SEM images of the blends (Figure 4.20) were examined how much the morphology of the HDPE changed and whether polyaniline aggregated or not. All surface images show different morphologies affected by the increasing PANI content

in HDPE blends. SEM images of $HP_{0.5}$ looks like a spider web with holes. This can be explained that some phase separation is observed when we add 0.5 wt% polyaniline to HDPE. When we increase the amount of polyaniline to 1%, the holes begin to fill and has taken shape like the leaves of the broad bean, when we increase it to 3%, the holes are completely filled, and shapeless agglomerations have begun and and white salt residues are visible on the surface. The intermolecular hydrogen bond N-H···N allowed the chains of PANI to interact closely with one another, and they clearly tended to agglomerate (Zhang et al., 2021).

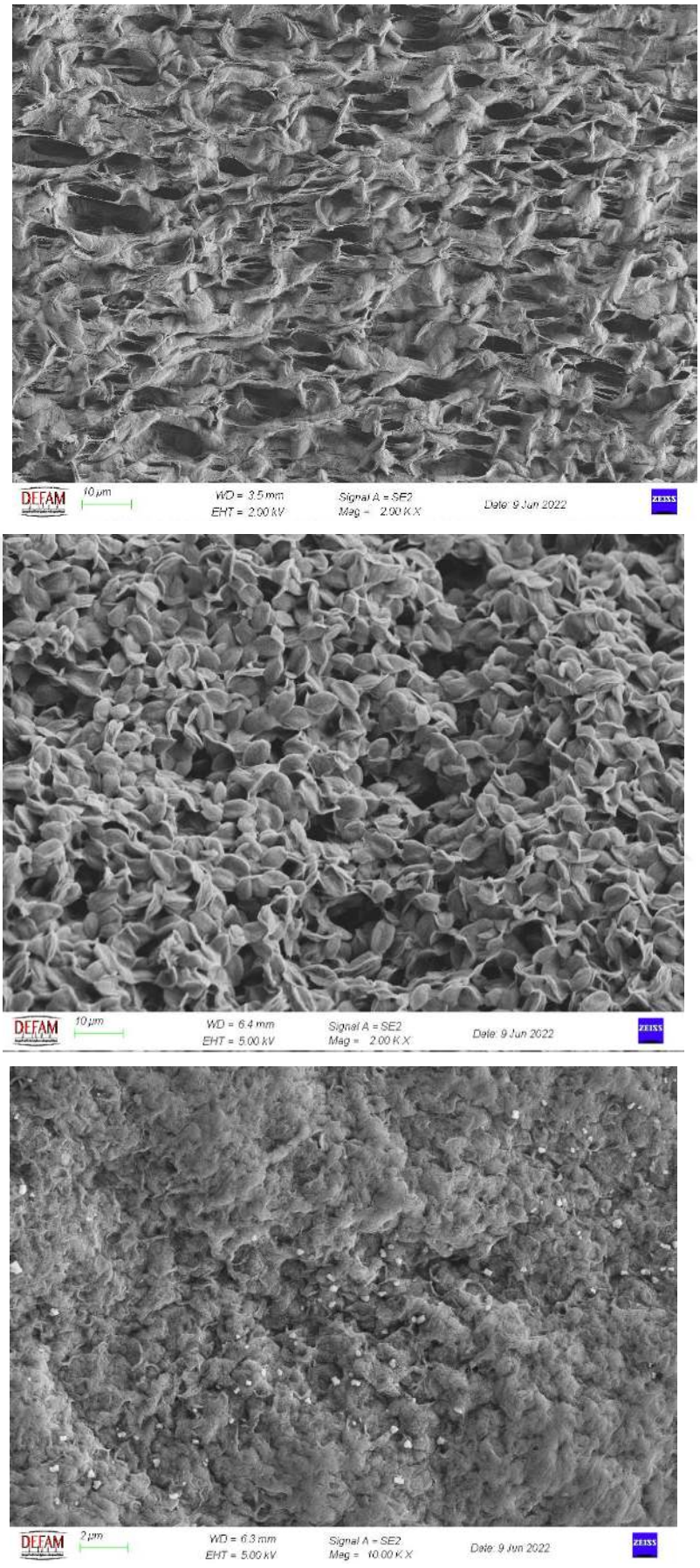

Figure 4.20. SEM Images of $HP_{0.5}$, HP_1 and HP_3 respectively.

4.3.7. Conductivity Measurements

The conductivities of the synthesized materials were measured in film form with a Keithley 2400 electrometer. The conductivities of blends and pure materials at three different temperatures are given in Table 4.13.

Table 4.13. Conductivity Measurements of Blends and Pure Materials.

Sample	Conductivity(24^0C) ($x10^{-10}$S/cm)	Conductivity(35^0C) ($x10^{-10}$S/cm)	Conductivity(50^0C) ($x10^{-10}$S/cm)
Pure HDPE	0.0091	0.063	0.071
$HP_{0.5}$	1.2	12	37
HP_1	4.9	51	63
HP_3	79	230	6700

According to the literature, it is seen that the conductivity value tends to increase as the conductive additive is added (Omastova,' et al., 1996). When we examine the conductivity measurements, it is seen that the conductivity value of HDPE, which is 9.1 10^{-13} S/cm, increases as PANI is added. In addition, when we examine the values in the Table 3, it is seen that the conductivity values increase with the increase in temperature. It is also seen in the literature (Joelma et al., 2007) that materials with a conductivity value within 10^{-6} -10^{-11} S/cm can be used as antistatic materials. The conductivity value of the blends we obtained varies between 10^{-7} and 10^{-10} S/cm. Therefore, all blends can be used as antistatic materials.

4.3.8. Electrostatic Charge Dissipation (ESD) Analysis

The dissipation time of static charge accumulation on the surface of the blends were determined. Various positive (3, 6, and 9 kV) and negative (3, -6, and -9 kV) corona voltages were applied to the blend's surface at ambient temperature. We detect the dissipation time of static charge accumulation on the surface of the blends. Firstly, ESD analysis of pure HDPE was carried out. It was observed that the HDPE surface could accept remarkably high surface voltages in both the positive and negative polarity of the charge decay time. As predicted, the static charge dissipation time (up

to 300 seconds) for aggregation on the surface of HDPE could not be measured. The results obtained from the measurements are summarized in Table 4.14.

Table 4.14. Polarity values of pure HDPE at various corona voltages.

Corona voltage *(V)*	Corona time *(s)*	Surface humidity *(%RH)*	Surface temperature *(^{0}C)*	Surface voltage *(V)*	1/e time *(s)*	%10 Cut-off time *(s)*	Surface charge *(nC)*	Capacitans
-9000	0.030	36.8	28.5	-2408.9	nr	nr	-47.85	8.54
-6000	0.030	34.6	29.1	-771.2	nr	nr	0.97	0.54
-3000	0.008	34.6	29.1	-425.8	nr	nr	-1.82	1.85
3000	0.008	33.6	28.2	-152.3	nr	nr	-2.034	5.703
6000	0.030	33.3	27.5	1568.7	nr	nr	1.02	0.28
9000	0.030	35.6	27.2	1864.4	nr	nr	53.62	12.35

nr:not reached

The length of time the static charge dissipates determines how well antistatic material performs. ESD performance is determined by the charge decay time of 10% of the voltage value or the charge decay time of 1/e, which is equivalent to around 37% of the voltage value. Therefore, any material which showed 1/e and 10% cut time standards smaller than 1s and 2s respectively, passes the requirements for usage as antistatic material. (Doğan et al., 2018).

With respect to the performance of various $HP_{0.5}$ corona voltages as given in Table 4.15, the blend at 3 kV corona voltage may be utilized as an ESD control material based on the 1/e criterion (1/e time: 1.029 s for 3 kV). Additionally, the "blend" had a cut-off time of roughly 2 s (%10 cut-off time: 2.385 s for 3kV).

Table 4.15. ESD values of $HP_{0.5}$ at various corona voltages.

Corona voltage *(V)*	Corona time *(s)*	Surface humidity *(%RH)*	Surface temperature *(^0C)*	Surface voltage *(V)*	1/e time *(s)*	%10 Cut-off time *(s)*	Surface charge *(nC)*	Capacitans
-9000	0.030	36.0	28.5	-2391.0	31.150	31.275	-22.95	4.13
-6000	0.030	35.2	29.8	-1495.6	nr	nr	-13.78	3.96
-3000	0.008	32.9	29.8	-385.9	54.636	54.761	-2.55	2.85
3000	0.020	32.4	22.0	418.6	1.029	2.385	nr	nr
6000	0.030	29.4	27.8	2241.9	nr	nr	-0.11	0.03
9000	0.030	34.2	26.9	1941.0	nr	nr	45.14	9.99

nr:not reached

Table 4.16 presents the performance of HP_1 at various corona voltages. The blend at 3 kV corona voltage (1/e time: 1.033 s; %10 cut-off time: 2.393s) could be used as ESD material according to the 1/e time and %10 cut-off time criterion.

Table 4.16. ESD values of HP_1 at various corona voltages.

Corona voltage *(V)*	Corona time *(s)*	Surface humidity *(%RH)*	Surface temperature *(^0C)*	Surface voltage *(V)*	1/e time *(s)*	%10 Cut-off time *(s)*	Surface charge *(nC)*	Capacitans
-9000	0.030	36.4	29.1	-2534.3	nr	nr	-33.96	5.76
-6000	0.030	36.2	29.4	-1519.0	48.026	48.026	-11.69	3.31
-3000	0.009	34.4	29.8	-370.1	39.526	39.526	-2.79	3.25
3000	0.020	32.4	22.4	403.4	1.033	2.393	nr	nr
6000	0.030	34.0	27.8	1926.2	29.400	29.463	1.69	0.38
9000	0.030	35.3	26.9	2143.2	nr	nr	32.38	6.49

nr:not reached

When the ESD values of HP_3 given in Table 4.17 at various corona voltages are examined, the blend at 3 kV Corona voltage, according to the 1/e time (1.025 s) and %10 cut-off time (2.361 s) could be used as an antistatic material.

Table 4.17. ESD values of HP_3 at various corona voltages.

Corona voltage *(V)*	Corona time *(s)*	Surface humidity *(%RH)*	Surface temperature *(^0C)*	Surface voltage *(V)*	1/e time *(s)*	%10 Cut-off time *(s)*	Surface charge *(nC)*	Capacitans
-9000	0.030	36.8	28.8	-2158.8	nr	nr	-57.87	11.52
-6000	0.030	34.9	29.1	-1516.4	nr	nr	-10.81	3.07
-3000	0.009	33.1	29.8	-368.5	71.338	71.588	-3.09	3.61
3000	0.020	32.4	22.4	-691.7	1.025	2.361	nr	nr
6000	0.030	35.1	27.5	1747.1	nr	nr	-0.13	0.04
9000	0.030	34.8	26.9	2083.1	nr	nr	35.74	7.37

nr:not reached

5. SUMMARY AND FUTURE WORK

Within the scope of this study, firstly, the emeraldine form of polyaniline was synthesized. The conductivity of polyaniline synthesized at 0°C was measured as $4.5x10^{-6}$ S/cm.

We have previously mentioned that polyaniline can exist in three different redox states: leucomeraldine, emeraldine (salt/base) and pernigraniline. Leucoemeraldine is composed of only benzenoid group, pernigraniline is composed of quinoid. Emeraldine consists of alternating reduced units (benzenoid) and oxidized units (quinoid). When the FTIR spectrum is examined, benzoid and quinoid ring vibrations are clearly seen in both spectra at 1468 cm^{-1} and 1566 cm^{-1} respectively. It was thought that the prominent peak at 1114 cm^{-1} indicated electron delocalization, making it a characteristic related to PANI conductivity.

TGA analysis of polyaniline showed a typical three step decomposition behavior. In the first step at approximately 100 °C, 8% weight loss is seen which attributed to loss of water. Second weight loss which is 18% may attributed to deprotonation of PANI. Last weight loss which is 34% represents the chain break of the polyaniline.

DSC analysis showed that polyaniline powder had a notable moisture content which are supported with the TGA results. These irreversible thermal transitions make finding the glass transition temperature difficult. MDSC seperates the reversing (melting, heat capacity and glass transition) and non-reversing heat flow (evaporation, crystallization, decomposition, cross-linking…) so glass transition temperature was found at 254.6°C.

In X-ray diffraction spectra, two small peaks were observed above the broad peak due to the almost amorphous structure of polyaniline.

SEM image of polyaniline showed cottony coral like appearance and there are networks which can be the reason of charge transport and the conductivity.

In the second part of the study low density polyethylene/polyaniline blends were prepared according to the solution blending method. Our goal is to give LDPE conductive properties for use in antistatic applications. To comprehend each polymer's interaction, a number of analyses were carried out.

Polymer blends are mixtures made from two or more polymers that have been physically combined rather than chemically bound. The goal of blending the polymers is to create new materials that have better properties than the individual components' physical attributes. Infrared spectroscopy showed that there are specific peaks of both materials, and this is the proof that these materials are physically blended. Most likely, because polymer blends are physically blended, host polymer allow electron transfer and acquires conductive properties due to double bonds of polyaniline.

Thermal gravimetric analysis of blends showed two-step weight loss behavior. First one is due to the solvent evaporation and second degradation is caused by decomposition of LDPE. The general expectation from additives is to obtain a blends without changing the thermal properties of the host polymer. It was observed that the temperature values corresponding to the highest degradation rate of pure LDPE and LP0.5, LP1and LP3 were around 478°C. This indicates that there is no change in thermal stability.

Since PANI and LDPE are immiscible, the amount of polyaniline does not seem to have a substantial effect on the melting temperature of LDPE. The addition of PANI to the LDPE matrix resulted in a melting temperature drop of about 1°C. However, the degree of LDPE crystallinity dramatically reduced as the amount of PANI in the blends increases. Since polyaniline is amorphous, the amorphous phase of the blends will expand, which means that as polyaniline concentration rises, the percentage of crystallinity in the composites will progressively decrease. It was also evident from the SEM images that polyaniline particles tended to gather to one side. This tendency makes it difficult for polyaniline to disperse well in LDPE. This aggregation is the reason why the crystallinity percentage and even mechanical properties decrease. According to the stress-strain results, there is a decrease in mechanical properties.

When X-ray diffraction patterns are examined, two distinct diffraction peaks similar to those of LDPE are seen. XRD patterns of all LDPE/PANI blends indicated the distinctive peaks of LDPE at approximately 21°, and 23° and other peaks.

SEM images of blends indicate that the solid particles started to agglomerate with the addition of pani to LDPE which was completely smooth. Beside these cluster of solid particles, LDPE blend, which is doped with 3 wt% polyaniline, shows regular structures and micro-channels resembling hexagons.

The conductivities of blends were measured at three different temperatures. The conductivity values increased as the temperature increases. It was previously stated that materials with conductivity values of 10^{-6} -10^{-11} S/cm can be used as antistatic materials. The conductivity values of the blends were found to be between 10^{-9} and 10^{-6} S/cm therefore, all blends can be used as antistatic material.

ESD analyzes were performed for antistatic applications. At room temperature, various positive (3, 6, 9 kV) and negative corona voltages (-3, -6, -9 kV) applied to the surface of the blends. The dissipation time of static charges accumulation on the surface of the blends were determined. At -3kV, 3kV and 6kV Corona voltage $LP_{0.5}$ blend and LP_3 blend could be used as antistatic material. LP_1 blend at 3kV corona voltage could be used as ESD material according to the 1/e and %10 cut-off time criterion.

Finally, HDPE/PANI blends were prepared by the solution blending method. To understand the interaction between PANI and HDPE, analyzes started with FTIR spectroscopy. According to the infrared spectrum, there are specific peaks of both materials, and this is the proof that these materials are physically blended.

Blends showed a two-step decomposition behavior, first step is thought to be due to solvent evaporation and second one is the breakdown of the blend's backbone structure. Based on DTG analysis, there is an increase of approximately 1°C at the maximum rate of decomposition. As a result, the degradation of HDPE will shift to higher temperatures.

DSC analysis indicated that, the addition of PANI to the LDPE matrix resulted in a melting temperature drop of about 1°C. However, the degree of LDPE crystallinity dramatically reduces as the amount of PANI in the blends increases. Since polyaniline is amorphous, the amorphous phase of the blends will expand, which means that as polyaniline concentration rises, the percentage of crystallinity in the composites will progressively decrease.

Two separate diffraction peaks that resemble pure HDPE are visible when X-ray diffraction patterns of blends are analyzed. XRD patterns of all HDPE/PANI blends indicated the distinctive peaks of HDPE at approximately 21°, and 23° and other peaks.

Molecular chains in HDPE are linear, and they are packed closer, which results in strong intermolecular forces and a more crystalline structure. Polyaniline tends to aggregate due to its structure. Therefore, the aggregation of polyaniline particles makes it difficult to establish a proper filler distribution in the HDPE matrix. Therefore, the mechanical properties of blends decrease.

It is clearly seen in the SEM images that as we add PANI to pure HDPE, a spider web appearance has begun to form. When we increased the amount of PANI, shapes similar to broad bean leaves were formed and finally shapeless agglomerations have begun and white salt residues are visible on the surface.

Conductivity measurements of the blends were made at three different temperatures. As the temperature increased, the conductivity of the blends also increased. Conductivity values between 10^{-7} and 10^{-10} S/cm were obtained, which are sufficient conductivity values to be used as an ESD material.

ESD analyses were carried out for antistatic applications. Various positive (3, 6, and 9 kV) and negative (-3, -6, and -9 kV) corona voltages were applied to the blend's surface at room temperature. The blends' surface static charge buildup dissipation time was determined. It has been observed that all PANI/HDPE blends at 3kV corona voltage can be used as ESD materials according to the 1/e time and 10% cut-off time criteria.

In light of the information mentioned above, the highest conductivity value at room temperature was obtained in the LP_3 blend and it was observed that all blends can be used as an effective ESD materials at 3kV. Blends of LDPE/PANI and HDPE/PANI may be suitable options for various kinds of electrical and electronic applications. The blends in this dissertation study were prepared by the solution blending method. In future studies, the two methods can be compared by preparing blends with a laboratory type single screw extruder. In addition, since conductive polymers have many application areas today, antistatic, and electromagnetic shielding applications can be studied by preparing blends of polyolefins and other conductive polymers.

6. REFERENCES

Abd Razak, S. I., Wan Abdul Rahman, W. A., Hashim, S., & Yahya, M. Y. (2014). Polyaniline and their Conductive Polymer Blends: A Short Review. *Malaysian Journal of Fundamental and Applied Sciences*, *9*(2). https://doi.org/10.11113/mjfas.v9n2.86

Abdelwahab, N. A., El-Nashar, D. E., & El-Ghaffar, M. A. A. (2011). Polyfuran, polythiophene and their blend as novel antioxidants for styrene- butadiene rubber vulcanizates. *Materials and Design*, *32*(1), 238–245. https://doi.org/10.1016/j.matdes.2010.06.003

Abraham, D., Bharathi, A., & Subramanyam, S. V. (1996). Highly conducting polymer blend films of polyaniline and nylon 6 by cosolvation in an organic acid. *Polymer Communications*, 37(23), 5295-5299

Akbari, M., Zadhoush, A., & Haghighat, M. (2007). PET/PP blending by using PP-g-MA synthesized by solid phase. *Journal of Applied Polymer Science*, *104*(6), 3986–3993. https://doi.org/10.1002/app.26253

Andrew Peacock. (2000). Handbook of polyethylene: Structures, properties, and applications. Marcel Dekker Inc.

A.R. West. (1987). Solid state chemistry and its applications (East Kilbride, Ed.). John Wiley & Sons Ltd.

Barlow, J. W., & Paul, D. R. (1981). Polymer blends and alloys—a review of selected considerations. *Polymer Engineering & Science*, *21*(15), 985–996. https://doi.org/10.1002/pen.760211502

Benabid, F. Z., Kharchi, N., Zouai, F., Mourad, A. H. I., & Benachour, D. (2019). Impact of co-mixing technique and surface modification of ZnO nanoparticles using stearic acid on their dispersion into HDPE to produce HDPE/ZnO

nanocomposites. *Polymers and Polymer Composites*, *27*(7), 389–399. https://doi.org/10.1177/0967391119847353

Beşergil, B. (2008) Polimer kimyası. Gazi Kitabevi

Bhadra, J., Al-Thani, N. J., Madi, N. K., & Al-Maadeed, M. A. (2016). High performance sulfonic acid doped polyaniline–polystyrene blend ammonia gas sensors. *Journal of Materials Science: Materials in Electronics*, *27*(8), 8206–8216. https://doi.org/10.1007/s10854-016-4825-6

Bhadra, S., & Khastgir, D. (2009). Glass-rubber transition temperature of polyaniline: Experimental and molecular dynamic simulation. *Synthetic Metals*, *159*(12), 1141–1146. https://doi.org/10.1016/j.synthmet.2009.01.052

Bhadra, S., Khastgir, D., Singha, N. K., & Lee, J. H. (2009). Progress in preparation, processing and applications of polyaniline. In *Progress in Polymer Science (Oxford)* (Vol. 34, Issue 8, pp. 783–810). https://doi.org/10.1016/j.progpolymsci.2009.04.003

Bhandari, S. (2017). In Polyaniline Blends, Composites, and Nanocomposite. Elsevier. https://doi.org/10.1016/B978-0-12-809551-5.00002-3

Buehler, F. U., Martin, C. J., & Seferis, J. C. (1998). Temperature-Modulated Differential Scanning Calorimetry Through Heat Diffusion Analysis. *Journal of Thermal Analysis*, *54*, 501–519.

Choudhary, H. K., Kumar, R., Patangrao Pawar, S., Anupama, A. V, Bose, S., & Sahoo, B. (2018). Effect of Coral-Shaped Yttrium Iron Garnet Particles on the EMI Shielding Behaviour of Yttrium Iron Garnet-Polyaniline-Wax Composites.*Chemistry Selec,*3,2120-2130.

Das, M., Sethy, P. P., & Sundaray, B. (2023). EMI shielding performance of graphene oxide reinforced polyaniline/polystyrene solution cast thin films. *Synthetic Metals*, *296*. https://doi.org/10.1016/j.synthmet.2023.117369

Depan, D., Chirdon, W., & Khattab, A. (2021). Morphological and chemical analysis of low-density polyethylene crystallized on carbon and clay nanofillers. *Polymers*, *13*(10). https://doi.org/10.3390/polym13101558

Deshmukh, K., Kovářík, T., Muzaffar, A., Basheer Ahamed, M., & Khadheer Pasha, S. K. (2020). In Polymer Science and Innovative Applications: Materials, Techniques, and Future Developments. Elsevier. https://doi.org/10.1016/B978-0-12-816808-0.00004-4

Dey, S., & Kar, A. K. (2019). Enhanced photoluminescence through Forster resonance energy transfer in Polypyrrole-PMMA blends for application in optoelectronic devices. *Materials Science in Semiconductor Processing*, *103*. https://doi.org/10.1016/j.mssp.2019.104644

Ding, L., Wang, X., & Gregory, R. V. (1999). Thermal properties of chemically synthesized polyaniline EB powder. *Synthetic Metals*, 104, 73-78.

Doğan, F., Şirin, K., Kolcu, F., & Kaya, İ. (2018). Conducting polymer composites based on LDPE doped with poly(aminonaphthol sulfonic acid). *Journal of Electrostatics*, *94*, 85–93. https://doi.org/10.1016/j.elstat.2018.07.004

Elhrari, W. (2018). The Influence of LDPE Content on the Mechanical Properties of HDPE/LDPE Blends. *Research & Development in Material Science*, *7*(5),1-7. https://doi.org/10.31031/rdms.2018.07.000672

Epp, J. (2016). X-Ray Diffraction (XRD) Techniques for Materials Characterization. In Materials Characterization Using Nondestructive Evaluation (NDE) Methods (pp. 81–124). Elsevier Inc. https://doi.org/10.1016/B978-0-08-100040-3.00004-3

Erdoğan, M. K., Karakişla, M., & Saçak, M. (2012). Preparation, characterization and electromagnetic shielding effectiveness of conductive polythiophene/poly(ethylene terephthalate) composite fibers. *Journal of*

Macromolecular Science, Part A: Pure and Applied Chemistry, *49*(6), 473–482. https://doi.org/10.1080/10601325.2012.676896

Ezzati, N., Asadi, E., Abdouss, M., & Ezzati, M. H. (2017). Polyaniline Nano-/Micromaterials–Based Blends and Composites. In *Polyaniline Blends, Composites, and Nanocomposites* (pp. 95–115). Elsevier. https://doi.org/10.1016/B978-0-12-809551-5.00004-7

Gulmine, J. V, Janissek, P. R., Heise, H. M., & Akcelrud, L. (2002). Test method Polyethylene characterization by FTIR. In *Polymer Testing*, 21,557-563.

Heeger, A. J. (2001). Semiconducting and metallic polymers: The fourth generation of polymeric materials. *Journal of Physical Chemistry B*, *105*(36), 8475–8491. https://doi.org/10.1021/jp011611w

Hideki Shirakawa, B., Louis, E. J., Macdiarmid, A. G., W A N K Chiang, C. H., & Heeger, A. J. (1977). Synthesis of Electrically Conducting Organic Polymers : Halogen Derivatives of Polyacetylene, (CH), *J.C.S. Chem. Comm, 578-580.*

Hwang, Y.-C. (2004). Electrostatic discharge and electrical overstress failures of non-silicon devices, dissertation, Maryland University, Maryland.

Ivanov, S., Mokreva, P., Tsakova, V., & Terlemezyan, L. (2003). Electrochemical and surface structural characterization of chemically and electrochemically synthesized polyaniline coatings. *Thin Solid Films*, *441*(1–2), 44–49. https://doi.org/10.1016/S0040-6090(03)00880-0

Joelma, M., Cardoso, R., Fogliato, M., Lima, S., & Lenz, D. M. (2007). Polyaniline Synthesized with Functionalized Sulfonic Acids for Blends Manufacture. In *Materials Research* (Vol. 10, Issue 4).

Joong T.Jeevananda, S. and J. H. L. (2018). Fabrication of carbon black/HDPE/polyaniline functionalized multi-walled carbon nanotube composites for enhancing PTC characteristics. In *Materials Today: Proceedings*

(Vol. 5). www.sciencedirect.comwww.materialstoday.com/proceedings2214-7853

Khan, S. A., Khan, S. B., Khan, L. U., Farooq, A., Akhtar, K., & Asiri, A. M. (2018). Fourier transform infrared spectroscopy: Fundamentals and application in functional groups and nanomaterials characterization. In *Handbook of Materials Characterization* (pp. 317–344). Springer International Publishing. https://doi.org/10.1007/978-3-319-92955-2_9

Kim, B. J., Oh, S. G., Han, M. G., & Im, S. S. (2001). Synthesis and characterization of polyaniline nanoparticles in SDS micellar solutions. *Synthetic Metals*, *122*(2), 297–304. https://doi.org/10.1016/S0379-6779(00)00304-0

Kondawar, S. B., & Patil, P. T. (2017). Conducting Polymer Nanocomposites for Sensor Applications, *Springer,* 223–267. https://doi.org/10.1007/978-3-319-46458-9_8

Kondratiev, V. V., & Holze, R. (2021). Intrinsically conducting polymers and their combinations with redox-active molecules for rechargeable battery electrodes: an update. *Chemical Papers*, 75(10), 4981–5007. https://doi.org/10.1007/s11696-021-01529-7

Kuleyin, H., Gümrük, R., & Çalişkan, S. (2022). The effect of ABS fraction on the fatigue behavior of PMMA/ABS polymer blends. *Materials Today Communications*, *33*. 104139.https://doi.org/10.1016/j.mtcomm.2022.104139

Kulkarni, M. V., & Viswanath, A. K. (2004). Comparative studies of chemically synthesized polyaniline and poly(o-toluidine) doped with p-toluene sulphonic acid. *European Polymer Journal*, *40*(2), 379–384. https://doi.org/10.1016/j.eurpolymj.2003.10.007

Kumar, V., Kalia, S., & Swart, H. C. (2017). Conducting Polymer Hybrids. Springer. http://www.springer.com/series/13173

Li, D., Zhou, L., Wang, X., He, L., & Yang, X. (2019). Effect of crystallinity of polyethylene with different densities on breakdown strength and conductance property. *Materials*, *12*(11), 1746. https://doi.org/10.3390/ma12111746

Li, Y., & Wang, X. (2012). Semiconducting Polymer Composites: Principles, Morphologies, Properties and Applications. Wiley-VCH Verlag GmbH & Co. KGaA. https://doi.org/10.1

María, M., Percino, J., Ictor, V. ´, & Chapela, M. (2013). Handbook of Polymer Synthesis, Characterization, and Processing. John Wiley & Sons, Inc.

Michael Dunlap & J. E. Adaskaveg. (1997). Introduction to the Scanning Electron Microscope.

Mishra, A. K. (2018). Conducting Polymers: Concepts and Applications. *Journal of Atomic, Molecular, Condensate and Nano Physics*, *5*(2), 159–193. https://doi.org/10.26713/jamcnp.v5i2.842

Molapo, K. M., Ndangili, P. M., Ajayi, R. F., Mbambisa, G., Mailu, S. M., Njomo, N., Masikini, M., Baker, P., & Iwuoha, E. I. (2012). Electronics of Conjugated Polymers (I): Polyaniline. *International Journal of Electrochemistry*, 7, 11859-11875. www.electrochemsci.org

Moučka, R., Mravčáková, M., Vilčáková, J., Omastová, M., & Sáha, P. (2011). Electromagnetic absorption efficiency of polypropylene /montmorillonite /polypyrrole nanocomposites. *Materials and Design*, *32*(4), 2006–2011. https://doi.org/10.1016/j.matdes.2010.11.064

Namsheer, K., & Rout, C. S. (2021). Conducting polymers: a comprehensive review on recent advances in synthesis, properties and applications. *RSC Advances,* 11(10), 5659–5697. https://doi.org/10.1039/d0ra07800j

Nand, A. V., Ray, S., Travas-Sejdic, J., & Kilmartin, P. A. (2012). Characterization of antioxidant low density polyethylene/polyaniline blends prepared via extrusion. *Materials Chemistry and Physics*, *135*(2–3), 903–911. https://doi.org/10.1016/j.matchemphys.2012.05.077

Nguyen, H. D., Nguyen, T. H., Hoang, N. V., Le, N. N., Nguyen, T. N. N., Doan, D. C. T., & Dang, M. C. (2014). pH sensitivity of emeraldine salt polyaniline and poly(vinyl butyral) blend. *Advances in Natural Sciences: Nanoscience and Nanotechnology*, *5*(4), 045001-0455006. https://doi.org/10.1088/2043-6262/5/4/045001

Novak, D., Plavan, V., & Bereznenko, N. (2019). Copper plated graphite, carbon nanotubes and polyaniline effect on the properties of electroconductive polyethylene compositions. *Materials Today: Proceedings*, *6*, 293–298. https://doi.org/10.1016/j.matpr.2018.10.107

Oliveira, L. B., Graeff, C. Z., Faria, P. V., Backes, E. H., Cristovan, F. H., & Passador, F. R. (2016). Preparation and characterization of conductive HDPE/LLDPE/Polyaniline blends. *AIP Conference Proceedings*, 1779, 080010-080015. https://doi.org/10.1063/1.4965554

Omastova, M., Kogna, S., Pionteck ', J., Janke ', A., & Pavlinec, J. (1996). Electrical properties and stability of polypyrrole containing conducting polymer composites. In *Synthetic MetaIs*, 81, 49-57.

Omastova, M., Pionteck, J., & Kosina, S. (1996). Preparation and characterization of electrically conductive polypropylene /polypyrrole composites. In *Eur. Polym. J.*, 32 (6), 681-689.

Passador, F. R., de Faria, P. V., Backes, E. H., Montanheiro, T. L. A., Montagna, L. S., de Souza Pinto, S., Pessan, L. A., & Rezende, M. C. (2017). Thermal, mechanical and electromagnetic properties of LLDPE/PANI composites. *Polymer Bulletin*, *74*(7), 2701–2717. https://doi.org/10.1007/s00289-016-1862-5

Pionteck, J. (2016). Handbook of Antistatics (pp. 1–15). Elsevier. https://doi.org/10.1016/b978-1-895198-95-9.50003-0

Posch, D. W. (2016). Applied plastics engineering handbook: processing, materials, and applications. (27–52). Elsevier Inc. https://doi.org/10.1016/B978-0-323-39040-8.00002-X

Pötschke, P., & Pionteck, J. (2016). Mechanisms of action of antistatic agents. In *Handbook of Antistatics* (83–101). Elsevier. https://doi.org/10.1016/b978-1-895198-95-9.50008-x

Prime, R. B., Vyazovkin, S., Gallagher, P. K., & Riga, A. (2009). Thermal Analysis of Polymers: Fundamentals and Applications, John Wiley & Sons, Inc.

Pud, A., Ogurtsov, N., Korzhenko, A., & Shapoval, G. (2003). Some aspects of preparation methods and properties of polyaniline blends and composites with organic polymers. In *Progress in Polymer Science (Oxford)*, 28(12), 1701–1753). https://doi.org/10.1016/j.progpolymsci.2003.08.001

Rashid, I. A., Hamza, A., Asim, S., Zubair, K., Shakir, H. F., Afzal, A., & Zubair, Z. (2023). Achieving enhanced electromagnetic shielding by novel flexible rubber based nanocomposite with the incorporation of nickel spinal ferrites and polyaniline. *Synthetic Metals*, 295, 117339. https://doi.org/10.1016/j.synthmet.2023.117339

Romero, J. A., Azarian, M. H., & Pecht, M. (2020). Life model for tantalum electrolytic capacitors with conductive polymers. *Microelectronics Reliability*, 104, 113550. https://doi.org/10.1016/j.microrel.2019.113550

Saini, P., & Choudhary, V. (2013). Electrostatic charge dissipation and electromagnetic interference shielding response of polyaniline based conducting fabrics. In *Indian Journal of Pure & Applied Physics*, 51, 112-117.

Saltan, F., Şentürk, S., Al, A. M., Özkan, A. N., & Şirin, K. (2023). Preparation, characterization and thermal properties of polypropylene/polyethylene/zinc borate composites: investigation of thermal degradation kinetics. *Journal of Polymer Research*, *30*(10), 391. https://doi.org/10.1007/s10965-023-03762-y

Sanches, E. A., Da Silva, J. M. S., Ferreira, J. M. D. O., Soares, J. C., Dos Santos, A. L., Trovati, G., Fernandes, E. G. R., & Mascarenhas, Y. P. (2014). Nanostructured Polyaniline Emeraldine-base form (EB-PANI): a structural investigation for different neutralization times. *Journal of Molecular Structure*, *1074*, 732–737. https://doi.org/10.1016/j.molstruc.2014.05.046

Sauter, D. W., Taoufik, M., & Boisson, C. (2017). Polyolefins, a success story. In *Polymers* 9(6), 185. https://doi.org/10.3390/polym9060185

Sharaf, S. M. (2020).Advances in Functional and Protective Textiles. (141–167). Elsevier. https://doi.org/10.1016/b978-0-12-820257-9.00007-2

Sirin, K. (2008). Preparatıon of polymer blends and their composites, and determination of their properties, dissertation, Ege University, İzmir.

Sirin, K., M., Zeybek, M. S. & Abali, Y. (2022). Effect of gamma irradiation on the thermal and mechanical behaviour of polypropylene and polyethylene blends. In *Radiation Physics and Chemistry*, 194, 110034. https://doi.org/10.1016/j.radphyschem.2022.110034

Sivakkumar, S. R., Howlett, P. C., Winther-Jensen, B., Forsyth, M., & MacFarlane, D. R. (2009). Polyterthiophene/CNT composite as a cathode material for lithium batteries employing an ionic liquid electrolyte. *Electrochimica Acta*, *54*(27), 6844–6849. https://doi.org/10.1016/j.electacta.2009.06.091

Sogancioglu, M., Yel, E., & Ahmetli, G. (2017). Pyrolysis of waste high density polyethylene (HDPE) and low density polyethylene (LDPE) plastics and production of epoxy composites with their pyrolysis chars. *Journal of Cleaner Production*, *165*, 369–381. https://doi.org/10.1016/j.jclepro.2017.07.157

Stejskal, J., Trchová, M., Bober, P., Humpolíček, P., Kašpárková, V., Sapurina, I., Shishov, M. A., & Varga, M. (2015). Conducting Polymers: Polyaniline. In Encyclopedia of Polymer Science and Technology (1–44). John Wiley & Sons, Inc. https://doi.org/10.1002/0471440264.pst640

Streetman, B. G., Sanjay & Banerjee, K. (2016). Solid state electronic devices. Pearson.

Taherian, R. (2018). Electrical conductivity in polymer-based composites: Experiments, modelling, and applications (1–18). Elsevier. https://doi.org/10.1016/B978-0-12-812541-0.00001-X

Tambakoozadeh, N., Youssefi, M., & Semnani, D. (2019). A composite polyaniline/graphene–coated polyamide6 nanofiber mat for electrochemical applications. *Polymers for Advanced Technologies*, *30*(11), 2819–2826. https://doi.org/10.1002/pat.4714

Thomas, S., Durand, D., Chassenieux, C., & Jyotishkumar, P. (2010). Handbook of biopolymer-based materials from blends and composites to gels and complex networks, Wiley-VCH Verlag GmbH & Co. KGaA.

Udayaraj, S., Annappa, M., Roopa, K. V., Mathad, G., Subramanya, K., & Pavithra, G. M. (2023). Optical, structural and conductivity properties of ferrous sulfate doped polyaniline. *Materials Today: Proceedings*. https://doi.org/10.1016/j.matpr.2023.05.384

Utracki, L. A. (2002). Polymer blends handbook. Kluwer Academic Publishers.

Vernon-Parry, K. D. (2000). Scanning Electron Microscopy: an introduction. *Analysis*, 1(4),40-44

Waremra, R. S., & Betaubun, P. (2018). Analysis of Electrical Properties Using the four point Probe Method. *ICENIS*, 73,13019 https://doi.org/10.1051/e3sconf/201873

Yadegari, A., Morshedian, J., Khonakdar, H.-A., & Wagenknecht, U. (2016). Influence of annealing on anisotropic crystalline structure of HDPE cast films. *Polyolefins Journal*, *3*(1), 1–9.

Yildirim, A., Tarkuc, S., Ak, M., & Toppare, L. (2008). Syntheses of electroactive layers based on functionalized anthracene for electrochromic applications. *Electrochimica Acta*, *53*(14), 4875–4882. https://doi.org/10.1016/j.electacta.2008.02.026

Yilmaz, F. (2007). Polyaniline: Synthesis, characterization, solution properties and composites, dissertation, Middle East Technical University, Ankara.

Yu, H., Xu, Z., Fang, T., Zhang, M., Xu, Y., Liu, J., & Tan, X. (2024). Preparation and corrosion resistance of polyaniline and waterborne polyurethane composite coating film. *Polymers for Advanced Technologies*, *35*(2), 6307. https://doi.org/10.1002/pat.6307

Zengin, H., Zhou, W., Jin, J., Czerw, R., Smith, D. W., Echegoyen, L., Carroll, D. L., Foulger, S. H., & Ballato, J. (2002). Carbon nanotube doped polyaniline. *Advanced Materials*, *14*(20), 1480–1483. https://doi.org/10.1002/1521-

Zhang, C., Kong, X., Liu, W., Yang, J., & Zhao, H. (2021). Regulation of PANI nanofiber conductivity and its influence on the DC dielectric properties of LDPE. *Polymer Testing*, 101, 107299. https://doi.org/10.1016/j.polymertesting.2021.107299

Zhang, Q. H., Wang, X. H., Chen, D. J., & Jing, X. Bin. (2004). Electrically conductive, melt-processed ternary blends of polyaniline/dodecylbenzene sulfonic acid, ethylene/vinyl acetate, and low-density polyethylene. *Journal of*

Polymer Science, Part B: Polymer Physics, *42*(20), 3750–3758. https://doi.org/10.1002/polb.20241

Zhang, Y., Pan, T., & Yang, Z. (2020). Flexible polyethylene terephthalate /polyaniline composite paper with bending durability and effective electromagnetic shielding performance. *Chemical Engineering Journal*, *389,* 124433. https://doi.org/10.1016/j.cej.2020.124433

Zhao, yanjun, Yao, W., Wang, Y., Wang, Q., Lou, F., & Guo Weihong. (2019). High-performance antistatic acrylic coating by incorparation with modified graphene. *Journal of Materials Research*, *34*(4), 510–518.

Zhu, A., Wang, H., Sun, S., & Zhang, C. (2018). The synthesis and antistatic, anticorrosive properties of polyaniline composite coating. *Progress in Organic Coatings*, *122*, 270–279. https://doi.org/10.1016/j.porgcoat.2018.06.004

ÖZGEÇMİŞ

Adı Soyadı : Ayşe Nur ÖZKAN

Doğum Yeri :

Yabancı Dili : İngilizce

E-posta :

Eğitim Durumu

Lise : Turgutlu Anadolu Lisesi (1999)

Lisans : Orta Doğu Teknik Üniversitesi (ODTÜ)
Fen-Edebiyat Fakültesi / Kimya Bölümü (2005)

Yüksek Lisans : Orta Doğu Teknik Üniversitesi (ODTÜ)
Fen Bilimleri Enstitüsü / Kimya Anabilim Dalı (2008)

Mesleki Deneyim

Analist	Drogsan İlaçları San. ve Tic. A.Ş.	2007 - 2008
Uzman	Orta Doğu Teknik Üniversitesi	2008 - 2014
Uzman	Manisa Celal Bayar Üniversitesi	2014 - 2018
Öğretim Görevlisi	Manisa Celal Bayar Üniversitesi	2018 -

Eserleri

Uluslararası Hakemli Dergilerde (SCI ve SCI Expanded) Yayımlanan Makaleler

Zora M., **Pinar A. N.**, Odabaşoğlu M., Büyükgüngör O., Turgut G. Synthesis of ferrocenyl pyrazoles by the reaction of 3-ferrocenylpropynal with hydrazinium salts. Journal of Organometallic Chemistry. 2008, 693, 145-154.

Atmaca H., **Özkan A. N.**, Zora M. Novel ferrocenyl pyrazoles inhibit breast cancer cell viability via induction of apoptosis and inhibition of PI3K/Akt and ERK1/2 signaling. Chemico-Biological Interactions. 2017, 263, 28-35.

Saltan F., Şentürk S., Al A.M., **Özkan A. N.**, Şirin K. Preparation, characterization and thermal properties of polypropylene/polyethylene/zinc borate composites: investigation of thermal degradation kinetics. Journal of Polymer Research. 2023, 30 (10), 391.